Applying Ozone to Accelerate Remediation of Petroleum-Contaminated Soils

by

Tengfei Chen

A Dissertation Presented in Partial Fulfillment
of the Requirements for the Degree
Doctor of Philosophy

Approved June 2018 by the
Graduate Supervisory Committee:

Bruce E. Rittmann, Chair
Paul Westerhoff
Rosa Krajmalnik-Brown
Anca G. Delgado

ARIZONA STATE UNIVERSITY

August 2018

ABSTRACT

Petroleum contamination is ubiquitous during extraction, transportation, refining, and storage. Contamination damages the soil's ecosystem function, reduces its aesthetics, and poses a potential threat to human beings. The overall goals of this dissertation are to advance understanding of the mechanisms behind ozonation of petroleum-contaminated soil and to configure an effective integrated bioremediation + ozonation remedial strategy to remove the overall organic carbon. Using a soil column, I conducted batch ozonation experiments for different soils and at different moisture levels. I measured multiple parameters: e.g., total petroleum hydrocarbons (TPH) and dissolved organic carbon (DOC), to build a full understanding of the data that led to the solid conclusions. I first demonstrated the feasibility of using ozone to attack heavy petroleum hydrocarbons in soil settings. I identified the physical and chemical hurdles (e.g., moisture, mass transfer, pH) needed to be overcome to make the integration of chemical oxidation and biodegradation more efficient and defines the mechanisms behind the experimental observations. Next, I completed a total carbon balance, which revealed that multiple components, including soil organic matter (SOM) and non-TPH petroleum, competed for ozone, although TPH was relatively more reactive. Further experiments showed that poor soil mixing and high soil-moisture content hindered mass transfer of ozone to react with the TPH. Finally, I pursued the theme of optimizing the integration of ozonation and biodegradation through a multi-stage strategy. I conducted multi-stages of ozonation and bioremediation for two benchmark soils with distinctly different oils to test if and how much ozonation enhanced biodegradation and vice versa. With pH and moisture optimized for each step, pre-ozonation versus post-ozonation was assessed for TPH removal and mineralization. Multi-cycle treatment was able to achieve the TPH regulatory standard when biodegradation alone could not. Ozonation did not directly enhance the biodegradation rate of TPH; instead, ozone converted TPH into DOC that was biodegraded and mineralized. The major take-home lesson from my studies is that multi-stage ozonation + biodegradation is a useful remediation tool for petroleum contamination in soil.

ACKNOWLEDGMENT

The research here was funded by Chevron Energy Technology Company.

Firstly, words fail to convey how grateful I am for having Dr. Bruce E. Rittmann as my Ph.D. advisor. In the past five years, he has been shaping me in every possible way towards a qualified Ph.D. From writing, presenting, and teaching to meeting and dealing with difficult situations, he is always the role model I can look up to and try to emulate. I'm lucky to be able to work with him.

My father-Shilong Chen and my mom-Hailian Huang are everything to me, I couldn't have gone this far without them. Words are too feeble to represent their love. To succeed is the most direct way to respond to their unconditional love.

I also would like to deliver my gratitude to my wonderful teammate Burcu M. Yavuz. I'm so indebted to her patience and help when we first started working together. Were it not for her, I wouldn't be able to have such an English proficiency today.

I must also express my million thanks to Dr. Anca G. Delgado. Her help on GC operation, oil extraction, bioremediation of soil, and paper revision was crucial to my research.

I'm also very grateful for Dr. Paul Westerhoff, who lent so much help on our ozone research. His comments and suggestions for my papers were hugely helpful.

I would like to thank Dr. Rosa Krajmalnik-Brown for her useful comments and editing on my papers.

Special gratitude is paid to our lab managers, Diane Hagner and Sarah Arrowsmith, and business manager, Carole Flores, for coordinating.

I also acknowledge all those people who have directly or indirectly aided me, either in my research life or personal life, over the past 5 years. They are (in no particular order) Dr. Chen Zhou, Zhuolin Liu, Dr. Paul Dahlen, Dr. Onur Apul, Dr. Yi Zuo, Dr. Roopa Kamath, Dr. Georgios. Papacharalampos., Alan Proctor, Rachel Von Gnechten, Delaney Won Winkle, and Brielle Januszewski, and all the lovely members in BSCEB.

Lastly, to my ex-girlfriends, thanks for being a ‘distraction’ and teaching me some important life lessons.

TABLE OF CONTENTS

Page

CHAPTER Page

LIST OF TABLES

LIST OF FIGURES

Figure Page

Figure Page

Figure Page

Figure Page

CHAPTER 1. INTRODUCTION

1.1 Foundation of my research—petroleum contamination

Every step within the petroleum industry, i.e., exploration, extraction, storage, transportation, and refining, opens potential for oil spills and leaks [1-5]. For example, oil pipelines convey nearly 70% of the petroleum from extraction fields to refineries [6], and this inevitably incurs oil spills and leaks. The Pipeline and Hazardous Materials Safety Administration (PHMSA) estimated crude oil lost via the pipeline transportation system across the entire U.S. since 2010 to be ~9 million gallons (https://undark.org/article/oil-pipeline-safety-dakota-access-standing-rock/).

Oil spilled in soil tends to migrate downwards and spread horizontally as a non-aqueous phase liquid (NAPL) at the top of the groundwater table when its quantity is large enough to saturate the soil pores [7, 8]. Since most oils are lighter than water, the gravitational infiltration will stop upon contacting groundwater saturated area, and the oil will float on the water table and spread into a plume in the direction of groundwater flow [9].

1.1.1 Petroleum's toxicity and regulations

The release of petroleum into soil and groundwater disturbs the soil eco-system and poses threats to human health. The major negative effects of petroleum intrusion on soil ecosystems are: (1) Reducing the germination of plants [10-15], attributed to embryonic damage caused by oil penetration or oil coating that prevents the seed from taking water and nutrients [11]. (2) Damaging existing plant tissues [11]. For example, roots directly contacting oil can be dissolved, and oil absorbed through root can be transported to leaves, which harms leaves' biological functions [11]. (3) Killing soil invertebrates, such as earthworms and collembola [14, 16-18] by disrupting their TCA cycles [19]. (4) Aggregating soil into water- and air-impenetrable clods, which retards water drainage, repels water, limits oxygen permeation, and alters soil's physical property [20-22]; this oxygen-blocking effect further impedes plants growth [20]. and (5) Affecting animals contacting the contaminated soil directly or via the food chain [23].

The impact of oil on human health is more complicated. From a bioavailability and mobility standpoint, crude oil is separated into $<C_{44}$ and $>C_{44}$ fractions (vacuum residue) in toxicity

assessment. Heavy hydrocarbons (>C_{44}) are nearly immobile and non-volatile and thus possess trivial macro-scale bioavailability; the only way human might be exposed would be direct contact with the soil via oral or dermal routes [7, 24]. Thus, very little attention has been paid to the effect of this fraction. The downside is a sparse data set for developing an accurate reference dose (RfD) [25]. Only one dermal RfD, 0.8 mg/kg/d, was established for the >C_{44} fraction (vacuum residue) by American Petroleum Institute (API) via two 28-day rabbit experiments. The rabbits exposed to 2000 mg/kg of vacuum residue suffered skin lesion and decreased appetite [26]. The oral RfD is believed to be much lower than dermal due to their bioavailability difference, and, for this, an oral RfD of 0.08 mg/kg/d was suggested [26].

For carbon length lower than C_{44}, a human might be exposed in various ways, including direct contact (e.g., kids rolling on the ground), volatile compounds inhalation, and contaminated groundwater ingestion [23]. Aliphatic and aromatic sub-fractions were assessed separately in the human health toxicology, because aromatics are normally more toxic than aliphatics [27, 28]. Each category was further divided into several carbon fractions, because toxicity is strongly related to fate and transport characteristics [9]. The Total Petroleum Hydrocarbon Criteria Working Group (TPHCWG) reviewed available toxicity data and developed RfD for oral ingestion and reference concentration (RfC) for vapor compounds. Table 1.1 below compiled these doses for different carbon fractions and the corresponding health effects [23, 25].

Table 1.1. Toxicity of petroleum hydrocarbons based on carbon fraction.

TPH fraction	Oral RfD mg/kg/d	Vapor RfC Mg/m^3	Health effect
Aliphatics			
C6-C8	5.0	18.4	Neurotoxicity
C8-C16	0.1	1.0	Hepatic and hematolotical changes
C17-C21	2.0	N/A (volatility not palpable)	Hepatic granuloma
C21-C35	2.0		
C35-C44	20		
Aromatics			
C5-C8	0.2	0.4	Neurotoxicity, hepatotoxicity
C9-C16	0.04	0.2	Decreased body weight, hemolytic anemia
C16-C21	0.03	N/A (volatility not palpable)	Lung abnormality, nephrotoxicity, hepatotoxicity
C21-C35	0.03		
C35-C44	0.03		

Total petroleum hydrocarbons (TPH), defined as the measurable amount of petroleum-based hydrocarbon in an environmental medium [9], has been used as the sole regulatory index for determining whether an environmental medium needs remedial action. TPH encompasses carbon lengths up to C_{44} (modified by API from the TPHCWG's original C_{35}) that can be detected and quantified by GC-FID [29] via EPA method 8015 M [30]. However, each state has adopted its own standard for TPH concentration. Some states use <1% (10,000 mg/kg soil), based on the oil not impeding vegetation growth or infiltrate into groundwater, but others have more stringent criteria, such as 0.1%. Examples are provided in Table 1.2 (adapted from [31]), though a survey conducted in 2014 updated the cleanup levels (CULs) in 11 states that loosened their regulatory limits based on different components of petroleum, such as gasoline range oil and diesel range oil, and potential exposure pathways [32].

Table 1.2. TPH regulations in some states for E&P sites in 1999

State	TPH Regulatory Limit mg/kg soil
Colorado	10,000
Louisiana	10,000
Michigan	10,000
New Mexico	100; 1,000; 5,000 (site specific)
Texas	10,000
Wyoming	1,000-10,000 (site specific)
Alberta, Canada	1,000

1.2 Challenge in removing of residual petroleum hydrocarbons using bioremediation

Depending on the composition of the original crude oil and the nature of the original release, soils can retain between 1% and 20% (w/w) petroleum residuals decades after a spill [33]. Natural "weathering" processes, i.e., photooxidation on the top layer, biodegradation, volatilization, dissolution and dispersion in groundwater [7, 9], gradually reduce the concentrations of oil components on its light end, but the heavy hydrocarbons (e.g., long-chain, branched, cyclo-alkane, and polycyclic-aromatic hydrocarbons (PAHs)) usually persist without remedial intervention [34-36]. These so-called "heavy hydrocarbon" residuals are the main subject of my research. The presence of such heavy-hydrocarbon residuals in soil is a long-term liability, and remediation costs range from tens to hundreds of US$ per cubic meter soil for technologies such as biopiles and biosparging [37].

Current field-applicable technologies for petroleum-contaminated soil include *in situ* and *ex situ* chemical, physical, and biological treatment processes. The commonly used ones are bioremediation (land farming, bioventing, biopile) [38-42], stabilization/solidification [43-45], chemical oxidation [46-48], soil washing [49, 50], and thermal technologies (desorption, incineration) [51-54]. Even direct reuse of the soil as a road material has been reported [55, 56].

Among these technologies, bioremediation has received a considerable amount of interest due to its relative cost-effectiveness, simplicity, and good performance [34, 57-59]. Practically, for a relatively biodegradable oil, a 1% TPH management level is achievable through bioremediation [31], which

involves the microbial degradation of different types of petroleum hydrocarbons (alkanes, branched-alkane, cycloalkane, and aromatics) in soil by stimulated indigenous or added microbial community.

Although bioremediation has shown great promise as a strategy for many organic contaminants [60-62], some residual hydrocarbons are not readily biodegradable. For example, the complex resonance structure of polycyclic aromatic hydrocarbons (PAHs) may require a co-metabolic mechanism [63] or energy and electron investments from microorganisms to initiate ring cleavage [64]. Moreover, hydrophobicity, complex structures, and toxicity also can hinder biodegradation [35, 65-69]. While long-chain n-alkanes are relatively susceptible to biodegradation in spite of low water-solubility [63], branched and cyclic alkanes are more persistent due to inherent recalcitrance. Labud et al. [70] reported that accumulation of these residual hydrocarbons inhibited the growth of microorganisms in the soil, further compromising the potential of bioremediation.

Lower API gravity (detailed below in 1.3.1) entails higher concentration of resins and asphaltenes and lower concentration of biodegradable hydrocarbons [71]. The recalcitrance that comes with a low API gravity results in a higher residual concentration, which is a phenomenon where TPH concentration gradually ceases to decline and plateaus at some point even if the abiotic conditions are optimal [35, 68, 72, 73]. Some researchers believed this was due to the lack of bioavailability as microbes couldn't access the TPH residing in soil's pores [74-76] . However, others attributed this to the inherent recalcitrance of the molecules with complex structures [77, 78] . Huesemann [68] assumed that the combined effect of the bioavailability issue and inherent recalcitrance was the real cause of this incomplete TPH reduction. In either case, the residual TPH, if higher than regulatory standard, needs to be treated with more aggressive strategies to reach the cleanup goal.

1.3 Petroleum

1.3.1 Crude oil composition

Crude oil is a mixture of hydrocarbons that exists in the liquid phase in underground reservoirs and that remains in the liquid phase at atmospheric pressure [79, 80]. Crude oil is composed mostly of the elements hydrogen and carbon at a mole ratio of approximately 1.85 (hydrogen):1 (carbon) [79]. In addition to hydrocarbons, petroleum contains fractions with nitrogen, sulfur, oxygen, and trace metals; these fractions may constitute less than 1% to as much as 8% of some crude oils [81]. Table 1.3 below lists the elemental fractions of an average petroleum.

Table 1.3. Elemental fractions of crude oils by weight

Element	Weight percentage
Carbon	82-87
Hydrogen	11-14
Oxygen	0.1-4.5
Sulfur	0.1-8
Nitrogen	0.1-1.8
Trace metals	<0.1

Adapted from [79] and [82]

Two non-hydrocarbon fractions are the asphaltenes and resins. They are the more polar fractions of the crude oil, and they contain multi-ring aromatics with O, N, and S fused in the rings [83, 84]. Resins and asphaltenes differ in molecular weight (asphaltenes > resin) and solubility in n-alkanes (resin > asphaltenes) [34, 67, 80, 85]. As the heaviest portion of crude oils, asphaltenes molecules not only have high molecular weight (MW) (500-2000 g/mol), but also self-associate to form nanoaggregate with MW up to 22,000 g/mol [86-88]. This feature can render asphaltenes relatively bio-resistant.

Hydrocarbons that typically comprise the largest fraction of crude oil are measured as total petroleum hydrocarbons (TPH). The traditional GC-FID method for TPH accesses ~40% of the total oil mass [89].

Most of the hydrocarbons consist of n-alkanes, branched-alkanes, cycloalkanes, and the mono-, and multi-aromatics (with or without alkylation). Tissot and Welte [90] quantitatively compiled the composition of 636 crude oils and reported that saturated made up roughly 40-80% of the total weight, aromatics had a proportion of 20-45%, and the range for asphaltenes and resins was 0-40%.

Boduszynski and Altgelt [91] proposed that crude oils are a continuum with respect to carbon number, molecular weight, boiling point, and aromaticity. The composition increases gradually and continuously with these parameters. And this continuity theory was later verified for carbon number up to C_{100} using Fourier transform ion cyclotron resonance mass spectrometry (FT-ICR MS) by a research team from Florida State University through a string of companion publications [86-89, 92, 93].

The color of petroleum varies from straw yellow to dark brown or black [82]. "Heavier" oil has a larger content of asphaltenes and has a darker color. The density of petroleum is an important characteristic that is expressed via its API gravity, whose formula is:

$$\text{API gravity} = \frac{141.5}{\text{Specific gravity at } 60^\circ \text{ F}} - 131.5 \qquad (1.1)$$

where the specific gravity of oil at 60°F is relative to water. The API gravity has a unit of degrees (°). Water, which has a specific gravity of 1, has an API gravity of 10°. Most crude oils are lighter than water, which means that their API gravity is above 10°.

A hydrocarbon's water solubility decreases with increasing carbon number, and aromatics are much more soluble than aliphatics with the same carbon range, as shown in Table 1.4.

Table 1.4. The solubility of petroleum hydrocarbons.

Compounds	Solubility (mg/L)
Aromatics	
C8-C10	65
C10-C12	25
C12-C16	5.8
C16-C21	0.65
C21-C35	2.9E-02
Aliphatics	
C5-C6	36
C6-C8	5.4
C8-C10	0.43
C10-C12	3.4E-02
C12-C16	7.6E-04
C16-C35	2.5E-06

(Adapted from Gustafson et al. [94])

1.4 Bioremediation of petroleum-contaminated soil

Quite a few variables can influence the efficacy of bioremediation, e.g., oxygen availability, moisture level, TPH concentration, pH, macro and micronutrients, salinity, and temperature [40, 67, 85]. Moreover, hydrocarbons differ in degradation rate depending on their structures; the general pattern of decreasing susceptibility to biodegradation is: n-alkanes > branched alkanes > low-molecular-weight aromatics > cyclic alkanes > PAH [67, 95]. Some high-molecular-weight PAHs appear to be intrinsically not biodegradable, even under optimal condition.

Understanding the mechanisms behind the bacterial conversions of different categories of hydrocarbons is crucial to (1) detecting the evidence that biodegradation is occurring and (2) tracking the fate and transport of the metabolites in soil and potentially in groundwater.

1.4.1 Aerobic bacterial degradation of alkanes

Alkanes with weight percentage ranging from 40%-80% are the saturated family of crude oil [96], and they can be divided further into n-alkanes, branched-alkanes, and cyclo-alkanes and grouped in three phases: gaseous (C_1–C_4), liquid (C_5–C_{16}) and solid (>C_{17}) [57]. Due to their sparing solubility

and the lack of functional group, alkanes are typically chemically stable; nevertheless, they are subject to biological attack when oxygen is available.

A major controlling factor is that the bacteria able to biodegrade the n-alkanes must for be able to take up (ingest) individual molecules. They cannot ingest the NAPL directly. Bacteria gain access to single molecules either through direct interfacial contact, where cell-membrane-embedded enzymes mediate the uptake of removal and uptake of single molecules; through a biosurfactant-facilitated uptake process, where biosurfactant is extruded to the outside to emulsify hydrocarbons [97]; or through normal dissolution to the aqueous phase.

The degradation pathway inside of a cell differs depending on the structure of the alkanes, but the common steps are initial mono- or di-oxygenation to insert –OH groups that make the molecules more water soluble and biochemically available. These oxygenation reactions require molecular oxygen as a direct reactant and consume intracellular electron donor, such as NADH [98]. Once the molecules have been activated by the addition of –OH groups, subsequent oxidations occur via normal hydroxylation and dehydrogenation reactions, such as occur in beta-oxidation. The subsequent reactions are electron and energy generating. Under aerobic condition, these hydrocarbons can be completely mineralized [40].

1.4.1.1 N-alkane Biodegradation

N-alkane biodegradation can be initiated by either terminal-methyl and sub-terminal-methyl mono-oxygenation [97, 99]. Terminal and sub-terminal oxidation can co-exist in some microorganisms, and their pathways are illustrated in Figure 1.1. For the former, the terminal methyl is mono-oxygenated to a primary alcohol, which is then converted to a corresponding aldehyde by an alcohol dehydrogenase and further hydroxyated to carboxylic acid via an aldehyde dehydrogenase. This is followed by β-oxidation, a process that releases the terminal two carbons as acetic acid in a process that oxidizes the new terminal C to a carboxylate. Sub-terminal oxidation of n-alkanes has the initial step involves generating a secondary alcohol by a mono-oxygenation. The alcohol is dehydrogenated to the corresponding ketone, oxidized by a Baeyer–Villiger monooxygenase to an ester, and then hydrolyzed by an esterase to generate an alcohol and acetate [57].

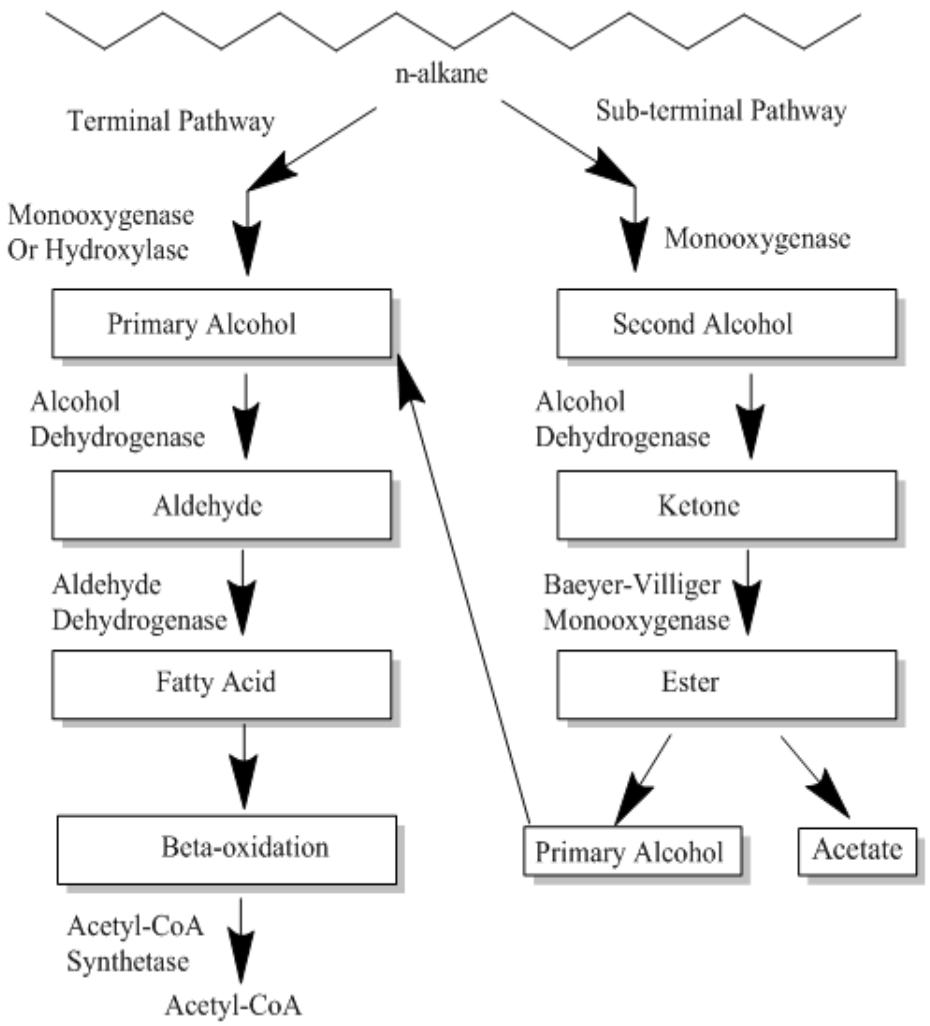

Figure 1.1. Two pathways associated with n-alkane biodegradation.

1.4.1.2 Branched-alkane Biodegradation

Methyl branching renders hydrocarbons less susceptible to microbial attack via □-oxidation. It requires an additional strategy, such as α-oxidation and ω-oxidation [85]. Figure 1.2 visualizes the two pathways. By removing the terminal carboxyl group of a branched chain fatty acid, alpha-oxidation enables subsequent β-oxidation. One good example is phytane degradation, where α-oxidation leads to the generation of pristanic acid that can be further degraded via β-oxidation [100]. In contrast, ω-oxidation first produces a dicarboxylic acid with a carboxyl group at each end of the chain; then, it generates a product that can be isomerized to succinyl-CoA. Peculiarly, β-oxidation

in the branched-alkane scenario not only releases acetyl-CoA, but also yields propionic-CoA at branch points [101].

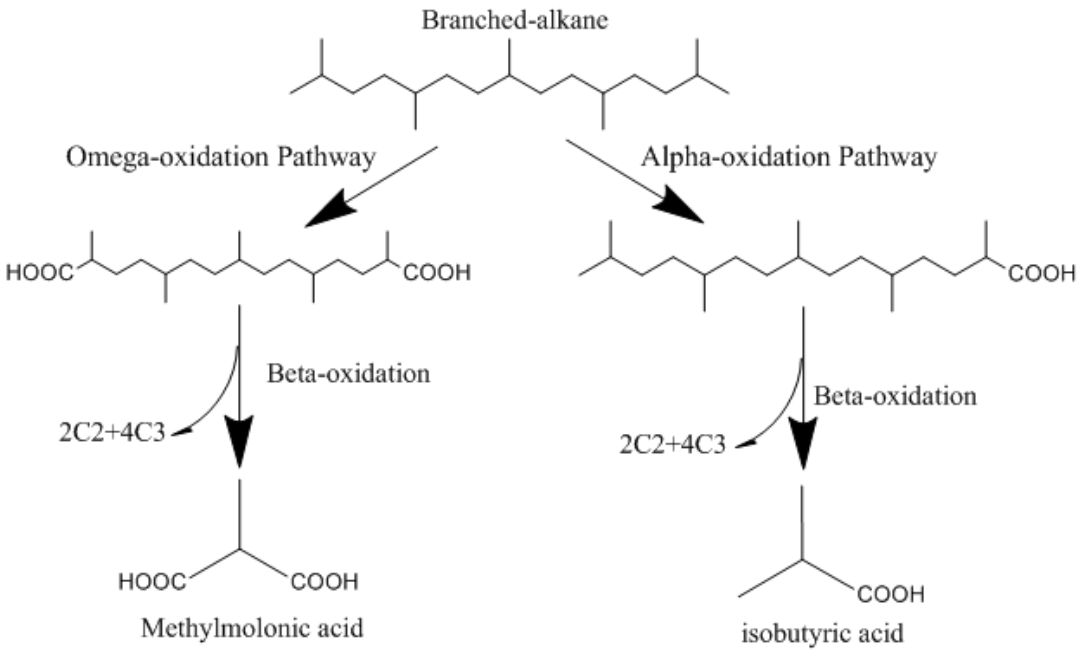

Figure 1.2. Two common pathways in biodegradation of branched-alkane.

1.4.1.3 Cycloalkanes

Cycloalkanes, major components in petroleum, are more recalcitrant than chained alkanes. In particular, complex polycyclic compounds, such as hopanes, are among the most persistent components of petroleum spillages in the environment [69, 102]. Nevertheless, they can be degraded via direct oxidation [85, 103, 104] and co-oxidation, which is a phenomenon where microorganisms oxidize the non-energy providing and non-growth compounds that are otherwise recalcitrant by using other growth-supporting substrates as the carbon source [85, 103, 105-107]. The intermediates generated from co-oxidation of the resistant compounds then can serve as energy and carbon source for other synergetic microorganisms.

Figure 1.3 exemplifies that oxidation pathways involved in cycloalkanes in either direct oxidation or co-oxidation are structure dependent. For cyclic alkanes without alkyl substitution, the attack is

initiated with an oxygen insertion by a monooxygenase, which produces an alcohol, and this alcohol further undergoes oxidation to a ketone; subsequently, a process known as Baeyer-Villiger oxidation driven by a Baeyer-Villiger monooxygenase leads to the ring cleavage, which then yields a dicarboxylic acid. The multi-ring structure is degraded in the same manner [108]. On the other hand, substituted cycloalkane can be more easily oxidized, as the side alkyl chain is more susceptible to microbial attack via β-oxidation; ring transformation to aromatic, which then is broken down through ring cleavage, as a pathway has also been established by other researchers [105].

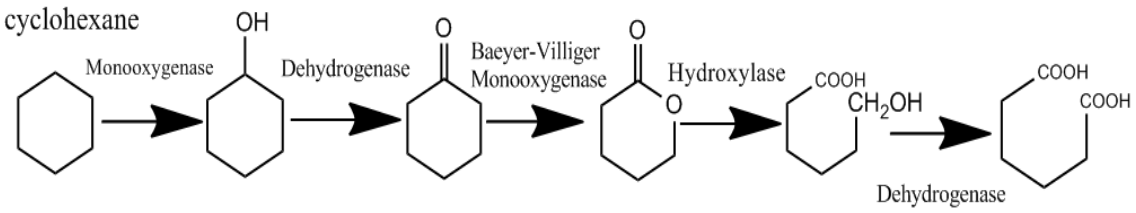

Figure 1.3. An example of cyclic alkane biodegradation.

1.4.2 Aerobic bacterial degradation of aromatics

Aromatics, another major component of petroleum, can be divided into single-ring compounds and polycyclic aromatic hydrocarbon (PAHs). These compounds also can be alkylated [109-111]. In aerobic conditions, single-ring aromatics, such as benzene and toluene, can be used as electron donors and carbon sources. The initial attack involves the addition of oxygen atom(s) onto the ring via mono- or di-oxygenase, and then the intermediate will be converted by a dehydrogenase to catechol [98], which will be cleaved via ortho pathway or meta pathway. Ring cleavage produces succinic, fumaric, pyruvic, acetic acids, and aldehydes, all of which can be utilized by microorganisms [58]. The pathways are shown in Figure 1.4.

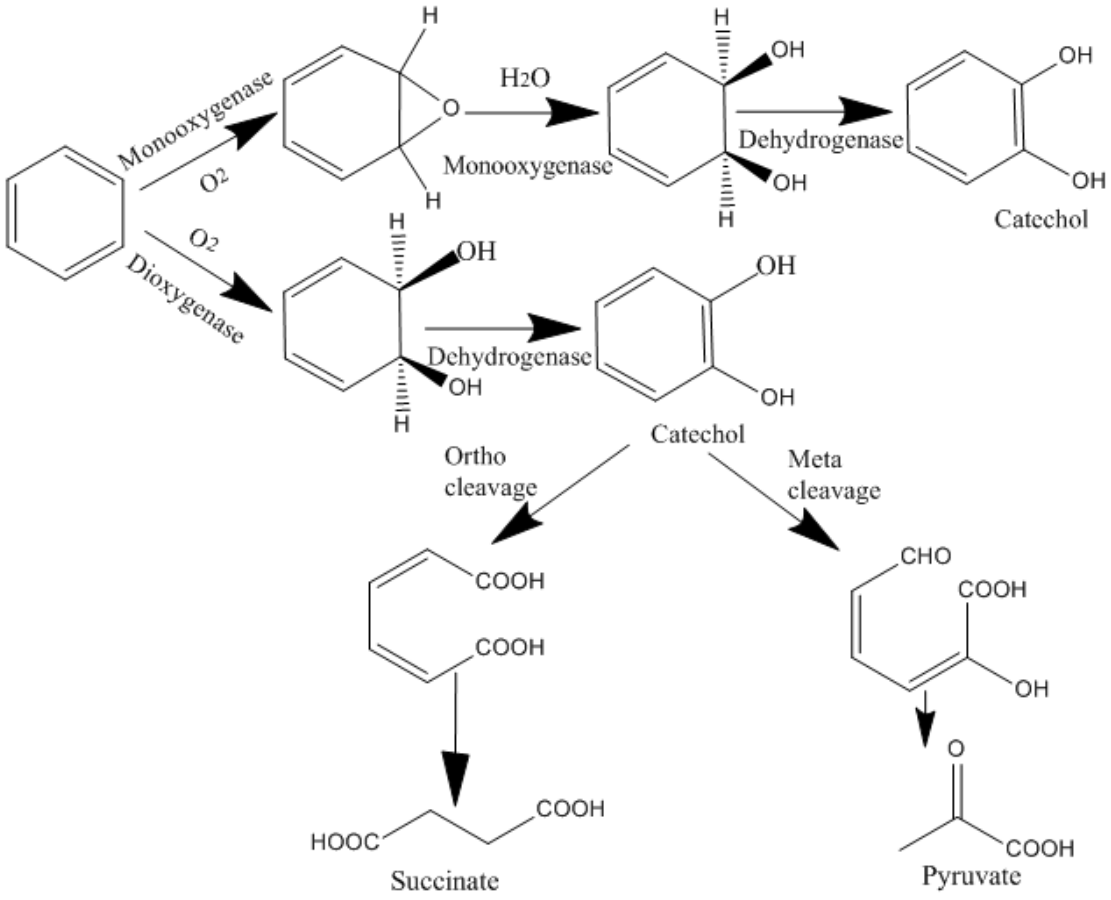

Figure 1.4. Exemplification of the biodegradation of single ring structure.

The ring attack step is usually the rate-limiting step [58, 112]. On the other hand, PAHs are more recalcitrant than single-ring compounds and sometimes require co-oxidation to be degraded [58, 113]. During co-oxidation, the degradation pathway of PAH is similar to the single-ring structure: oxygen insertion followed by ring split. Once the first ring is opened, the second ring will be cleaved in a similar fashion[112]. Angular PAHs are thermodynamically more stable than the linear form [114-116]; however, the angular area is more susceptible to enzymatic attack, making angular PAH more biodegradable [115]. One example of PAH (Benzo[a]pyrene) degradation pathway is illustrated in Figure 1.5.

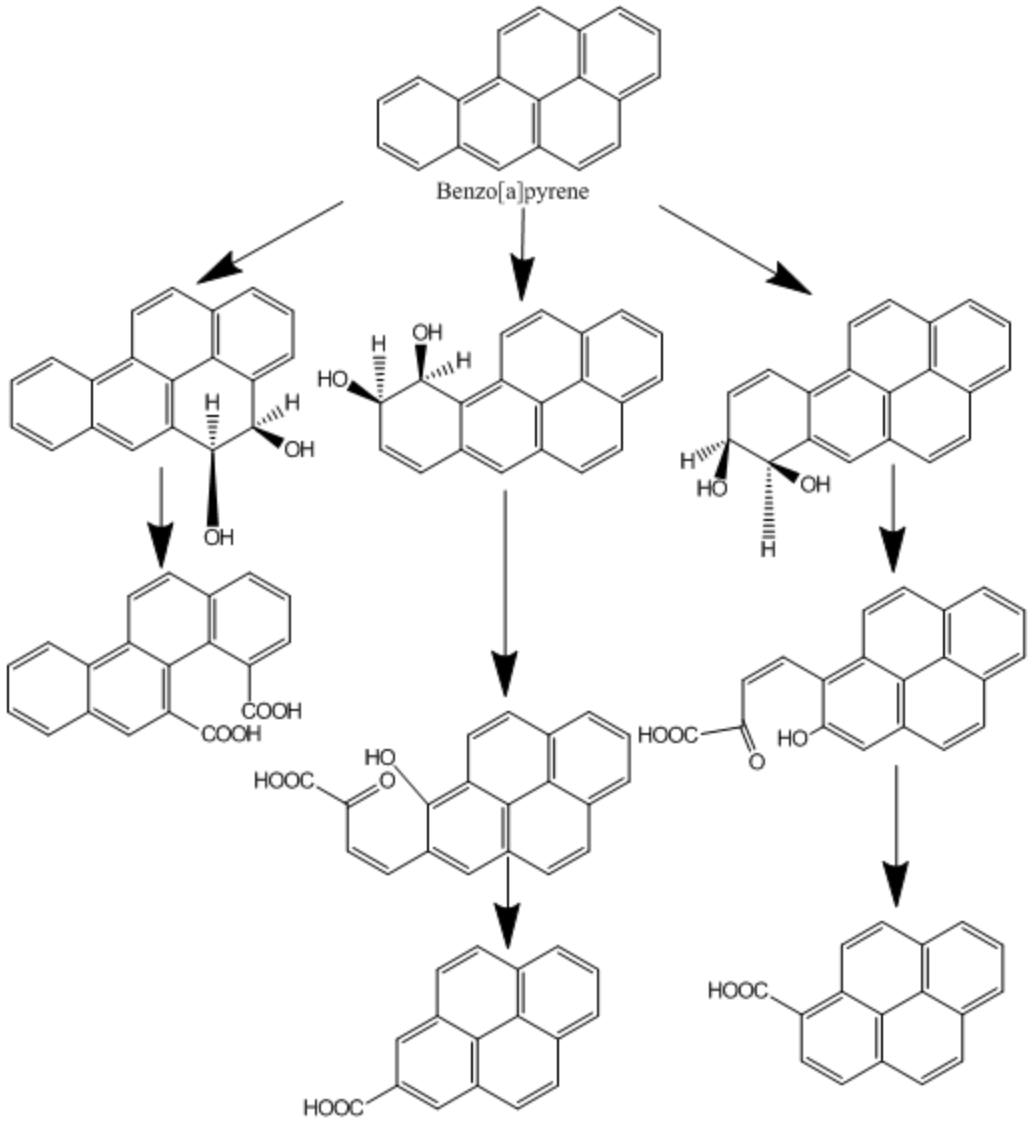

Figure 1.5. Partial biodegradation pathway of Benzo[a]pyrene at different initial positions.

Alkylated aromatics have been observed to possess significant toxicity [110, 111, 117]. The presence and the position of alkyl group can greatly affect the biodegradation rate, and many reported that the biotransformation rate of PAH decreased with increasing alkylation [118-120]. This is believed to be because alkyl branches replace the binding position for dioxygenase on the ring, resulting in the inability of dioxygenase to attack [121]. Biodegradation of alkylated aromatics can start from the alkyl group or the ring [122-124], the alkyl chain will be cut in the same manner as alkane, and the ring cleavage follows the pattern of an unsubstituted aromatic compound.

1.4.3 Abiotic Factors Affecting Biodegradation of Petroleum Hydrocarbons

Microorganisms need proper conditions to degrade petroleum hydrocarbons. A suite of abiotic factors influencing the biodegradation of petroleum hydrocarbons have been identified. Successful implementations of bioremediation thus depend on how favorable the following factors are.

1.4.3.1 Temperature

A decrease in temperature reduces microbial enzyme activity, oil viscosity, oil volatility, and oil water-solubility, resulting in a slowdown in biodegradation rate [67, 125]. Though successful bioremediation of crude oils attributed to psychrophilic bacteria has been achieved in cold environments, such as Antarctic/sub-Antarctic and Artic/sub-Arctic areas [126-128], the general observed pattern is biodegradation rate of crude oils decreases with a decreasing temperature. For example, Balks et al. [129] observed that biodegradation rate at an optimal temperature was 4 times faster than at a colder temperature. An optimal range has been reported to be 30-40℃ in soil environment [34, 67]. Although microbial degradation does not fully stop in winter, a summer condition is always favorable.

1.4.3.2 Oxygen

O_2 not only serves as the terminal electron acceptor for aerobic biodegradation, but it also is a required component for oxygenation of hydrocarbons via mono- or di-oxygenation. Thus, its availability and concentration determine the biodegradation rate. In subsurface soil setting, O_2 availability depends on diffusion, which is controlled by O_2 consumption rate, soil composition, and soil moisture level [67]. O_2 supply via natural attenuation is not sufficient to maintain an oxic condition in many oil-contamination cases, such as a high soil water content that blocks the diffusion of O_2 and high concentration of oil that deplete O_2 faster than it can diffuse. In these scenarios, adding O_2 through air injection, tilling, or water saturated with O_2 is necessary to ensure an aerobic environment.

1.4.3.3 pH

The optimal pH reported for a desirable biodegradation of oil is circumneutral (7-8) [67, 130-133]. However, a soil's pH can vary over a wide range, from extremely acidic (2) to extremely basic (11)

[134], and these extreme conditions have negative effects on biodegradation of hydrocarbons [67, 135], i.e., either too acidic or too alkaline pH retards biodegradation rate. Thus, pH modification (HCl or lime) is indispensable for non-neutral soils, particularly when bioremediation is combined with chemical pre-oxidation, as chemical oxidation, such as ozonation, can produce organic acids, further lowering the pH [136, 137].

1.4.3.4 Macronutrients

Bioavailable macronutrients, nitrogen and phosphorus, are indispensable elements for microbial anabolism during the consumption of petroleum hydrocarbons; thus, their availability dictates the growth of microbial community and thereby limits the overall biodegradation rate. Several suitable ratios of C: N: P, such as 100:10:1 [85, 130, 138, 139] and 100:15:1[125], for a significant biodegradation rate have been reported; however, the infusion of large amount of oil into soil, which typically contains insufficient concentration of nutrients to produce a desirable C/N/P ratio, can significantly reduce the indigenous available nutrients [140-143], resulting in an unfavorable condition. Therefore, implementing biostimulation usual requires nutrients addition. A common way is applying commercial fertilizer, while Okolo [144] observed an improved biodegradation of oil with animal manure. The amount of fertilizer to be added depends on the oil concentration.

1.4.3.5 Soil water content

Water in soil is essential to microbial activities, not only because it is required for bacterial growth, but also because it serves as the medium for mass transfer of the substrate. However, moisture content cannot be too high; otherwise it will block the porous space and hinders O_2 transfer. A generally suitable moisture content (by weight) ranges from 15% to 20% or close for typical bioremediation strategies, such as land farming [37, 145, 146]. Moisture content over 30% makes the soil sticky and inhibits O_2 diffusion because O_2 diffuses in water around 10^4 times slower than in air [147]; a much lower level (<10%) will be insufficient to drive substrate mass transfer. Water losses occurs through evaporation overtime; thus, constantly adding water to maintain a 15-20% moisture content is essential.

1.4.3.6 Salinity

A high concentration of salts impairs microbial activities in two major ways: (1) increased osmotic potential that causes microbial cells to dehydrate; and (2) direct damage on enzymatic activities, cell structure [148-150] , and genes [151]. Though some microbes can resist high salinity by synthesizing osmolytes in their cells to offset the osmotic stress, this process is energy-intense and compromises growth and degradation activity [147]. Quite a few studies have demonstrated that increasing salinity led to a reduction in hydrocarbon biodegradation [149, 152-154], due to the aforementioned reasons. Thus, for a highly salinized soil, removing excessive salts, such as by leaching, might be needed as a pre-treatment step.

1.5 Ozonation of Petroleum Hydrocarbons

Chemical oxidation relying on ozone (O_3) to remediate the soil has been gaining incremental attention over the past few decades. Ozone's strong oxidizing power should overcome the heavy fraction's residual problem by making them more soluble (thus more bioavailable) and simpler in structure (more biodegradable). Ozone and the hydroxyl radical (OH•), which can be produced form ozone, can react with all types of hydrocarbons and produce hydrophilic compounds, but through different mechanisms. The dominant oxidation pathways for OH• are hydrogen abstraction and OH• addition. In contrast, ozone attacks hydrocarbons via molecule addition, which leads to bond breaking. This section compiles and highlights the major oxidation pathways for each category of the petroleum hydrocarbons.

1.5.1 Physical-chemical Properties of Ozone

O_3 is a trioxygen molecule with a bond angle of 116.8° and a bond length of 1.278 Å. O_3 gas, a colorless gas with a unique color at low concentration, takes on a blue color in the concentrated form [155, 156]. The characteristic odor can be discerned by human olfaction at a concentration as low as 0.01 ppm [157], which acts as an exposure indicator, alerting humans of the hazard due to ozone's high toxicity. At ambient pressure and a temperature of 161.3 K, ozone gas liquifies into a dark blue fluid [156, 158], which is highly explosive. Even a volume concentration of ozone higher than 10-11% could trigger an explosion through its rapid self-decomposition [159].

Table 1.5, which lists the half-lives of O_3 in gas and water, shows that ozone decays rapidly in water solution at ambient temperatures, but persists longer in the gas phase unless the temperature is high.

Table 1.5. The half-lives of ozone in air and water over a range of temperatures

Gas phase		Aqueous phase	
T/°C	Half-life	T/°C	Half-life
-50	180 d	15	30 min
-35	10 d	20	20 min
-25	8 d	25	15 min
20	3 d	30	12 min
120	1.5 h	35	8 min
250	1.5 s		

Adapted from Gonçalves [160]

Figure 1.6 illustrates that O_3 exists in four resonance forms that render O_3 simultaneously electrophilic and nucleophilic, which means that it can launch attacks on chemical bonds and on the nucleus [161]. The resonance forms result from a delocalized pi pond that enriches one atom with electrons (nucleophilic, - sign in the Figure) and peels off electrons from another (electrophilic,+). This feature gives ozone a much stronger oxidation potential (E^0 = 2.07 V) compared to O_2 (E^0 = 1.23 V). Ozone's solubility is also 10-20 times higher than O_2 at room temperature [157, 162].

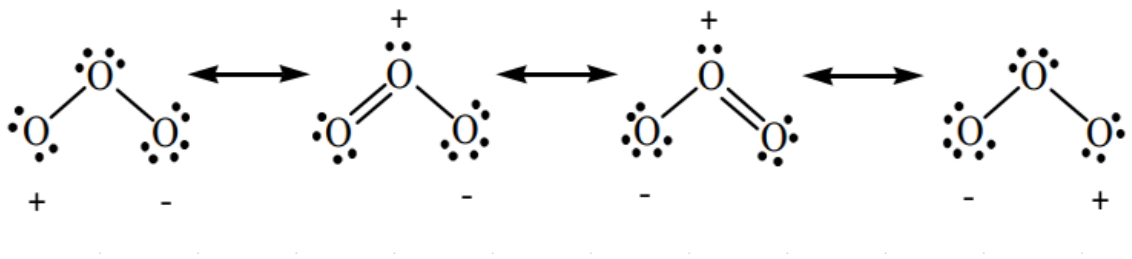

Figure 1.6. The four resonance forms of O_3.

1.5.2 Producing ozone

Commonly used ozone generators are based on corona-discharge [163], which applies a high voltage between two electrodes. The high voltage breaks down O_2 molecule to O radicals that attach to O_2 molecule to form O_3 molecules. Generators relying on other technologies, such as radiation and electrolysis, are also on the market, but they are less efficient and more expensive than corona discharge generators.

1.5.3 Ozone toxicity to humans

Because ozone attacks membrane lipids and amino acids in proteins and enzymes [164-166], ozone in the ambient environment can be dangerous to human health. The primary targets of ozone are airways and lungs [167-171], and if the exposure is extended, ozone may enter the bloodstream and transport to the central nervous system [164, 172]. For example, a 4-6-week exposure to 0.2 ppmv ozone caused lung distensibility (an inability to increase lung volumes [167, 173]), and prolonged ozone exposure (3-12 months, 0.8 ppm) also triggered increased pulmonary resistance and impaired airway stability [174]. A concentration of 10,000 ppmv caused death in 30 seconds [162]. The Occupational Safety and Health Administration (OSHA) set a standard of 0.1 ppmv for personnel exposure over an 8-hour shift (https://www.osha.gov/dts/chemicalsampling/data/CH_259300.html). The U.S. EPA has an even more stringent regulation for ambient exposure, no more than 0.07 ppmv over 8 hours (https://www.epa.gov/criteria-air-pollutants/naaqs-table).

1.5.4 Ozone decay

Along with being highly reactive, O_3 also is highly unstable and decays quickly upon entering water [161, 175, 176] or contacting soil surface with metal oxides or organic matter [177-180]. In water, the decay is launched by the reaction of O_3 with the hydroxyl ion (OH^-) and then proceeds to generating various hydroxyl, O_2, and O_3 radicals that are highly reactive in chain reactions that lead to rapid loss of O_3 [181]. In a soil matrix, the contact of O_3 and the soil surface in the presence of water leads to the production of the hydroxyl radical and the decay of O_3 [161].

1.5.5 Ozone Reactivity

Ozone and the hydroxyl radical react with a wide range of organic compounds, including hydrocarbons, but through different mechanisms. The dominant oxidation pathways for OH• are hydrogen abstraction and OH• addition [182-187]. Section 1.4.5.1-1.4.5.7 include some good examples.

In contrast, O_3 attacks hydrocarbons via electrophilic and nucleophilic addition, which leads to bond breaking [161, 175, 188]. Good examples of the O_3 reactions are also shown below.

This dual-oxidizing effect makes ozonation an attractive remediation method for wastewater and contaminated soil. In a soil setting, this feature can be further amplified because metal oxides in soil promote ozone's decay to form hydroxyl radicals [189-193]. This is of importance, since OH• shows reaction rates many orders of magnitude higher than does O_3. Table 1.6 compares the reaction rates of various organic contaminants with ozone and hydroxyl radical (Adapted from [194]).

Table 1.6. Typical reaction rates of O_3/OH with diverse types of organics

Organic compound	O_3 / $M^{-1}s^{-1}$	Hydroxyl radical/ $M^{-1}s^{-1}$
Phenols	10^{-1} - 10^{3}	10^{9} - 10^{11}
N-containing Organics	10 - 10^{2}	10^{8} - 10^{10}
Ketones	1	10^{9}-10^{10}
Aromatics	1-100	10^{8} - 10^{10}
Alcohols	10^{-2}-1	10^{8} – 10^{9}
Alkanes	10^{-2}	10^{6} – 10^{9}

1.5.5.1 Reactions between the ozone molecule and saturated hydrocarbons

Hellman and Hamilton [195] proposed a possible mechanism in which the O_3 molecule attacked saturated compounds via 1,3-dipolar insertion, and this insertion led to an intermediate of ROOOH that then decomposed to R and OH radicals. This mechanism, which was later supported [196], can be illustrated by the following pathway:

$$RH + O_3 \rightarrow R\cdot + HO_3\cdot \rightarrow ROOOH \rightarrow R\cdot + HO\cdot + O_2 \rightarrow R{=}O + ROOH$$

$$\downarrow$$

$$ROH + O_2\bullet$$

ROH, R=O, and ROOH are the corresponding hydrophilic products. More recently, other researchers put forward H abstraction theory where O_3 abstracts a hydrogen atom from the C-H bond to form a HOOO radical, which subsequently performs the second H abstraction to generate HOOOH [197-199]. The two H abstractions lead to a double bond that can be attacked directly by the O_3 molecule, and the HOOOH decays into H_2O and O_2 [197].

ROH, R=O, and ROOH can be further oxidized by O_3 through a similar mechanism to HOOOH pathway; however, the kinetics have been reported to be much slower than their precursors due to the stronger electron-withdrawing power of the functional group [200, 201].

1.5.5.2 Reactions between hydroxyl radical and saturated hydrocarbons

H-atom abstraction predominates in the oxidation of alkanes, cycloalkanes, and branched alkanes by OH• radical [187, 202, 203]. The room-temperature rate constants increase with decreasing C-H bond dissociation energy. H-atom abstraction entails one hydrogen atom being liberated by the radical, and the hydrocarbon becoming a radical (R•). The general equation can be expressed by:

$$R + OH\cdot \rightarrow R\cdot + H_2O$$

R· then undergoes reactions with O_2 or self-decomposition to form more water-soluble products. Figure 1.7 uses C_4H_{10} as an example [187].

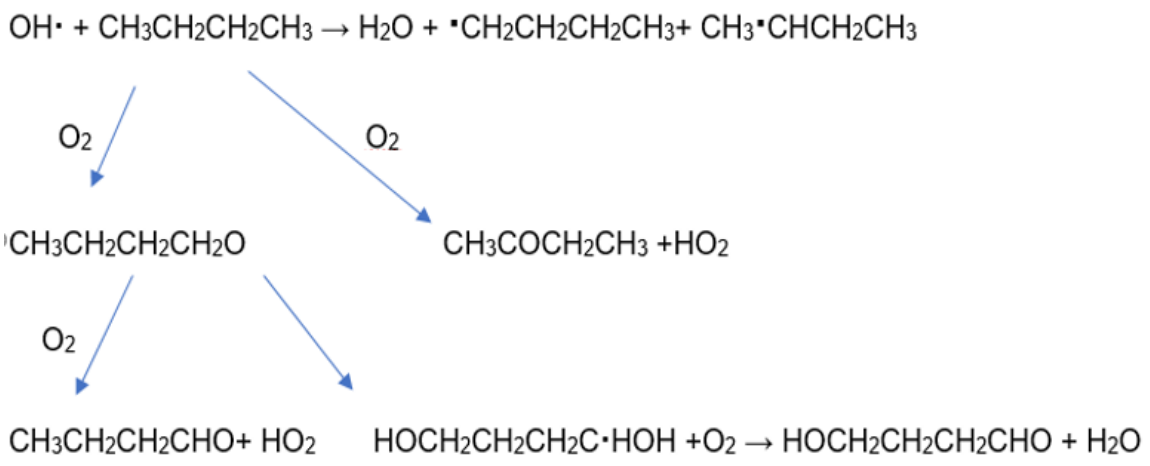

Figure 1.7. Pathway of C_4H_{10} oxidation via hydroxyl radical

H abstraction can take place at two locations, which means that a variety of hydrophilic products is possible. The produced oxygenated compounds are susceptible to further HO-radical attack, in which they will experience another H abstraction. This continued process breaks down the long chain into smaller molecules and eventually converts them to CO_2 and H_2O.

1.5.5.3 Reactions between ozone molecule and aromatics

O_3 can vigorously attack unsaturated carbon bonds due to its dipolar feature via 1,3-dipolar cycloaddition. For example, carbon double bond reacts with ozone molecule through the pathway below in Figure 1.8 [201, 204-206]:

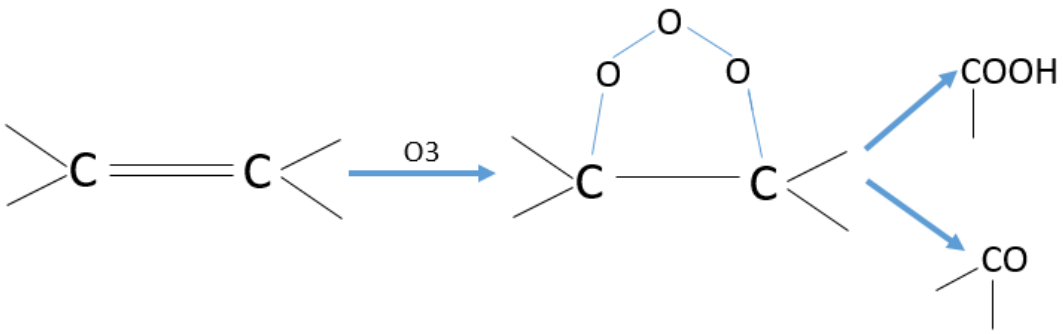

Figure 1.8. O_3 attacking C=C double bond.

The addition of O_3 molecule onto the double bond eliminates the double bond and creates a labile intermediate. This process can lead to the C-C bond breaking and the production of carboxylic acid and ketone.

The benzene ring exhibits higher resistance towards O_3 oxidation, probably due to its resonance structure that renders the ring relatively stable [161]. Figure 1.9 elucidates that ring cleavage of aromatic rings during ozonation can occur via both bond and atom attacks [201]. The bond attack follows the pattern of 1,3-dipolar cycloaddition, and the atom attack is launched by the electrophilic and nucleophilic properties of ozone. Single ring (benzene) mostly undergoes addition reaction. The addition of O_3 results in either bond splitting or the generation of phenol, which can be further oxidized to dicarboxylic acid. The final products will be CO_2 and H_2O if sufficient O_3 exists.

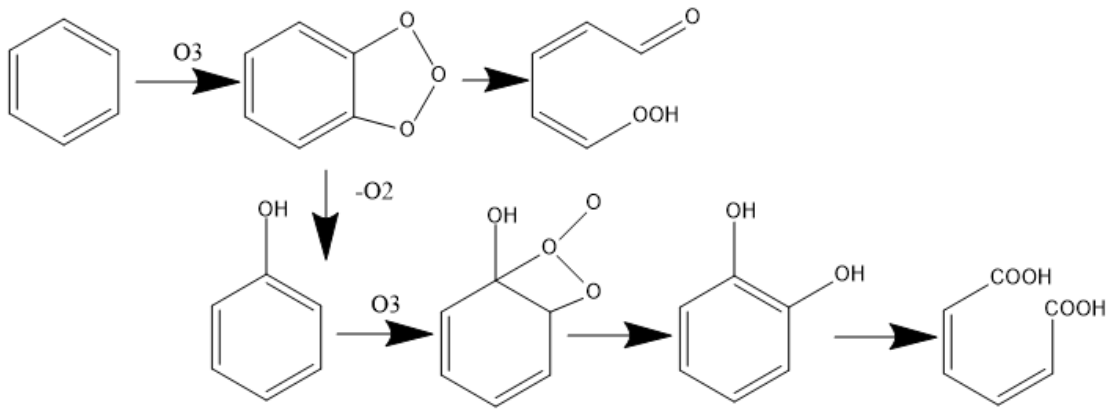

Figure 1.9. Ozonation of benzene.

Polycyclic aromatic (PAH) compounds, though more stable and more complex, are also more susceptible to atom attack due to the condensed electron accumulation. Bailey [201] proposed several different reaction pathways for various PAHs including naphthalene, pyrene, benzo[a]pyrene, and anthracene. These pathways are grouped by how the attack proceeds. Figure 1.10 and Figure 1.11 lay out examples of phenanthrene and pyrene that may undergo 1,3-dipolar addition, while benzo[a]pyrene is more likely subject to a series of electrophilic attacks. The rest of the rings can be cleaved in the same manner, resulting in the birth of various ketones, carboxylic acids, and aldehydes.

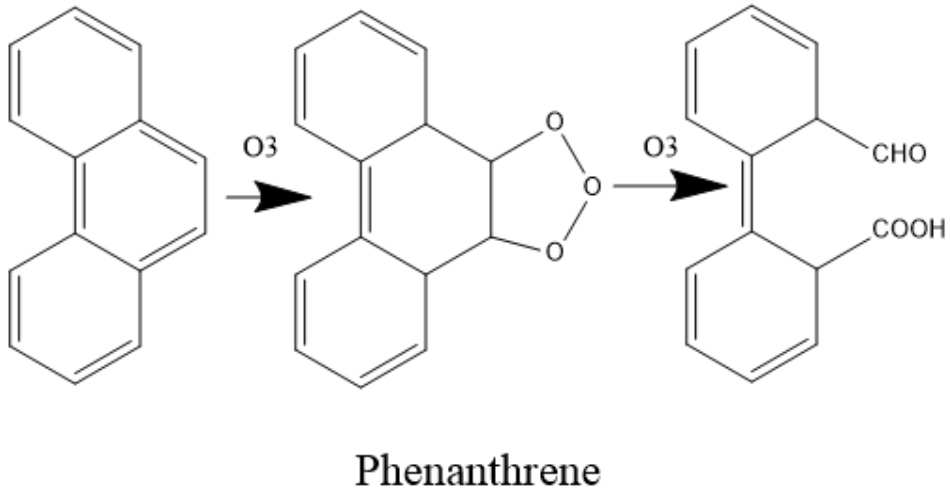

Figure 1.10. 1,3-dipolar addition of ozone on phenanthrene.

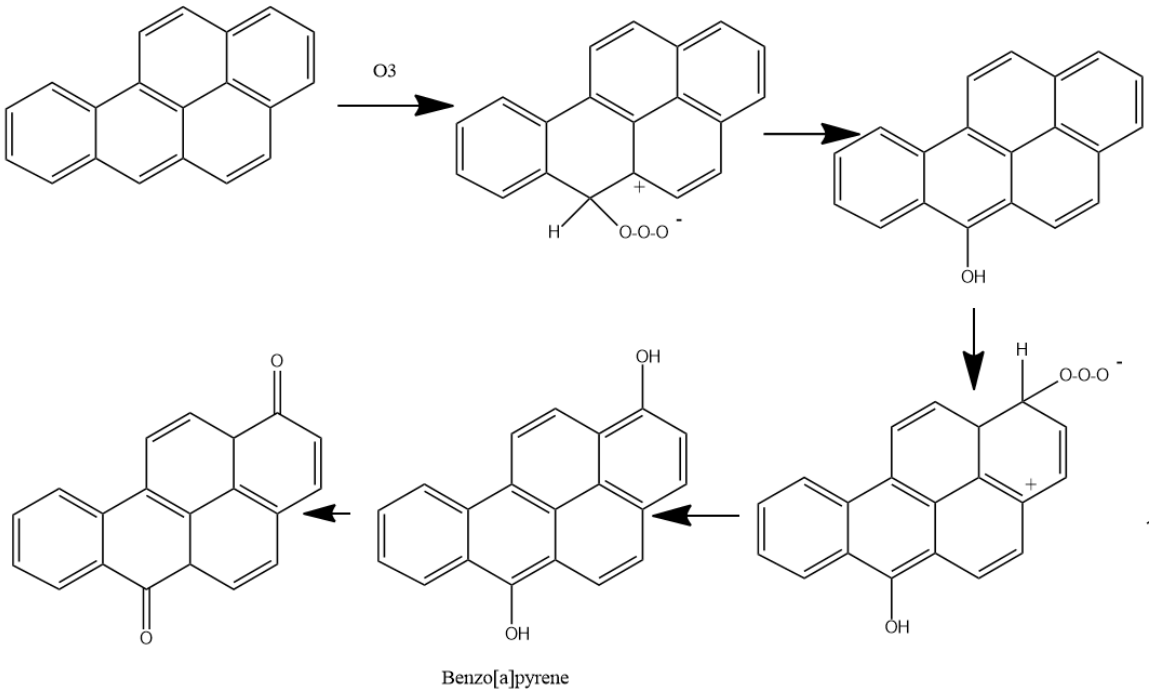

(Adapted from Bailey [201])

Figure 1.11. Electrophilic attack on B[a]P.

Other pathways are possible. Zeng et al. [207] traced and quantified the byproducts of the ozonation of BaP, and they proposed a new pathway in which O_3 attack transpired at a different carbon position. Given the diverse active sites on BaP, it is reasonable to infer that atom attack can follow multiple leads. In any cases, these processes could all result in ring cleavage and the emergence of simpler substances.

1.5.5.4 Reactions between hydroxyl radical and aromatics

The oxidation by the hydroxyl radical, in the presence of oxygen, initiates a complex cascade of reactions that lead to mineralization. Pure PAHs haveno group that may act as leaving groups for substitution reactions. Substitutions are more commonly observed in haloarenes, where a halogen atom may act as a leaving group. Therefore, OH addition in conjunction with H abstraction complete the attack [187, 208-211]. Using benzene as an example for visualization in Figure 1.12, the attack is initiated by a hydroxyl addition and then continues with the mechanism shifting to H atom abstraction.

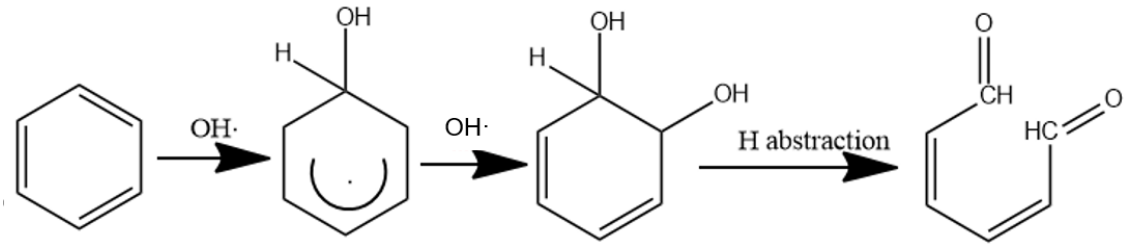

Figure 1.12. The oxidation of benzene by hydroxyl radical

PAHs with more than one ring have been given multiple plausible pathways. Bunce et al. [210] proposed 5 schemes in which the reactions progressed with different combinations of abstraction and addition. Ananthula et al. [208] also reported that H atom abstraction could start with either α position or β position of anthracene, and the position affected the overall oxidation kinetics.

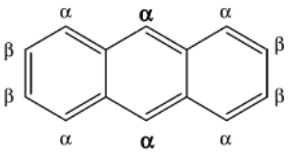

(anthracene)

Dang et al. [212] deduced that seven possible combinations of H atom abstraction from the C-H bonds and the addition of OH to the C=C bond could exist. Each reaction pathway was associated with different △H. Nevertheless, all the pathways would lead to ring splitting and yield more hydrophilic and less aromatic compounds.

1.5.5.5 Reactions between ozone molecule and NSO-aromatics

Resins and asphaltenes (NSO-aromatics) also can be oxidized by ozone due to their unnegligible reactivity towards ozone. N, S, and O have a higher electronegativity than carbon; thus, when N, S, and O form bonds with carbon, they tend to draw electrons towards themselves. This character creates an asymmetric electron distribution, which exposes both aggregated electrons and nucleus to ozone attack. Using phenanthridine as a model in Figure 1.13, the initiation takes place at the carbon next to the nitrogen atom due to a nucleophilic attachment, while the following step is driven by electrophilic addition onto the N atom due to the surrounding aggregated electrons. These steps lead to the breaking of N-C bond and finally the release of oxidized N compounds [201]. The mechanism for nitro-aromatics is analogous to that for S-containing compounds, and S will be liberated during that process in the form of SO_3.

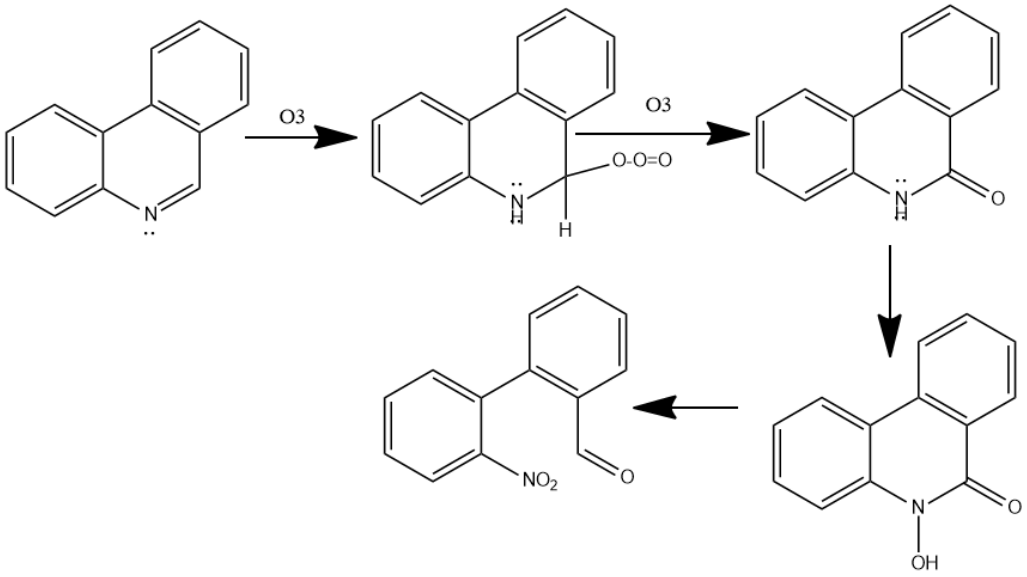

Figure 1.13. Partial pathway of ozonation of phenanthridine

1.5.5.6 Reactions between hydroxyl radical and NSO-aromatics

H abstraction could be achieved on carbon and NSO atoms when NSO atoms are attached to a hydrogen atom. The strength of the NSO-H bond relative to C-H bond dictates the preferential position for the H abstraction [187]. The general equations of the reactions can be written as follows:

$RH(NSO) + OH\cdot \rightarrow R\cdot (NSO) + H_2O$ (a)

$R(NSO)H + OH\cdot \rightarrow R(NSO)\cdot + H_2O$ (b)

The relative fraction of (a) and (b) cannot be predicted when NSO-H bond strength is unknown. In the presence of O_2, both pathways produce simpler and more oxidized compounds.

OH radical addition is also a viable scenario, and the addition could occur either on the aromatic ring or on NSO atoms. However, there is meager information on the full reaction mechanisms as to which pathway dominates and how the reactions lead to the final products. This 'shadow zone' necessitates further research.

1.6 Combining ozonation and biodegradation

As shown in Figures 1.7 - 1.13, the products (e.g., ketone, alcohol, carboxylic acids) from oxidation by ozone or the hydroxyl radical ought to be directly utilized by microorganisms without them launching the initial electron-consuming enzymatic attack. This combination can thus save microorganisms' energy and accelerate their metabolic processes. One good example comes from pairing Figure 1.1 and Figure 1.7. The ketone produced in Figure 1.7 can allow the microbes to bypass the mono-oxygenation (activation) of the alkane, and this shortcut saves the need for electrons from NADH. Comparing Figure 1.4 and Figure 1.12, it is clear that the ring cleavage involving O_2 and NADH can be outsourced to ozone. The integration of ozonation and biodegradation should be able to attain TPH reduction as well as total organic carbon removal via the relay.

1.7 The structure of this dissertation

This dissertation highlights the core research outcomes I have produced over the past five years. Much of my work involved colleagues and co-authors, and they are identified in the chapters that follow. I was the primary driver of all research presented in this document.

To provide a better overview of the dissertation, I organize the contents of Chapters 2-5 in the form of the research questions each Chapter addresses.

- Chapter 2: Does application of gaseous ozone to soil reduce TPH and produce water soluble DOC?
  - I test the ability of ozone to remove TPH and convert TPH to more water-soluble and simpler compounds on a weathered soil (BM1) in Chapter 2.

- Chapter 3: (1) How can the mass transfer of ozone in petroleum-contaminated soil be improved? (2) What are the interactions between ozone and different organic carbon fractions (TPH, SOM, and DeOC) for a more recalcitrant oil?
  - A comprehensive carbon balance on a new weathered soil (BM2) advances the knowledge gained from Chapter 2 and elucidates the interaction between O_3 and the soil matrix.

- Chapter 4: What is the effect of water content on TPH transformation and reduction during ozonation?
  - Chapters 2 and 3 focus only on air-dried soil. Therefore, I investigate the effect of moisture on the efficiency of ozonation on BM2 and BM3 soils, as wet soil is more prevalent. Chapter 4 shows that high moisture content slows ozonation, but some moisture is necessary.

- Chapter 5: (1) Does the sequence of ozonation and biodegradation (pre- versus post-ozonation) affect the overall TPH removal? (2) What synergies exist between ozonation and biodgradation of TPH contaminated soils, for both TPH and DOC removal?

- Chapters 2, 3, and 4 lay the groundwork for applying ozone effectively. Here, I pursue the theme of optimizing the integration through a multi-stage strategy with alternating ozonation and biodegradation. With pH and moisture optimized, I assess pre-ozonation versus post-ozonation on TPH removal efficiency and TPH mineralziation for a readily biodegradable oil and a more recalcitrant oil.

Chapter 6 summaries the major take-home lessons from Chapters 2-5 and highlights the path forward.

CHAPTER 2. OZONE ENHANCES BIODEGRADABILITY OF HEAVY HYDROCARBONS IN SOIL

This chapter was published in a modified format in *Journal of Environmental Engineering and Science*. DOI: https://doi.org/10.1680/jenes.16.00002.

Chen, T., Delgado, A.G., Yavuz, B.M., Proctor, A.J., Maldonado, J., Zuo, Y., Westerhoff, P., Krajmalnik-Brown, R. and Rittmann, B.E., 2016. Ozone enhances biodegradability of heavy hydrocarbons in soil. *Journal of Environmental Engineering and Science*, *11*(1), pp.7-17.

2.1 Introduction

Part of this section has been rearranged and merged into Chapter 1 to avoid repetition.

Liquid, gaseous, and solid-phase oxidants are plausible to add to soils either *in situ* or *ex situ*. Among the oxidants, ozone (O_3) (E^0 = 2.07 v) offers advantages compared to others, such as hydrogen peroxide (E^0 = 1.15 v) and potassium permanganate (E^0 = 1.49 v): facile delivery as a gas, relatively lower cost, a higher oxidizing potential, and generation of hydroxyl free radicals (E^0 = 2.33 v), which are even stronger oxidants than O_3 itself [180, 213]. Added as a gas, O_3 can diffuse into soil aggregates. Furthermore, soils can be reused after ozonation [214, 215], as O_3 reverts to O_2 within a short period of time. This contrasts with other gas-phase oxidants (e.g., chlorine dioxide (E^0 = 1.5 v)), which forms chlorite or chlorate as a by-product. Gas-phase O_3 should be advantageous over O_3 dissolved in water, since the O_3 concentration in the gas phase is several orders of magnitude higher than in the aqueous phase [216] and gas delivery is simpler as long as the soil has sufficient gas porosity.

Combining ozonation and bioremediation already has shown high-efficiency for accelerating the biodegradation of a range of other recalcitrant organic contaminants in soil (e.g., PAHs, substituted phenolics) [214, 215, 217-220].

Oxidation via O_3 can occur in two ways. (1) direct attack by O_3 on electron-rich bonds and nucleus centers due to its electrophilic and nucleophilic features; and (2) indirect attack by O_3-created hydroxyl free radicals (HO•) on delocalized bonds in the aromatic ring, double-bonds, and bonds

with certain non-C components. Hydroxyl free radicals (HO•) is initiated by O_3 reacting with organic molecules, inorganic surfaces or simply hydroxide ions in soil pore water [175, 221, 222]. The former pathway can break aromatic rings to produce carboxylic acids or aldehydes [175, 223, 224]. The free radicals of the second pathway, being non-selective and having a stronger oxidizing capacity than O_3 itself [222], also can attack organic molecules at saturated and ring structures and at certain non-carbon components. Free-radical attack introduces O (mainly as an –OH group), cleaves aromatic rings, and releases nitrogen or sulfur from heterocyclic compounds [225]. This free-radical attack can be especially advantageous because it is energetically powerful and acts on many chemical structures relevant to heavy hydrocarbons, such as PAHs and alkanes [225, 226]. Moreover, metal oxides in the soil catalyze the generation of free radicals from the decay of O_3 [190-193].

The structural complexity and low bioavailability of heavy hydrocarbons make them recalcitrant to biodegradation, which can make bioremediation unreliable. Integrating advanced oxidation with bioremediation is a means to increase the biodegradability and water-solubility of recalcitrant organic compounds such as humics in natural waters, PAHs, and organics in landfill leachate [180, 213, 227-232], thus allowing microorganisms to mineralize the residuals.

Previous research has addressed the ozonation of PAH model compounds, diesel-range hydrocarbons, and crude oil (up to C_{32}) in soil for biodegradation [137, 188, 193, 217, 233-238]. Wang et al. [237] reported the compositional change of the crude oil (C_{12}-C_{40}) during ozonation but aimed to totally destroy the petroleum rather than use ozone for pre-treatment to facilitate biodegradation. However, ozonation of soil containing residual petroleum hydrocarbons with carbon length from C_{12} to C_{40} and higher for the purpose of stimulating biodegradation has not been broached before now. These hydrocarbons dominate the heavy residuals in weathered soil and generally are recalcitrant and toxic components.

No information is available concerning the proper dose of O_3 that gives minimal mineralization but benefit substantially subsequent biodegradation. Totally mineralizing the hydrocarbons is not cost-effective; the better strategy is to generate partially oxidized products that can be readily

mineralized by more economical biodegradation [239]. Since O_3 is a disinfectant, ozonation can affect the indigenous microorganisms [213], and this may require post-ozonation bioaugmentation to recover the microbial community structure. Therefore, it is important to assess the degree to which the indigenous microorganism can withstand ozonation.

Here, we systematically 1) evaluate the degree to which partial oxidation of residual hydrocarbons using O_3 can lead to chemical structures that are readily biodegradable; 2) determine a benchmark O_3 dose that balances between the desired outcome (conversion to biodegradable products) versus the undesired outcome (total mineralization by O_3) using various indicators: BOD_5, DOC, SCOD, and TOC; and 3) assess the viability of soil bacteria and evolution of the microbial community during biodegradation post ozonation.

2.2 Materials and Methods

2.2.1 Soil characterization and preparation

The test soil (BM1) was a homogenized mixture of 4 soils that had been contaminated with petroleum hydrocarbons with an API gravity of 40 and weathered on-site for many years. The test soil was classified as sandy, and the physical-chemical characteristics of the mixed soil are summarized in Table 2.1. Particle-size distribution was performed by the Weatherford Laboratory (Houston, TX, USA) using Laser grain-size analysis. we measured the pH in 1:5 (w/w) soil/water mixture with a Thermo Scientific Orion 2 Star pH probe (Thermo Fisher Scientific Inc., MA, USA) and the metal content using particle-induced X-ray emission (PIXE) [240]. The initial total petroleum hydrocarbons (TPH) concentration and total organic carbon (TOC) concentrations were 10600 (±400) mg/kg and 33±1.8 g/kg, respectively, measured with methods described below. The soil had an initial moisture content of ~18%, which tightly clumped the soil together; thus, we air-dried the soil (moisture ~1%), passed it through a 2-mm sieve to remove plant roots and rocks, and stored it at 4°C before any chemical treatments and analyses.

Table 2.1. Physical-chemical properties of the mixed soil

Parameter	Value
Sand	95% (wt)
Silt	1% (wt)
Clay	2.4% (wt)
Al	6760 mg/kg
Ca	6910 mg/kg
Fe	5790 mg/kg
K	742 mg/kg
Mg	1620 mg/kg
Mn	42 mg/kg
Na	220 mg/kg
Zn	19 mg/kg
TPH	10600±400 mg/kg
pH	7.9±0.3
TOC	33±1.8 g/kg

2.2.2 Experimental set-up for ozonation

Figure 2.1 shows the configuration for applying O_3 gas to air-dried contaminated soil. O_3 was generated using an Ozonia Triogen laboratory ozone generator (Triogen Ltd., UK) and passed through a gas humidifier (Chemglass Life Science, NJ, USA) to remove NO_x or other contaminants and to partially humidify the gas. For BM1 soil, we exposed 250 g of soil to the same ozone gas for 1.5 h, 2 h, 2.5 h, and 3 h. we also set up a 2-h oxygen-only flow control with the same amount of soil to trace any loss of TPH via volatilization. The soil was held in a 250 mL ACE glass 7166 gas washing bottle (ACE glass Inc., NJ, USA) with a glass diffusion plate at the bottom for even gas distribution. The inlet and outlet gas-phase O_3 absorbance was measured with a DR-5000 spectrometer (Hach Company, CO, USA) at a wavelength of 258 nm; we converted the absorbance to concentration using a molar extinction coefficient of 3000±30 L mol^{-1} cm^{-1}. The outlet O_3 concentration was measured for 15 min starting from 15 min after the onset of ozonation; 90 to 95%

of the input O_3 was consumed in the soil. It is possible that the fractional O_3 consumption declined later in the experiment, but it was large and stable in the first 30 minutes.

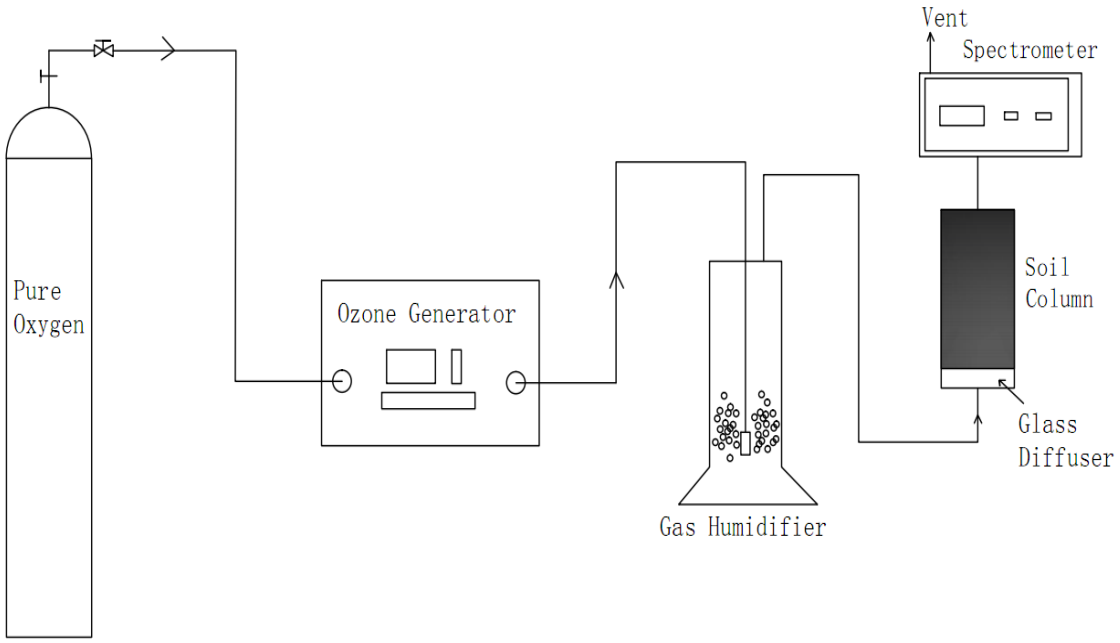

Figure. 2.1. Schematic diagram of the ozonation procedure.

2.2.3 Soluble Chemical Oxygen Demand (SCOD), Dissolved Organic Carbon (DOC), and Total Organic Carbon (TOC)

We used the extraction protocol established by Jones and Willett [241] for assaying soluble organic matter for non-treated control and ozone-treated soils. Briefly, we added 5 g air-dried and 2-mm sieved soil to 25 mL of 0.5-M K_2SO_4 (Sigma-Aldrich Co. Ltd., MO, USA) in a 50-mL centrifuge tube (VWR, PA, USA). The tubes were shaken with a standard heavy-duty vortex mixer (VWR, PA, USA) at a speed of 3000 RPM for one hour at room temperature. Then, we centrifuged the soil + water mixture at 4000 RPM for 20 min and filtered the liquid fraction through a 0.2-µm nylon membrane filter (VWR, PA, USA) to yield the soluble organic components. Extracts were stored at 4°C before assay.

SCOD was assayed using a Hach COD digestion kit (Hach Company, CO, USA) (range of 20-1500 mg/L) according to the manufacturer's instructions. We adopted the method from Kim et al. [242] for measuring DOC. We assayed organic carbon in the soil using a Shimadzu TOC Solid Sample Module SSM-5000A (Shimadzu Corp., MD, USA).

2.2.4 Bioavailable nutrients determination

We extracted ammonium and nitrate from ozonated soil and control soil with a 2M KCl at a 1:5 (w/v) soil/KCl solution ratio. To extract bioavailable phosphorus, we used the method of Pierzynski [243]. Ammonium and nitrate were measured using Hach TNT 832 ammonium and Hach TNT 836 nitrate kits, and phosphorus was assayed with a Hach TNT 844 reactive phosphorus kit (Hach Company, CO, USA).

2.2.5 Unseeded 5-day Biochemical Oxygen Demand (BOD_5)

We added 5 g of air-dried soil into 300 mL of BOD-dilution water [244] and stirred it vigorously to form a homogeneous slurry. Subsequently, we took out 5, 10, and 15 mL of the slurry and diluted each in 300-mL BOD_5 bottles to yield a 60-fold, 30-fold and 20-fold dilution, respectively. The diluent water was prepared according to the formula in USEPA BOD_5 protocol [244]. We also set up two blanks to monitor the effect of the dilution water; each dilution and blank was run in duplicate. The bottles were incubated at room temperature in the dark for 5 days. We measured the dissolved oxygen concentration (DO) with a PRO BOD YSI DO probe (YIS Inc., OH, USA) before and after the incubation and calculated BOD_5 of the soil with equation 1:

$$\mathrm{BOD}_{soil} = \frac{(DO_0 - DO_5) \times \rho \times 0.3}{5} \quad (2.1)$$

where BOD_{soil} is the BOD of the soil, g/kg; DO_0 is the initial DO, mg/L; DO_5 is the DO after 5 days of incubation, mg/L; ρ is the dilution factor, 0.3 is the volume of the bottle, L; and 5 is the mass of the soil for the slurry, g.

2.2.6 Hydrocarbon-degrading culture and seeded BOD_5

We enriched a microbial culture capable of biodegrading medium-API (30.2) crude oil. The microbial inoculum came from soil containing heavy hydrocarbons, clean top soil, and compost. The enrichment liquid was 20 mM HEPES-buffered medium containing salts, trace minerals, and vitamins as previously described [245]. The culture was grown in a 1-liter Celstir reactor (Wheaton, USA) with agitation at 30°C and was maintained in semi-batch mode.

Seeded BOD_5 was carried out to investigate whether bioaugmentation would be needed to offset the disinfecting effects of O_3 gas. The procedure for seeded BOD_5 was the same as for unseeded BOD_5, except that we added 1 mL of the enriched culture into each bottle. We calculated BOD_5 of the soil based on equation 2:

$$\mathrm{BOD}_{ss} = \frac{[(DO_0 - DO_5) - DO_{seed}] \times \rho \times 0.3}{5} \quad (2.2)$$

where BOD_{ss} is the BOD of the soil with seed, g/kg, and DO_{seed} is the DO consumed by seed, mg/L.

2.2.7 TPH extraction and quantification

We used a Gerhardt® Soxtherm automatic extractor (C. Gerhardt GmbH & Co. KG, Germany) to extract TPH and ozonation products. We thoroughly mixed 1 g of air-dried soil with 1 g of anhydrous Na_2SO_4 (Sigma-Aldrich Co. Ltd., MO, USA) to dry the soil; the moisture content of the soil samples was < 1%. TPH was extracted with 125 mL of dichloromethane (DCM). The extraction and concentration program was as follows: the temperature of the heating plate ramped up to 140°C, followed by 50 min of hot extraction and 6 intervals of concentration, with each interval lasting for 3.5 min. Then, we filtered the extract through 0.2-µm nylon membrane (VWR, PA, USA) and assayed it using a gas chromatograph (GC) (Shimadzu GC-2010) equipped with a flame ionization detector (FID) (Shimadzu Corp., MD, USA).

We measured TPH according to the guidelines recommended in USEPA method 8015d [30] and MA EPH [246]. The column and analytical conditions were as follows: chromatographic column, Restek Rxi®-1HT, 30 m x 0.25 mm I.D., 0.25 µm wall thickness; oven temperature program: initial 60°C,

hold time 1 min, ramp of 8°C/min to 290 °C, hold time 30 min; total run time: 59.75 min; sample/autosampler injection: 1 µL; carrier gas, H_2 at 3 mL/min; oxidizer, air at 400 mL/min; fuel, H_2 at 32 mL/min; Injector, AOC-20i auto injector with a SPL injection unit, injection port temperature: 285°C; and FID temperature: 315°C.

We defined TPH as the collective concentration of all hydrocarbon compounds eluting from n-nonane (C_{12}) to n-tetracontane (C_{40}). We generated calibrations for aliphatic hydrocarbons by diluting an alkane C_{12}-C_{40} standard mixture (Sigma-Aldrich Co. Ltd. MO, USA) at five or six concentrations. All compound calibrations were linear within the concentrations used. The lower detection limit of the method for aliphatic and aromatic hydrocarbons was 1 mg/L. In order to quantify TPH in contaminated soil, we obtained calibration factors (CF) from the standard calibration mixtures according to Equation 3:

$$\mathrm{CF} = \frac{\text{Area of peak}}{\text{Conc.injected (mg/L)}} \tag{2.3}$$

The concentration of TPH (mg/kg_{soil}) was calculated from Equation 4:

$$TPH = \frac{(A_x)(V_s)(D)}{(W_d)(Range_{CF})} \tag{2.4}$$

where A_x is the area count summation for TPH, V_s is the volume of extract (mL), D is dilution factor (dimensionless), W_d is the dry weight of soil (g), and $Range_{CF}$ is average calibration factor for range TPH. Our estimated concentrations were within 16% deviation from the concentrations obtained by Eurofins Lancaster laboratory.

We subtracted the area of non-TPH products identified by GC-MS when calculating TPH for ozone-treated soil. We estimated the TPH contributed by ozonation products' concentrations using the aliphatic calibration factors.

2.2.8 Products identification using GC/MS

GC-detectable and separable products of oxidation were identified by GC/MS performed at the Eurofins Lancaster laboratory (PA, USA) using an Agilent GC6890 instrument (Agilent Technologies, CA, USA) equipped with an Agilent DB-5MS column (20 m x 0.18 mm x 0.18

µm) and a mass spectrometry detector (MS) 5973 inert MSD with the HP Chemstation software (Hewlett Packard Co.,CA,USA). A scan range from m/z 35 to m/z 550 was used. The NIST11 library was used for species identification. Soil after ozonation was extracted with USEPA method 8015d [30], and 1 µL of the extract was injected into the GC/MS.

2.2.9 Microbial community analysis:

We extracted DNA from an unseeded BOD_5 test using a PowerWater® DNA isolation kit (MO BIO Laboratories, Inc., USA) according to the manufacturer's instructions. The soil used in this test had been treated with O_3 for 2.5 h. We performed amplicon sequencing of the V4 region of the 16S rRNA gene using the barcoded primer set 515F/806R in Caporaso et al. [247]. Library preparation and sequencing was performed at the Microbiome Analysis Laboratory at the Krajmalnik-Brown Laboratory in the Swette Center for Environmental Biotechnology (http://krajmalnik.environmentalbiotechnology.org/microbiome-lab.html). The library preparation was done according to the protocol from Earth Microbiome Project (http://www.earthmicrobiome.org/emp-standard-protocols/). Sequencing was performed in a MiSeq Illumina sequencer (Illumina Inc., USA) using the chemistry version 2 (2x150 paired-end).

We used the Quantitative Insights into Microbial Ecology software ((QIIME, version 1.8 [248]) for analysis of the 16S rRNA gene sequences. The obtained operational taxonomy units (OTUs) were clustered against the Greengenes database using an identity threshold of 97% by using the RDP Classifier v.2.2 algorithm [249]. We removed singletons and rarefied the OTU table to the minimum number of sequences obtained among the samples (25,485 sequences) as previously described [250].

2.3 Results and Discussion

2.3.1 Effect of ozonation on TPH in contaminated soil:

We evaluated the effect of ozonation time and dose on TPH in the soil. Figure 2.2 presents GC-FID chromatograms of the mixed soil before ozonation and after 3-h of O_3 treatment. (Chromatograms for 1.5-h, 2-h, and 2.5 h are shown in Figure 2.3). Figure 2.4 highlights that sparging with O_2 gave virtually the same chromatogram as the non-ozonated control, indicating that gas sparging did not lead to losses by volatilization. Ozonation transformed the heavy hydrocarbons (mainly from C_{16}-C_{40}) to lighter compounds, and Table 2.2 lists the identified as n-monocarboxylic acids. Liang et al. [137] observed a similar pattern for carbon chains up to C_{32} when they ozonated soil contaminated by crude oil. Figure 2.2 also shows that the unresolved "hump" decreased substantially after ozone treatment.

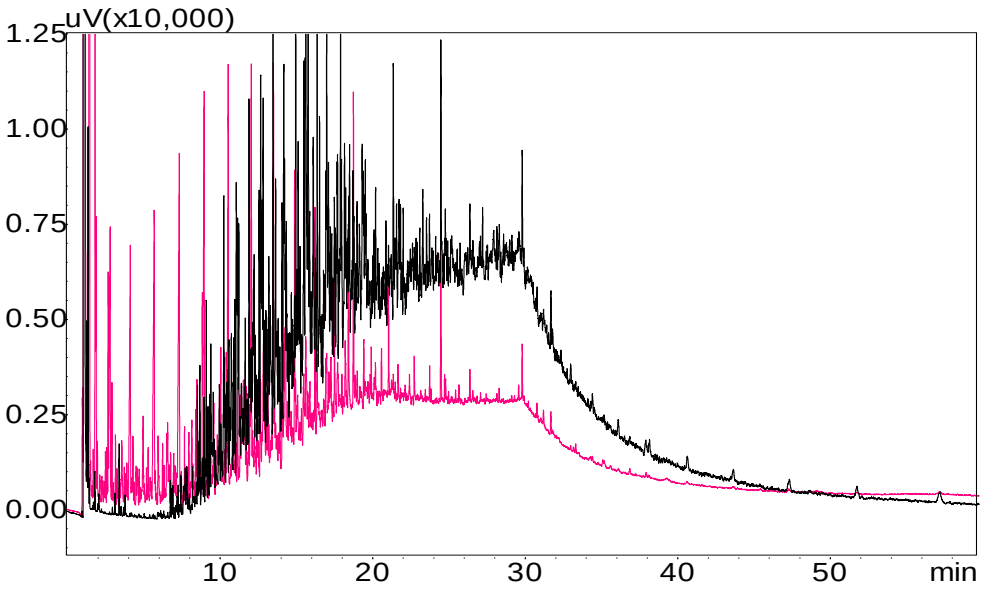

Figure. 2.2. GC-FID traces of the control soil and after ozonation 3 h. Black is the unozonated control, and pink is after 3-h of ozonation.

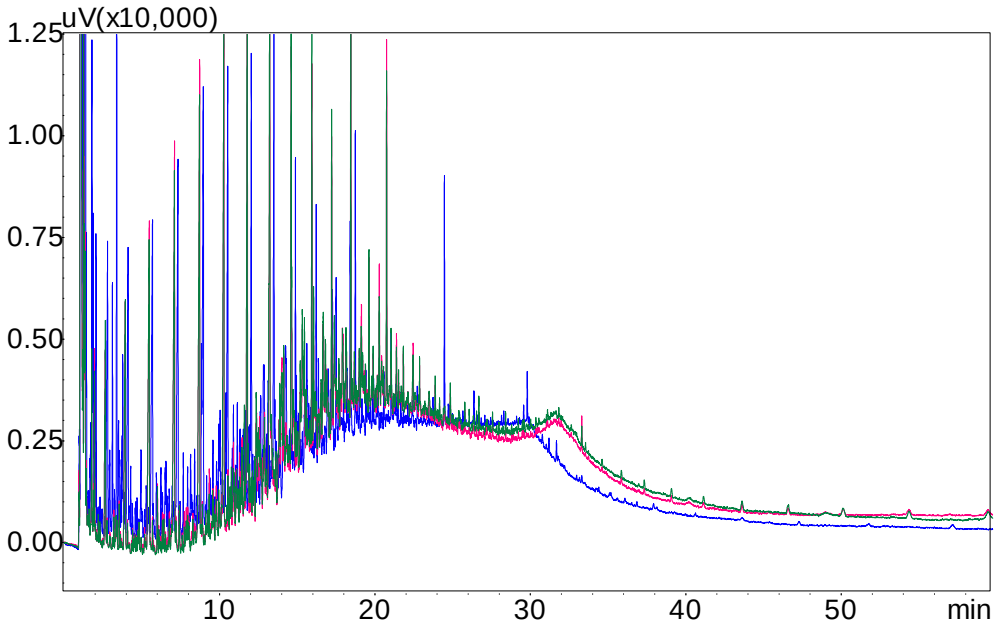

Figure. 2.3. GC-FID chromatograms of soils after ozonation for 1.5 h (green), 2 h (red), and 2.5 h (blue). Comparing these with the unozonated and 3-h ozonated chromatograms in Figure 2.3 shows the progression of towards lighter products with continued ozonation.

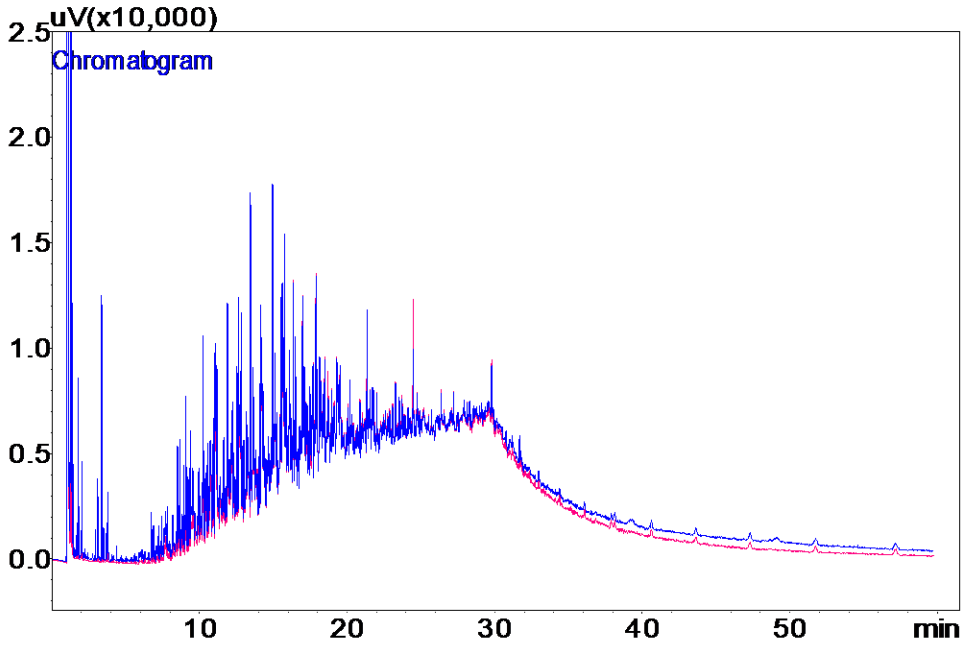

Figure. 2.4. GC-FID chromatograms of oxygen-only control soil (Blue) and non-ozonated control soil (pink). They almost overlap each other, which demonstrates no significant change occurred due to the gas flow.

Table 2.2. GC-MS identification of ozonation by-products based on retention times in the GC-FID chromatograms in Figure 2.3.

Retention time (min)	**Analyte name**
2.72	Unknown Carboxylic Acid
4.42	Hexanoic acid
5.84	Heptanoic acid
7.38	Octanoic acid
9.20	Nonanoic acid
10.54	n-Decanoic acid
12.06	Unknown Carboxylic Acid
13.70	Dodecanoic acid
15.02	Tridecanoic acid
16.29	Cyclohexane, undecyl-
17.59	Unknown
18.79	n-Hexadecanoic acid
21.07	Unknown
24.55	Unknown
29.96	Unknown

The decline of true TPH concentration after ozonation is shown in Figure 2.6. True TPH for the ozonated soil does not include the carboxylic acids; their inclusion would result in an over-estimation of TPH. For example, the carboxylic acids in the 2.5-h sample contributed ~500 mg/kg of TPH. We subtracted the mass of carboxylic acids to compute the concentration of true TPH. Declines are evident for the whole range of carbon lengths, even for the small peaks with size > C_{40}. The total TPH for the control was 10,600 mg/kg, and this value declined to 6,500 mg/kg for 1.5-h, 5,700 mg/kg for 2-h, 4,920 mg/kg for 2.5-h treatment, and 4,740 mg/kg for 3-h treatment.

The O_3 dose corresponding to each time point was computed by 20 mg/L (ozone concentration) × 5 L/min (gas flow rate) × time (min) / (10,600 mg/kg TPH × 0.25 kg soil). The O_3 doses for 1.5, 2, 2.5, and 3 h were, respectively, 3.6, 4.8, 6, and 7.2 kg O_3/kg initial TPH.

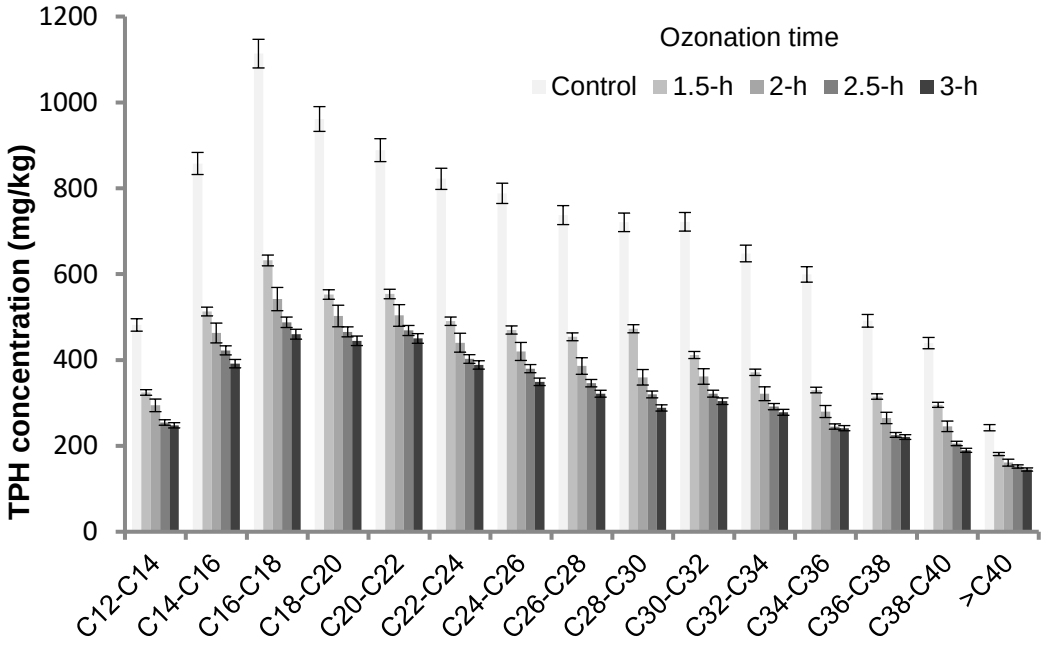

Figure. 2.5. True TPH reduction after 1.5-h, 2-h, 2.5-h, and 3-h ozonation according to carbon range. The data are averages of three replicate experiments and the error bars are standard deviations around the mean.

2.3.2 Trends in TOC, SCOD, DOC, and BOD_5 with ozonation time

Figure 2.6 summarizes how the soil's TOC, SCOD, COD, and BOD_5 changed with increased ozonation. The 12% decline in TOC – a loss of 4.1 g/kg from 33.0 g/kg – roughly corresponded to the TPH reduction and illustrated that ozonation gave only a small amount of mineralization. SCOD and DOC increased substantially with ozonation up to 3 h, showing the profound impacts of partial oxidation of making the hydrocarbons more water soluble. SCOD increased from an initial value of 0.7 gCOD/kg to as high as 23.3 gCOD/kg with 3-h ozonation, while DOC rose from 0.28 to 7.7 gC/kg. Increases in BOD_5 mirrored the trends with SCOD and DOC: more than a 4-fold increase, from 2.4 to 10.5 gBOD_5/kg.

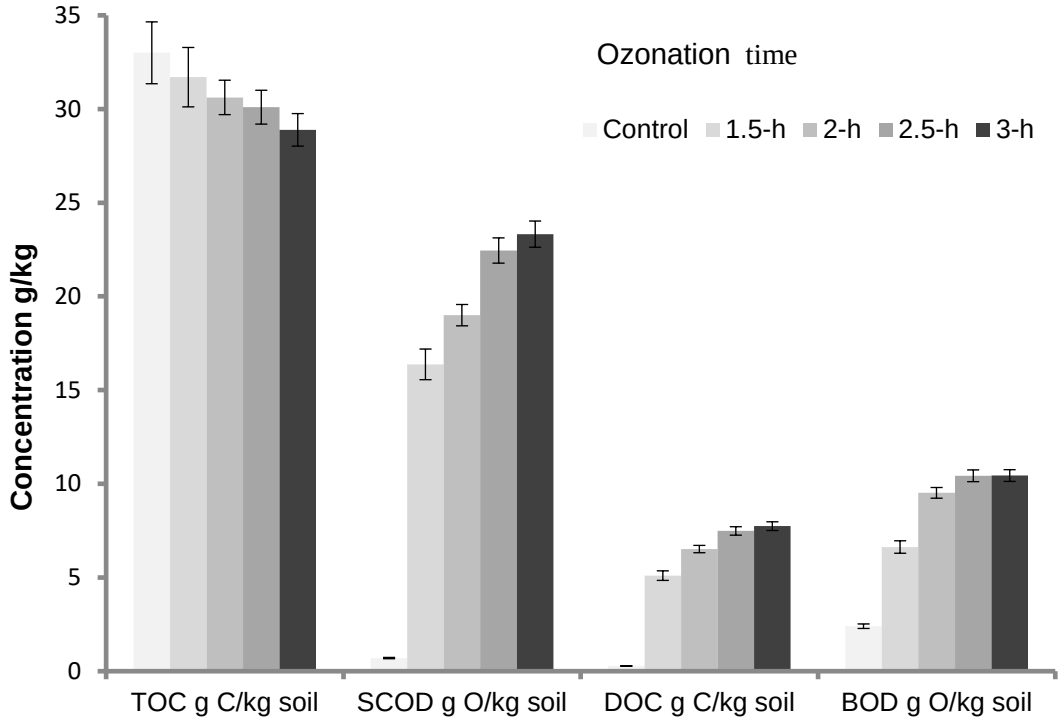

Figure. 2.6. Concentrations of TOC, SCOD, DOC, and BOD_5 with increasing ozonation time. Each TOC, SCOD, and DOC bar is the average of three replicates. The BOD_5 bars are the average of 6 replicates (three dilution factors with each duplicate). Error bars are standard deviations around the mean.

The large increments in SCOD, DOC, and BOD_5 were directly related to the formation of carboxylic acids, although other water-soluble, partial-oxidation products were important, since the increase in DOC (7.4 gC/kg) was much higher than the DOC concentration of carboxylic acids (about 0.5 gC/kg). The large increase in DOC concentration could be partially due to the oxidation of soil organic matter (SOM) [180, 251], as ozonation and free-radical attack are non-selective. The observed large increases in SCOD, DOC, and BOD_5, coupled with a small loss of TOC, is the desired outcome of ozonation, because the goal of our ozonation approach is to make the heavy hydrocarbons biodegradable, not to fully mineralize them.

SCOD, DOC, and BOD_5 started to plateau after 2.5 h of ozone treatment. As the marginal effects declined with additional ozonation, we established a benchmark O_3 dose with 2.5-h treatment = 6 kg O_3/kg TPH.

2.3.3 The release of bioavailable nutrients via ozonation:

Figure 2.7 shows that nitrate, ammonium, and reactive phosphorus concentrations increased with the duration of ozonation, with nitrate showing the largest release. Ozonation increased the nitrate from 7.5 mg/kg to 118 mg/kg after a 3-hr ozonation period, during which ammonia increased from 8 to 19.5 mg/kg. For the same ozonation conditions, reactive phosphorus increased from 1.5 mg/kg to 15 mg/kg. Releases of bioavailable N and P probably came from N- and P-containing compounds, such as resins, asphaltenes, and SOM [251, 252], although proteins and phospholipids in microorganisms could have been small sources. The large increase in nitrate probably was due to oxidation of NH_4^+ and organic N by ozonation. The release of nutrients should facilitate biodegradation and lower the need to add macronutrients to stimulate bioremediation.

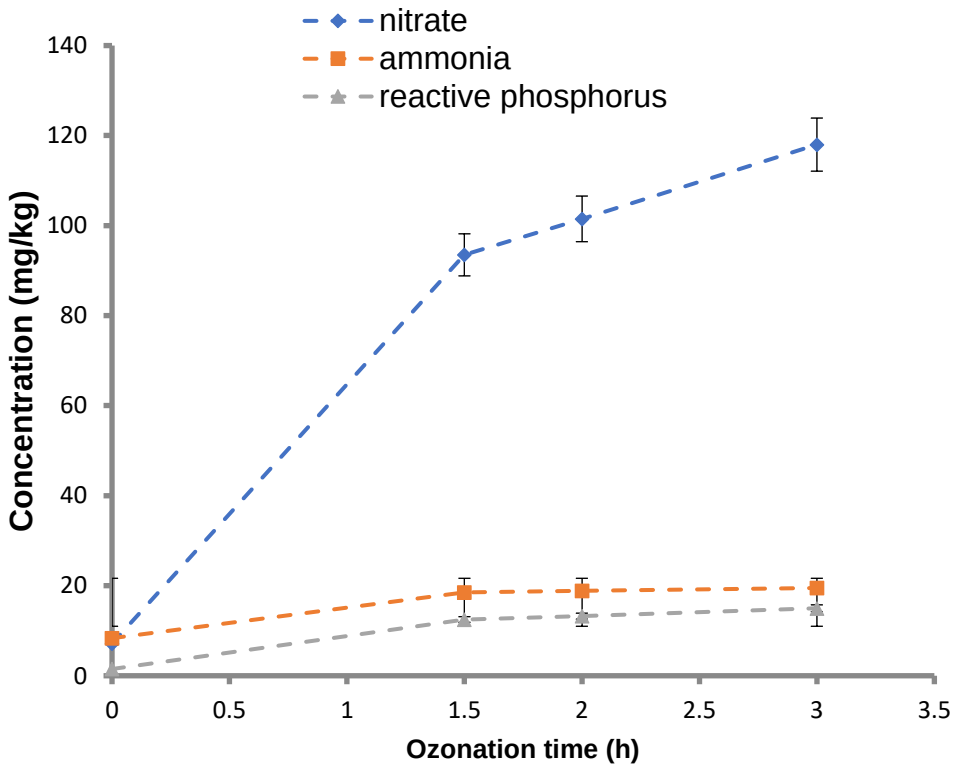

Figure. 2.7. Fate of NO_3^-, NH_4^+, and PO_4^{3-} concentrations with increasing ozonation time. NO_3^- had a large increase. NH_4^+ and PO_4^{3-} also increased, but to a smaller extent.

2.3.4 Seeded versus unseeded BOD_5

Figure 2.8 illustrates the difference between unseeded and seeded BOD_5 of soil for control and 2-h O_3-treated soils. Adding a diverse microbial seed had a negligible impact on the BOD_5 value of the O_3-treated soil (both around 9 $gBOD_5/kg$), although it increased the value of the control soil from 2.4 to 5.3 $gBOD_5/kg$. The results for the O_3-treated soil indicate that the soil retained a substantial microbial community capable of biodegrading the water-soluble and biodegradable products of ozonation. Thus, bioaugmentation was not necessary and offered no advantage after ozonation in this case. For the control soil, the increase in BOD_5 was related to the fact that we used an inoculum previously enriched with petroleum-hydrocarbon degraders. Adding enriched hydrocarbon degraders had a significant beneficial impact only when the heavy hydrocarbons were not made more biodegradable by ozonation.

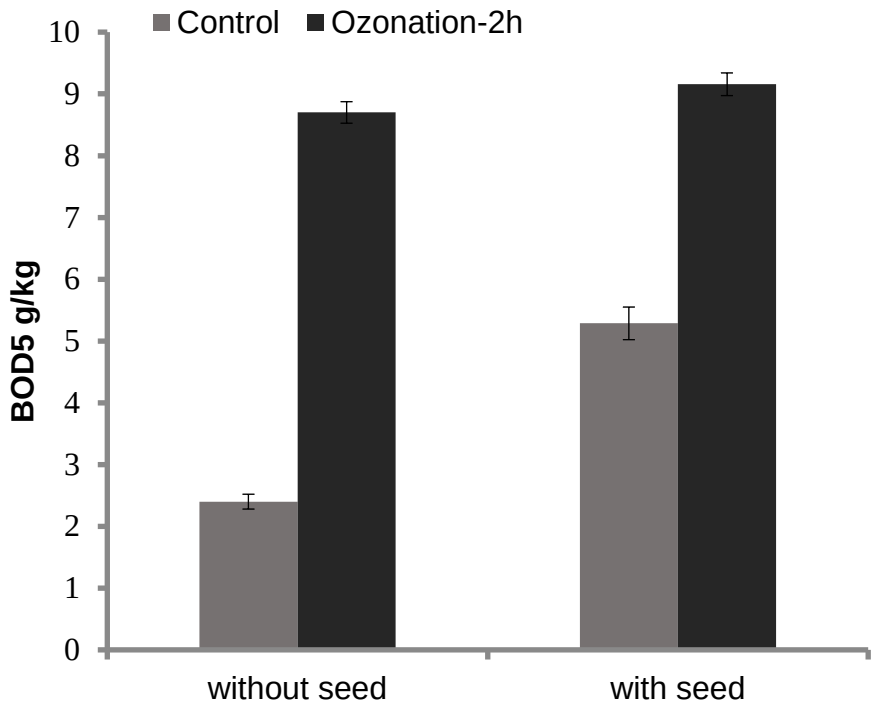

Figure. 2.8. BOD_5 concentrations with and without seed for control and 2-h O_3-treated soil. The data are averages of 6 replicates (three dilution factors with each duplicate), and the error bars are standard deviations around the mean.

2.3.5 Bacterial community structure during unseeded BOD_5 experiments:

Figure 2.9 shows the bacterial community structure at the genus and family levels for day 0 (immediately after O_3 treatment), day 3, and day 5 during a non-seeded BOD_5 test. At the genus level, *Pseudomonas* was the most abundant phylotype in the microbial community in the beginning, followed by *Sphingomonas*. Both genera naturally exist in petroleum-contaminated soil (also in non-contaminated soil) and are capable of biodegrading crude oil components, including alkyl aromatics, n-alkanes, and PAHs [253-256].

The bacterial community became more diverse during the BOD_5 test. *Pseudomonas* and *Sphingomonas* were gradually outcompeted, with phylotype sequences spread among *Variovorax, Methylobacterium, Phenylobacterium, Peredibacte*, and the families of *Sphingobacteriaceae, Comamonadaceae, Bradyrhizobiaceae*, and *Caulobacteraceae*. Higher diversity was most likely due to the fact that the large range of substrates produced by ozonation of the TPH, which reduced environmental selective pressure and allowed a more diverse community to thrive. *Variovorax* gradually became dominant as incubation time increased. This genus is able to biodegrade carboxylic acids [257], along with a variety of recalcitrant organics, such as atrazine, nitrotyrosine, 2,2-dithiodibenzoic acid, 3-(3,4-dichlorophenyl)-1-methoxy-1-methylurea, and acyl-homoserine lactones [258, 259]. Another potentially important strain was *Methylobacterium*, which can consume used engine oil (contains aliphatics, aromatics, and branched alkanes), aldehydes, and nitro-aromatics [260-262]. In summary, the increased diversity and changes in predominant bacterial types underscore that ozonation produced a range of products readily biodegradable by the native soil bacteria.

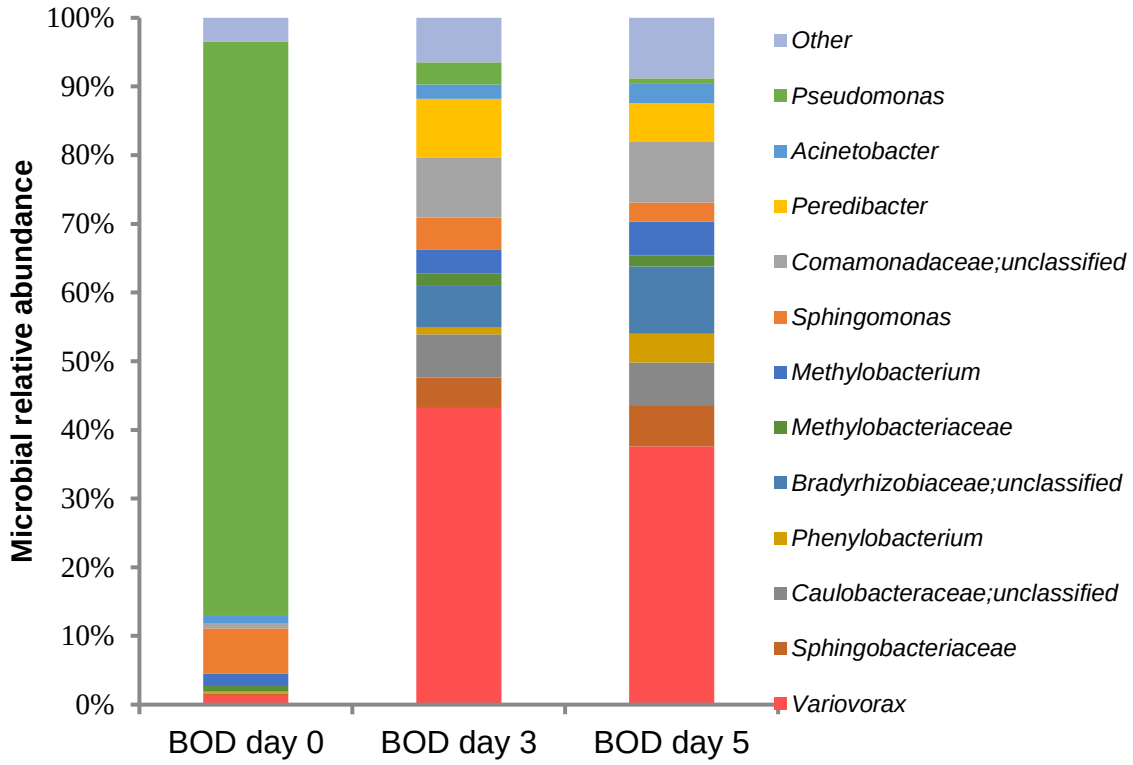

Figure. 2.9. Genus- and family-level abundances of sequences from an unseeded BOD_5 test of a 2.5-h ozonated soil. The relative abundance of a genus is defined as the number of sequences affiliated with that genus divided by the total number of sequences. Some bacteria did not give genus-level resolution, and the family level is presented instead.

Liang et al. [137] identified genes associated with the microorganism before and after the bioremediation of crude-oil-contaminated soil, but the community impact differed remarkably from our study. The microbial community recovered after ozonation during biodegradation in their study consisted mainly of *Mycobacterium*, *Pectobacterium*, *Mesorhizobium*, *Rhodopseudomonas*, *Bacillus*, *Sphingomonas*, *Rhodobacter*, *Mycobacterium*, and *Rhodopseudomonas*, most of which existed before ozonation. No species that initially was trivial was enriched during biodegradation after ozonation. In contrast, we observed strong enrichment of *Variovorax* and loss of *Pseudomonas* and *Sphingomonas* during biodegradation after ozonation. These differences reflect major differences in oil composition and composition of original microbial communities.

2.4 Conclusions

Ozonation of soil contaminated with heavy residuals of weathered petroleum hydrocarbons achieved substantial reductions in true TPH and simultaneous increases in soluble and biodegradable organics. For example, a dose of 6 kg O_3/kg TPH gave a nearly 50% decrease in true TPH, a >20-fold increase in SCOD, and a >4-fold increase in BOD_5, but with only a 12% loss of TOC. Ozonation converted TPH molecules to partially oxidized products, many identified as carboxylic acids. Bacterial seeding had a negligible effect on the BOD_5 of the ozonated soil, which means that indigenous bacteria survived and were capable of rapid biodegradation of ozonation products. DNA sequencing over the time course of BOD_5 tests showed changes in the predominant genera and increased diversity and changes in predominant bacteria, both of which underscore that the ozonation products were readily biodegradable by soil bacteria. Because ozonation transforms residual organics into oxidation products that are readily biodegradable, including organic acids, and releases nitrate and reactive phosphate, it should be able to accelerate the rate of TPH reduction during bioremediation, such as land farming, and reduce the need for external addition of large amounts of fertilizers. Coupling ozonation and bioremediation thus can be a promising means for removal of heavy petroleum hydrocarbons in the field.

CHAPTER 3. INTERPRETING INTERACTIONS BETWEEN OZONE AND RESIDUAL PETROLEUM HYDROCARBONS IN SOIL

This Chapter has been published in a modified format in *Environmental Science & Technology*. DOI: 10.1021/acs.est.6b04534

Chen, T., Delgado, A.G., Yavuz, B.M., Maldonado, J., Zuo, Y., Kamath, R., Westerhoff, P., Krajmalnik-Brown, R. and Rittmann, B.E., 2017. Interpreting Interactions between Ozone and Residual Petroleum Hydrocarbons in Soil. *Environmental science & technology*, *51*(1), pp.506-513.

3.1 Introduction

Part of this Introduction has been modified and relocated to Chapter 1 to avoid repetition.

Approaches to remediate organic contaminants in soil include thermal treatment, soil washing, chemical oxidation, and bioremediation [37, 40, 263, 264]. Using strong oxidants has gained considerable attention as a means to transform a wide range of organic molecules that are persistent due to their structures. The reactions insert O groups that increase the water solubility and biodegradability of target compounds, as has been demonstrated for PAHs, polychlorinated biphenyls (PCBs), and phenolics [188, 214, 225, 229, 239, 265-269]. The inherent recalcitrance of residual weathered hydrocarbons should be overcome when the oxidant partially oxidizes the organic compounds so that they are more soluble and biodegradable. Mineralizing the hydrocarbons by chemical oxidation is not cost-effective; instead, the partially oxidized products can be mineralized by the more economical biodegradation [239]. Thus, the goal of pre-oxidation in this context is to modify the residual hydrocarbons just enough to be biodegradable.

Combining ozonation and bioremediation already has shown good efficiency in laboratory studies for accelerating the biodegradation of a range of recalcitrant organic contaminants (e.g., PAHs, diesel range oil, substituted phenolics, COD in landfill leachate, and weathered crude oil) [137, 217-220, 228, 235, 251]. We studied the biodegradability-increasing effect of gas-phase ozonation on hydrocarbon residuals (up to $>C_{40}$) in a soil originally contaminated with crude oil of API gravity of 40 and identified an O_3 dose that increased BOD_5 and DOC [136].

In this study, we ozonated air-dried soil with much heavier and more recalcitrant crude-oil residual (API gravity of 20) than that (API gravity of 40) in Chen et al. [136]. We systematically use a carbon balance, which to our knowledge no one else has done before, to advance understanding in how ozone interacts with organic carbon in soil that contains petroleum hydrocarbons. The specific objectives of the study are to (1) determine a benchmark ozone dose, using DOC, SCOD, and BOD_5 as indicators, that enables subsequent biodegradation, but with minimal mineralization, (2) quantitatively assess how different carbon pools interact with ozone, and (3) evaluate the impacts of ozone mass transfer to the residual hydrocarbons on ozonation efficiency within the soil matrix.

3.2 Materials and Methods

3.2.1 Soil preparation and characteristics

The soil was a homogenized mixture of two sludgy soil samples (~ 20 L each) with the crude oil having an API gravity of 20 from an oil production/refinery location, an Arizona topsoil (from a local landscape material supplier, ~ 150L and with negligible hydrocarbons), and ~ 40 L of Quikcrete Playsand (The Quikreter® Companies, AZ, USA). The details of the soil preparation were described in Apul OG et al. [270]. The sludgy soils had a high silt and clay content, but the mixture was classified as a sandy loam with the physical and chemical characteristics in Table 3.1. The particle-size distribution was performed by the Weatherford Laboratory (Houston, TX, USA) using Laser grain-size analysis. The pH was measured in 1:5 (w/w) soil/water mixture with a Thermo Scientific Orion 2 Star pH probe (Thermo Fisher Scientific Inc., MA, USA), and the metal content and TKN were assayed using total acid digestion in EPA method 3051a [271] in the Soil, Plant, and Water Laboratory at University of Georgia. The TPH and TOC contents of the soil in this study -- 18000 (±600) mg/kg and 49000±800 mg/kg, respectively – are substantially higher than in Chen et al. [136]– 10600 mg/kg and 33000 mg/kg, respectively. We air-dried the soil (moisture content ≤1%), passed it though a 2-mm sieve to remove plant roots and rocks, and stored it at 4°C before conducting ozonation and other chemical and biological experiments. All the units ending with /kg are based on air-dried soil; for simplicity, we use /kg hereafter.

Table 3.1. Physical and chemical properties of the mixed soil

Parameter	Value
Sand	79.5% (wt)
Silt	5.1% (wt)
Clay	12.5% (wt)
Al	12000 mg/kg
Ca	37000 mg/kg
Fe	17000 mg/kg
K	2560 mg/kg
Mg	6900 mg/kg
Mn	200 mg/kg
Na	1400 mg/kg
Zn	37.9 mg/kg
P	330 mg/kg
S	36000 mg/kg
TKN	699 mg/kg
pH	7.9±0.3
TPH	18000±600 mg/kg
TOC	49000±800 mg/kg

3.2.2 Gas-phase ozonation of soil:

The apparatus and configuration are the same set as in Chen et al. [136], and details can be found there. The only difference was that we exposed 300 g of air-dried soil (≤1% moisture content) to a gas flow having an O_3 concentration of 10,000 ppmv (20 mg/L) and a gas flow rate of 5 L/min for 1 h, 2 h, 3 h, or 4 h. The inlet and outlet concentrations of O_3 gas were measured by an ozone monitor (Model 465M, Ozone Solutions Inc., IA, USA). The ozone dose corresponding to each time point was computed by 20 mg/L (ozone concentration) × 5 L/min (gas flow rate) × time (min) / (18000 mg/kg TPH ×0.3kg soil). The O_3 doses for 1, 2, 3, and 4 h were, respectively, 1.1, 2.2, 3.4, and 4.5 kg O_3/kg initial TPH.

To investigate the influence of gas channeling in the soil on TPH reduction, we thoroughly remixed the 300 g of soil after 2 h of ozonation and then ozonated it again for another 2 h; the control for comparison was continuous 4-h O_3 treatment.

3.2.3 Soluble Chemical Oxygen Demand (SCOD), Dissolved Organic Carbon (DOC), Total Organic carbon (TOC), Unseeded 5-day Biochemical Oxygen Demand (BOD5), Bioavailable nutrients, TPH extraction and quantification, and Products identification using GC/MS

All these analytical methods and their detection limits are elaborated in Chen et al. [136].

3.2.4 SARA analysis

Saturated, aromatic, resin, and asphaltene (SARA) fractionations in control soil and ozonated soil were performed by the Weatherford Laboratory (Texas, USA) following IP 143 (for asphaltenes) [272] and the SAR method that they developed. Briefly, 30 g of soil was extracted with dichloromethane (DCM) using a Soxhlet extractor, the SARA components were recovered by evaporating the DCM, and the recovered components were "topped" using an N-Evap at 60°C for at least 42 hours to stabilize their weight. The residual oil was then mixed with a measured volume of heptane to precipitate the asphaltene. The de-asphaltened (i.e., SAR) components then were separated into saturated, aromatic, and resin fractions using extraction into known volumes of heptane, toluene, and chloroform/methanol (78:22), respectively. All fractions were dried under nitrogen at 40°C until a stable weight was obtained. The weights of each fraction were determined by a gravimetric balance and used to calculate the percentage of each from the original sample.

3.2.5 Organic carbon mass balance before and after 3-h ozonation

We split organic carbon into four categories: TOC, DCM-extractable organic carbon (DeOC), DOC, and residual organic carbon (ROC). TOC and DOC measurements were detailed in Chen et al. [136]. DeOC was first extracted with DCM and then analyzed using the TOC solid module after all the DCM was evaporated by heating at 70°C for 2 h. ROC refers to the organic carbon left in the soil after DCM extraction, which was measured using the same TOC protocol. Remaining DOC (after DCM extraction) also was assayed using the method described above. DOC in DeOC was computed by total DOC minus remaining DOC. All carbon fractions were normalized to g C/kg soil.

3.3 Results and Discussion

3.3.1 Ozonation of TPH

We assessed how ozonation affects the TPH in soil by measuring the TPH concentration and identifying the intermediates formed during treatment. Figure 3.1 presents the TPH concentrations by carbon fraction for air-dried soil samples before and after ozonation. TPH concentrations declined roughly by one-half, with nearly equivalent reductions for each range of carbon-chain length, even for compounds with size > C_{40}. Increasing applied ozone dosages, achieved through longer durations of O_3-gas addition, reduced the starting TPH of ~18000 mg/kg to ~13000 mg/kg, ~12000 mg/kg, ~11500 mg/kg, and ~11000 mg/kg with ozone doses of 1.1, 2.2, 3.4, and 4.5 kg O_3/kg initial TPH, respectively. The relatively small additional decline after a dose of 2.2 kg O_3/kg initial TPH may have been due to the selective loss of the most readily oxidized components in the first 2 hours, poor O_3 transport to part of the TPH, or a combination. We discuss this aspect below.

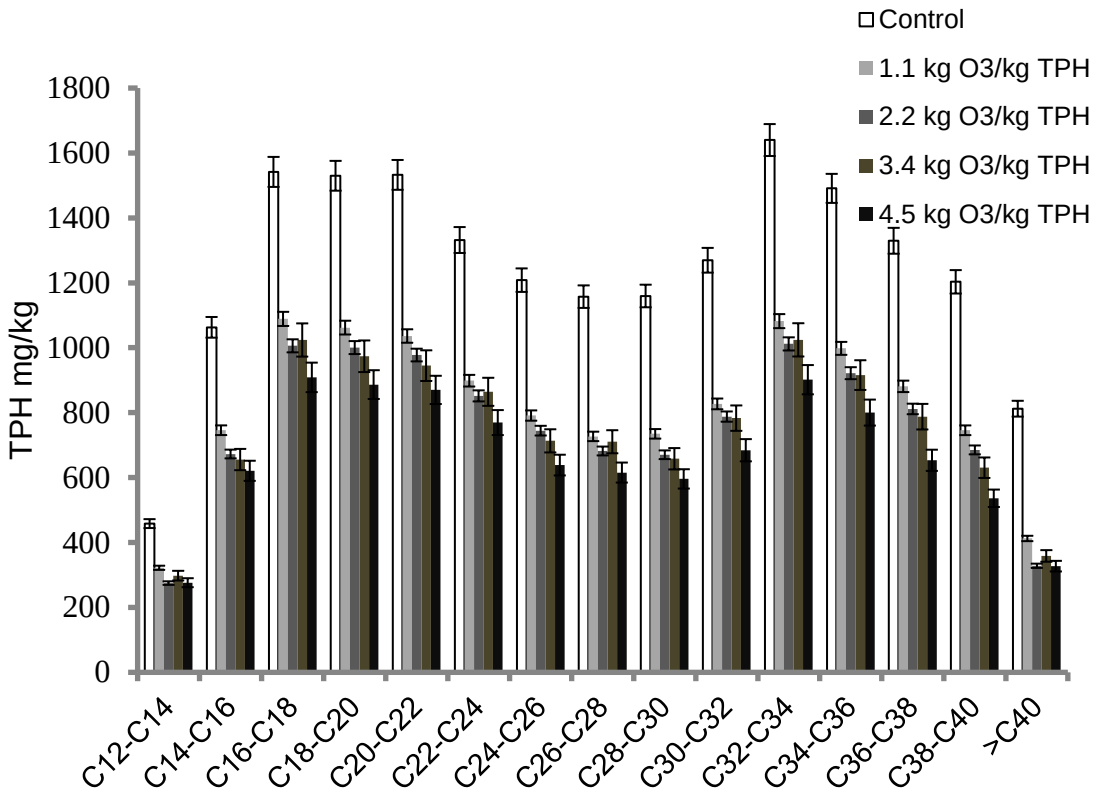

Figure 3.1. Reduction in TPH concentrations according to C-size range after applying O_3 doses of 1.1, 2.2, 3.4, and 4.5 kg O_3/kg initial TPH. The control is non-treated soil. The data are averages of three replicate experiments, and the error bars are one standard deviation around the mean.

In conjunction with the loss of gross TPH, ozonation transformed residual hydrocarbons and possible soil organic matter [180, 251] into smaller and more water-soluble compounds by inserting O groups. For example, the n-monocarboxylic acids, such as nonanoic acid and n-decanoic acid, likely were derived from *n*-alkanes[188]. Organic ozonation products tentatively identified from GC/MS outputs are compiled in Table 3.2. Most products were carboxylic acids, which are readily biodegradable. Tentative quantification of the products using TPH carbon-range calibration (by the Eurofin Lancaster Laboratory) indicated a concentration range of 30 to 500 µg/kg (noted in Table 2), with heptaonic acid having the highest concentration.

3.3.2 The effect of gas channeling

The formation of stable gas channels in the soil could result in short-circuiting and diminished mass transport of O_3 to TPH bound to the soil particles. As the gas ascends due to buoyancy and moves outward due to applied pressure, the gas forms a network of interconnected gas channels [266, 273]. Figure 3.2 demonstrates the likely negative impact of gas channeling on TPH reduction. For the same total ozonation of 4 h, remixing the soil after 2 h led to a lower final TPH concentration (~8,700 mg/kg) than continuous flow without remixing (~11,000 mg/kg), as remixing broke up channels and exposed more TPH to ozone gas. The positive impact of remixing was evident for all C sizes, including $>C_{40}$. Chromatograms comparing continuous 4-h and 2h+2h are presented in Figure 3.3, and corroborate that remixing played a positive role in reducing the hump size of the chromatograms and overcoming the plateau of TPH reduction. This finding could imply a field application related to enhancing mass transfer, such as tumbling contactor.

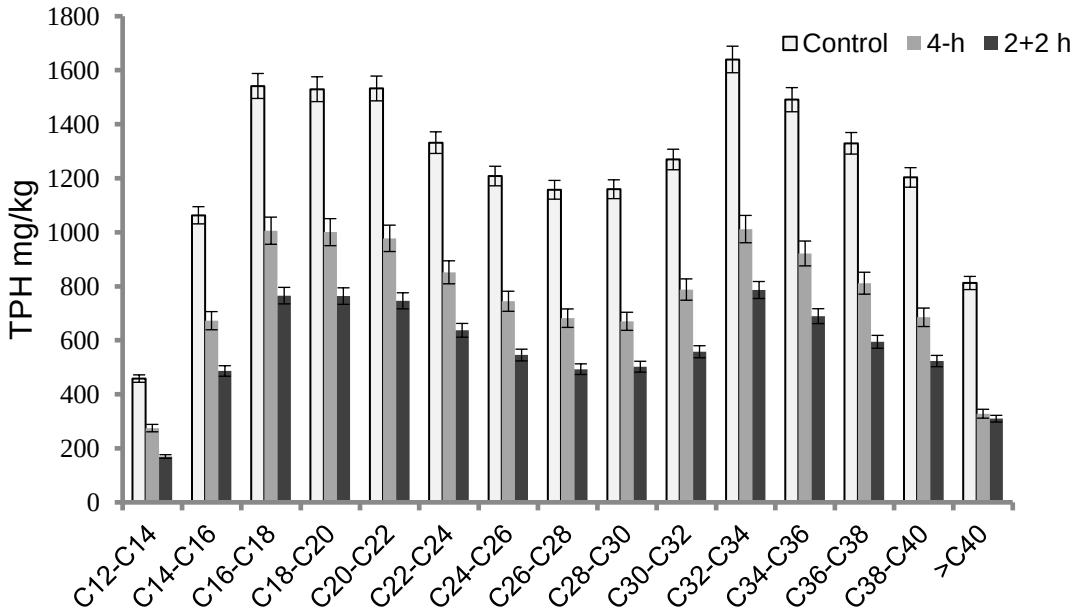

Figure 3.2. TPH concentration by carbon range for control, 4-h treated soil, and 2-h + remix + 2-h treated soil. The data are averages of three replicate experiments, and the error bars are one standard deviation around the mean. Corresponding TPH concentrations were ~18,000 mg/kg for control, ~11,000 mg/kg for 4-h treated soil, and ~8,700 mg/kg for 2h+2h soil.

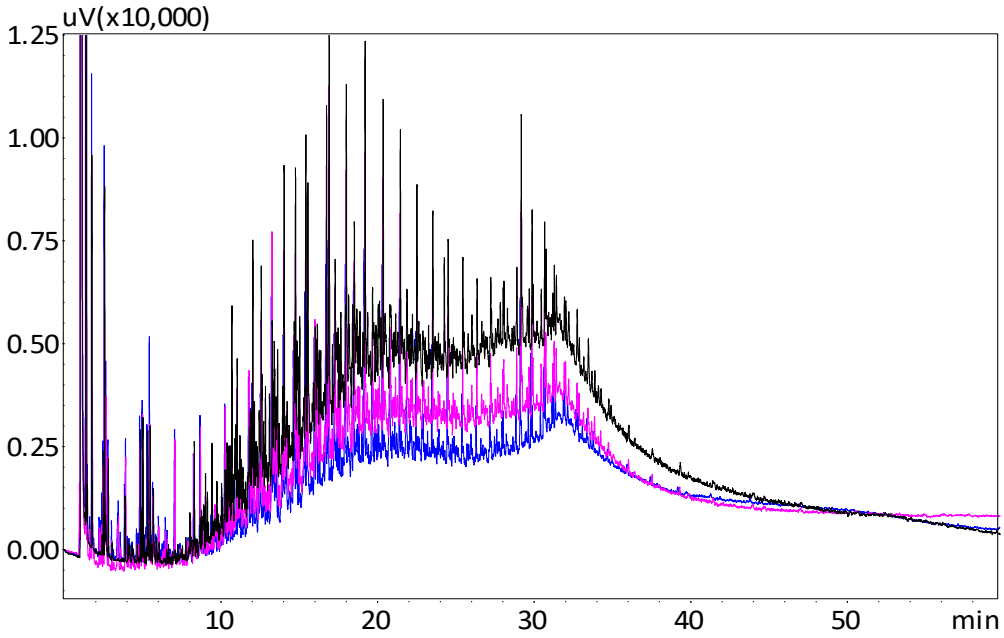

Figure 3.3. GC-FID traces for control soil (black), continuous 4-h ozonated soil (pink), and 2h+2h treated soil (blue).

3.3.3 Trends in TOC, SCOD, DOC, and BOD5 with Ozone Dose

Measures of bulk organics after ozonation provide critical information on the ability of ozone to be used as a pretreatment for accelerated bio-treatment. Figure 3.4 summarizes changes in TOC, SCOD, COD, and BOD_5 upon ozonation. Soil TOC declined by only ~10%, whereas TPH declined by ~45%. This means that TPH-extractable and GC-MS-detectable organics were transformed, rather than mineralized, because TOC would have declined by a corresponding amount if oxidation to CO_2 had occurred.

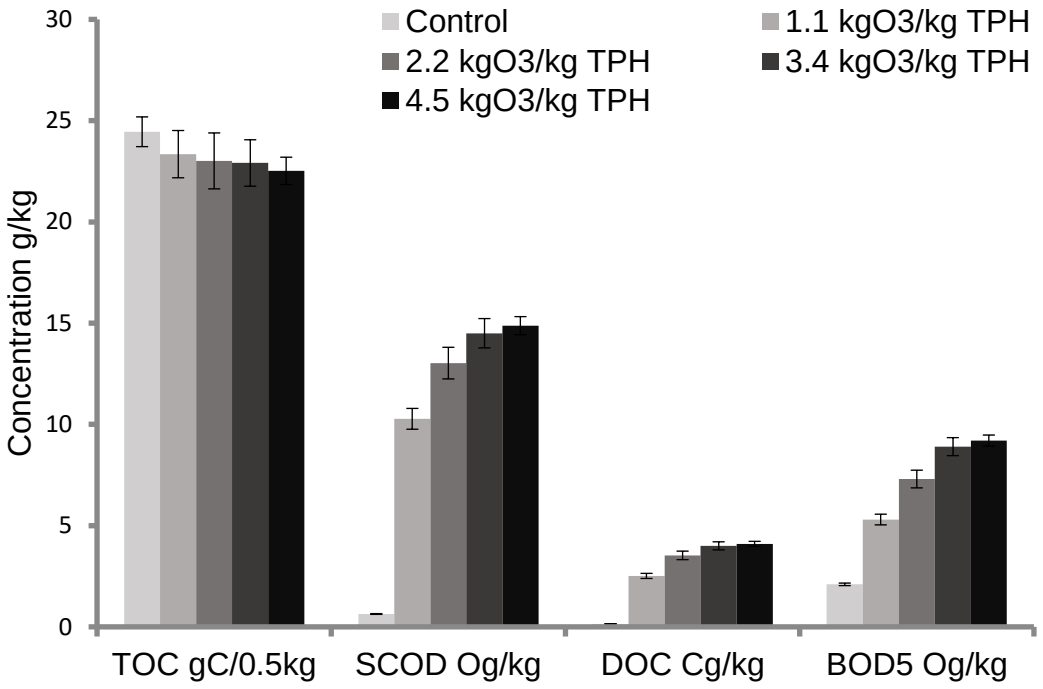

Figure 3.4. Concentrations of TOC, SCOD, DOC, and BOD_5 with increasing ozone dose (in kg O_3/kg initial TPH). Each TOC, SCOD, and DOC bar is the average of three replicates. The BOD_5 bars are the average of six replicates (three dilution factors with each duplicate). Error bars are one standard deviation around the mean.

SCOD and DOC increased substantially with ozonation, showing the profound impacts of partial oxidation making the hydrocarbons more water soluble. SCOD increased from an initial value of 0.64±0.02 gCOD/kg to as high as 15±0.4 gCOD/kg with 4.5 kg O_3/kg TPH, while DOC rose from 0.15±0.02 to 4.1±0.1 gC/kg. Because ozone and free-radical attacks are non-selective, ozonation probably oxidized a combination of TPH, the non-TPH part of DeOC, and soil organic matter (SOM), all of them being transformed into more water soluble organic matter detected as SCOD and DOC, with small losses due to mineralization [180, 251].

Much of the released water-soluble organics were biodegradable, based upon the four-fold increase in BOD_5 (from 2.1±0.1 to 9.2±0.3 gBOD_5/kg), which mirrored the trends of SCOD and DOC. The direct quantitative linkage of the increases in BOD_5 and DOC is evident by comparing the ratio of the increases. For example, the concentrations for the O_3 dose of 3.4 kg O_3/kg initial

TPH were 8.9 g BOD_5/kg soil and 4 g DOC/kg soil: thus, the ratio of ΔBOD_5 to ΔDOC, i.e., (8.9-2.1)/(4-0.15) = 1.8 g BOD_5/g DOC, matched that of the typical soluble hydrocarbon, heptanoic acids (Table 2), which has an ultimate BOD (BOD_L) to DOC ratio of 2.6 kg BOD_L/kg DOC. The experimental ratio of BOD_L-to-BOD_5 then would be 1.5 kg BOD_L/kg BOD_5, which is consistent with rapid biodegradation with synthesis of biomass [274].

SCOD, DOC, and BOD_5 started to plateau after 3.4 kg O_3/ kg initial TPH, and this parallels the trends for TPH components in Figure 3.1; the possible reason for the plateau was explained in the preceding section (Figure 3.2). From this, we established a benchmark O_3 dose of 3.4 kg O_3/kg initial TPH, which corresponds to a dose of 8.7 kgO_3/kg TPH removed.

3.3.4 Carbon mass balance

We built a carbon balance for the soil that received the benchmark dose of 3.4 kg O_3/kg initial TPH. Figure 3.5 illustrates how carbon was distributed before and during ozonation. The soil originally had a TOC of 49±0.8 gC/kg, which portioned into 59±1% DeOC and 38±1% ROC, with DOC of 0.3±0.03% included in the ROC. The missing part can be attributed to losses during extraction, evaporation, and transferring, along with measurement variability. We assumed that C was 85% of the measured TPH for both situations; this corresponds to the $C_nH_{2.1n}$. Then, the C in TPH in the control was 15.3±0.5 gC/kg and 9.3±0.4 gC/kg in the sample after ozone treatment.

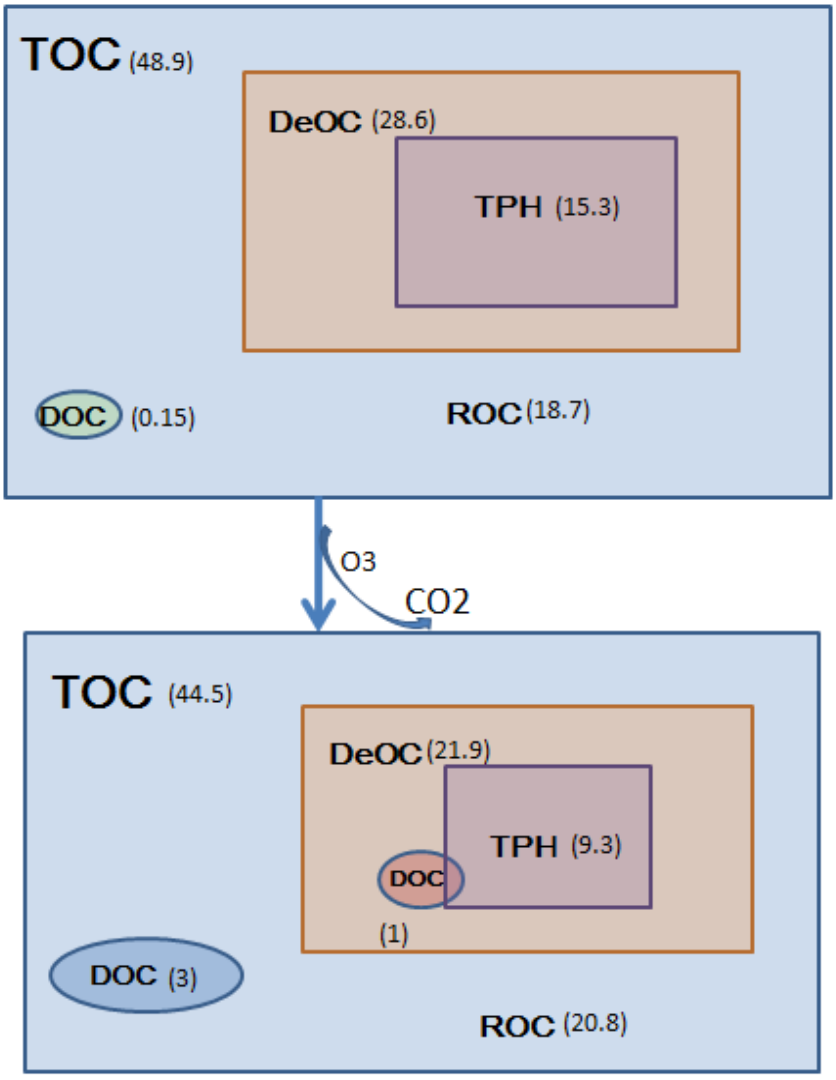

Figure 3.5. Organic-carbon distribution before and after ozonation at a dose of 3.4 g O_3/g initial TPH. TOC: total organic carbon, DeOC: DCM extractable organic carbon, DOC: dissolved organic carbon, ROC: residual organic carbon after DCM extraction, and TPH: C in TPH. Numbers in parentheses show the mass of C in grams, and the areas are proportional to the mass.

During the ozonation, carbon shifted among the different categories, i.e., TOC, DeOC, and TPH squares in Figure 3.5 shrank to different degrees, while DOC and ROC were enriched through the process. Clearly, TPH was more reactive than general organic carbon, as the TOC declined by about 9%, while TPH declined by about 45%. TPH carbon was only a modest fraction of DeOC before and after ozonation, and it declined from ~53% of DeOC to ~42% due to ozonation.

DOC not part of DeOC increased more than did DOC that was included in DeOC. This means that a portion of the original hydrophobic carbon became more polar and non-DCM-extractable, probably due to O-group insertion. Thus, part of the reduction of TPH resulted from its conversion to compounds not extracted by DCM. The slight overlap between DOC in DeOC and TPH, based on that the total estimated concentration of all identified water-soluble products in the organic phase (Table 3.2), was only about 5% of the DOC value in DeOC; this also corroborates that ozonation could lower the GC-detectable TPH in part by making these materials more polar and, thus, not detected when using GC with a column for non-polar hydrocarbons.

Although TPH was the most reactive component, O_3 reacted with all 3 categories of organic carbon (non-TPH DeOC, TPH, and ROC) in the soil, since O_3 and free radicals are widely reactive with many organic structures [175, 187, 222]. This means that the amount and reactivity of other forms of organic matter also contribute to O_3 demand, even though TPH is the target.

Table 3.2 Tentative GC/MS identification of products after 4 h of ozonation. The compounds shown are new compared to control (not treated) soil sample.

Retention time, min	Compound Name	QUAL*	Concentration**µg/kg
3.1	Butanoic acid	86	3300
3.719	Butanoic acid, 3-methy-	87	810
4.76	Pentanoic acid,4-methyl-	64	1400
5.037	Hexanoic acid	74	1800
5.548	4-methyl-hexanoic acid	74	770
5.736	Heptanoic acid	53	5200
5.86	5-Amino-3-methyl-1,2,4-oxadiazole	59	500
6.372	Octanoic acid	86	3100
6.466	Hexanoic acid,anhydride	83	430
6.954	Nonanoic acid	74	2200
7.507	n-Decanoic acid	80	800
7.525	Oxalic acid, 6-ethyloct-3-yl-isobutyl ester	64	510
8.466	Bacchotricuneatin c	90	2000
8.525	Dodecanoic acid	83	1900
8.842	Dodecanoic acid, 1-methylethyl ester	81	1400
8.889	Sulfurous acid, butyl pentadecyl ester	64	450
8.995	Tridecanoic acid	93	1230
9.877	Pentadecanoic acid	68	670
10.289	n-hexadecanoic acid	86	820
12.171	4,7,7-trimethyl-3-oxo-2-oxabicyclo[2.2.1	83	360
13.707	Pyridine-2,5-dicarboxylic acid bis-cyclo	59	420
14.489	β-iso-Methyl ionone	60	2500
14.871	Urs-20-en-16-ol	72	1300

* QUAL means quality of identification: A higher number indicates greater certainty in the identification. 100 is with absolute certainty. Only the compounds with a QUAL higher than 50 are listed.

** The concentrations are approximate and based on TPH calibration factor.

3.3.5 Evidence for oxidation of resins and asphaltenes

All SARA fractions belong to DeOC. The SARA results in Figure 3.6 show that the weight proportions of aliphatics and aromatics decreased, while resin and asphaltenes fractions increased. Liang et al. [137] also observed a decline in aliphatic and aromatics and a growth in resin during ozonation of crude-oil contaminated soil, but the asphaltenes part only changed trivially; however, they did not offer a reason of the changes in resin and asphaltenes. Oxidation of DeOC can account for the losses of aliphatics and aromatics during ozonation, as O_3 attacks unsaturated and saturated structures [188, 237]. The gains in resin and asphaltenes can be attributed to the insertion of O-groups in any SARA component, and this led to more oxygenated compounds (O_3-O_8) [275] that had increased polarity, a trend consistent with the increase of DOC in DeOC (Figure 3.5). As asphaltenes are measured as the fraction of DeOC that is insoluble in the non-polar solvent hexane, some polar oxidation products may be measured as asphaltenes even if they do not meet the structural definition. Furthermore, others have observed that free-radical-induced conjugation-addition reactions and polymerization of aliphatics and aromatics also can produce resins and asphaltenes [276-280]. In our experiments, TPH transformations that removed aliphatics and aromatics may have produced resins and asphaltenes through similar conjugation mechanisms.

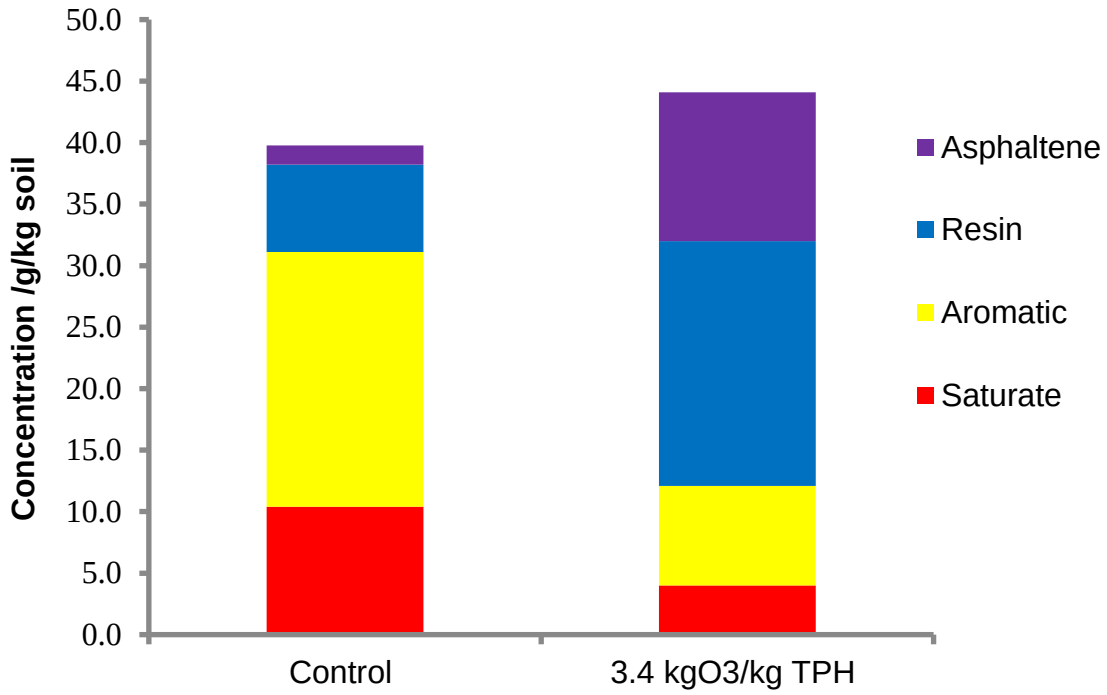

Figure 3.6. The distribution of SARA components before and after ozonation.

3.3.6 Release of inorganic nutrients and ions

Figure 3.7 demonstrates that N, S, and P bound in the residual petroleum and soil organic matter were oxidized and released as NO_3^-, PO_4^{3-}, and SO_4^{2-} during ozonation. Whereas non-ozonated soil contained ortho-phosphate of only 0.3±0.02 mg PO_4^{3-}-P/kg, soil ozonated at a dose of 4.5 kg O_3/kg TPH had ten-fold more ortho-phosphate (3.1±0.2 mg PO_4^{3-}-P/kg). Similarly, nitrate increased from 13.5±0.8 to 97.5±1.5 mgNO_3^-N/kg, while no nitrite and little ammonium (less than 0.7 mg/kg) were detected. If any ammonium was released during ozonation, it was likely oxidized by O_3 to NO_3^- [281]. Inorganic sulfur was present as sulfate, and ozonation increased sulfate from 1100±60 to 1890±90 mgSO_4^{2-}/kg. Others have observed that, when O_3 oxidizes organic compounds (model organic compounds and humic matter in soil) containing N (amines, amides, heterocyclic N) or S (thiols), inorganic ions are released as NO_3^- and SO_4^{2-}, with NH_4^+ reported as a possible intermediate [251, 281-283].

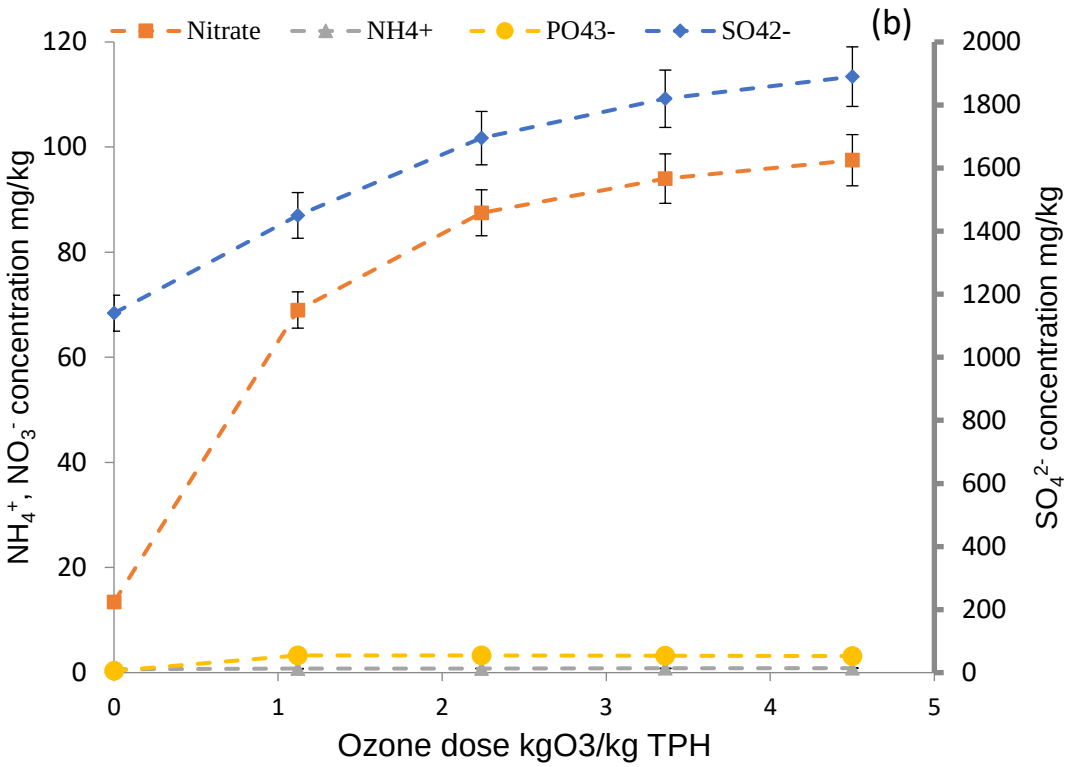

Figure 3.7. NH_4^+, NO_3^-, PO_4^{3-}, and SO_4^{2-} concentrations during ozonation. The SO_4^{2-} concentration is on the right y-axis. The error bars for PO_4^{3-} and ammonium are too small and covered by the data points.

The production and release of inorganic nutrients (NO_3^-, PO_4^{3-}, and SO_4^{2-}) should help stimulate microbial growth after ozonation. A ratio of 5 to 20 gN:gP is usually suitable to support microbial growth [85, 130, 138, 139]. The N:P ratio was 400 in the untreated soil, since the bioavailable P concentration was very small, but it became 31:1 gN:gP after ozonation. This suggests that ozonation could minimize the need for an external addition of fertilizers. Figure 3.7 also shows that most of the oxidation and release of inorganic N, P, and S was achieved at the lowest O_3 dose, and higher ozone doses resulted in relatively small incremental transformations.

3.4 Conclusion

We evaluated how gas-phase O_3 interacts with residual petroleum hydrocarbons in soil. Total petroleum hydrocarbons (TPH) were 18±0.6 g/kg soil, and TPH carbon constituted ~40% of the dichloromethane-extractable carbon (DeOC) in the soil. At the benchmark dose of 3.4 kg O_3/kg initial TPH, TPH carbon was reduced by nearly 6 gC/kg soil (40%), which was accompanied by an increase of about 4 gC/kg soil in dissolved organic carbon (DOC) and a 4-fold increase in 5-day biochemical oxygen demand (BOD_5). Disrupting gas channeling in the soil improved mass transport of O_3 to TPH bound to soil and increased TPH removal. Ozonation resulted in two measurable alterations of the composition of the organic carbon. First, part of DeOC was converted to DOC (~4.1 gC/kg soil), 75% of which was not extractable by dichloromethane. Second, the DeOC containing saturates, aromatics, resins, and asphaltenes (SARA), was partially oxidized, resulting in a decline in saturates and aromatics, but increases in resins and asphaltenes. Ozone attack on resins, asphaltenes, and soil organic matter led to the production of NO_3^-, SO_4^{2-}, and PO_4^{3-}. The results illuminate the mechanisms by which ozone gas interacted with the weathered petroleum residuals in soil to generate soluble and biodegradable products.

CHAPTER 4. IMPACTS OF MOISTURE CONTENT DURING OZONATION OF SOILS CONTAINING RESIDUAL PETROLEUM

This chapter was published in a modified format in *Journal of Hazardous Materials*

DOI: https://doi.org/10.1016/j.jhazmat.2017.11.060

Chen, Tengfei, Burcu M. Yavuz, Anca G. Delgado, Garrett Montoya, Delaney Van Winkle, Yi Zuo, Roopa Kamath, Paul Westerhoff, Rosa Krajmalnik-Brown, and Bruce E. Rittmann. "Impacts of moisture content during ozonation of soils containing residual petroleum." *Journal of Hazardous Materials* 344 (2018): 1101-1108.

4.1 Introduction

Soils containing petroleum-derived organics -- ranging from moderately biodegradable compounds, such as BTEX, to refractory residual crude oils [66, 67, 284-287] -- are widespread around the globe. Rapid remediation approaches are needed to eliminate ecosystem and health risks, while returning the soil to beneficial uses. Chemical oxidation relying on gaseous ozone (O_3) to attack residual petroleum-derived hydrocarbons in soil is being intensively studied in laboratory settings [136, 188, 214, 235, 237, 239, 266, 288, 289], as well as being executed in field tests [290-292]. O_3 is a strong and cost-effective oxidant, and it can be readily applied as a gas-phase oxidant for *in-situ* and *ex-situ* settings. Oxidation during ozonation can occur through direct O_3 attack and indirect reaction caused by free radicals generated via O_3 decomposition catalyzed by metal oxides or soil organic matters [293, 294]. Both mechanisms can generate more biodegradable and hydrophilic compounds [224] that enhance the possibility of bioremediation of recalcitrant contaminants, such as polycyclic aromatic hydrocarbons (PAHs) [239, 295], diesel fuel [236, 296], and residual petroleum [137, 297].

Our team has demonstrated that gas-phase ozonation of air-dried soil led to direct reductions in total petroleum hydrocarbons (TPH) and to the transformation of TPH to more hydrophilic and bioavailable products, such as carboxylic acids [136, 297]. Increases in soluble chemical oxygen demand (SCOD), dissolved organic carbon (DOC), and biochemical oxygen demand (BOD_5) were good indicators of the benefits of ozonation for subsequent bioremediation.

While ozonation of dry soil (<1% moisture) is possible for small quantities of soil, a three-phase (gas-water-soil) scenario is more realistic for field application. The three-phase scenario is especially important when ozone is applied in concert with bioremediation, because microbial activity depends on having a moisture content of >10% [37, 298]. The presence of water in soil has been reported to retard ozonation performance. Masten and Davies [289] found that higher moisture content led to a higher O_3 demand for PAH removal in soil. Goi and Trapido [299] similarly reported that three-phase ozonation of PAH-contaminated soil was associated with lower PAH removal and higher O_3 doses than two-phase ozonation. More recently, O'Mahony et al. [288] documented that an increase in soil water content remarkably reduced phenanthrene removal efficiency by ozonation. Parallel findings were obtained by Kulik et al. [191] and Luster-Teasley et al. [300] for PAH removal and Gomez-Alvarez et al. [301] for anthracene decomposition.

All of these moisture-related studies focused on degradation of PAHs; no information on the effects of moisture content on ozonating other crude oil hydrocarbons in soil has been published. Although PAHs are a part of crude oils, they account for less than 8% of the hydrocarbon in petroleum.[302, 303] Instead, the main constituents of residual petroleum in soils are saturates, aromatics, resins, and asphaltenes (SARA) [67].

The negative impacts of soil water can be explained by at least four phenomena. First, O_3 mass transport is much faster in the gas phase than in the water phase; thus, the accessibility of O_3 to contaminants could be limited when water occupies too much soil-pore space [191]. Second, O_3 (having a Henry's constant, H_c, of 77 $m^3 \cdot atm/mol$) can have aqueous-phase concentrations several orders of magnitude lower than in the gas phase, thus, slowing the kinetics of the reactions when O_3 dissolves into excessive water [216, 289]. Third, soil-based metal oxides (e.g., Fe_2O_3, NiO, CuO, and Mn_2O_3) can catalyze O_3 decomposition to form free radicals that are stronger oxidants than O_3 itself [177-180]; however, hydrated surfaces mask the sites for the generation of free radicals [178, 179]. Fourth, water has a large heat-absorbing capacity, which can suppress temperature increases that can accelerate all the oxidation reactions [304, 305].

Given that dry soil is rarely attainable in field conditions, in this study we performed ozonation on two types of soils with a range of relevant moisture contents (from air-dried to 20% w/w). The soils were distinctly different. One soil (BM2) had TPH ~18,000 mg/kg and oil API gravity ~20, while the second soil (BM3) had a much higher TPH concentration (~33,000 mg/kg) and had lighter hydrocarbons (API gravity of ~40). We evaluated the role of water content on TPH removal and the formation of more soluble and biodegradable products. We also report that BM3 soil smoldered without an external ignition source when the moisture content was low (<5%), although BM2 soil did not smolder. Smoldering is operationally defined as slow and flameless combustion.

4.2 Materials and Methods

4.2.1 Soil characteristics

We conducted ozonation experiments with two distinctly different soils that contained residual petroleum hydrocarbons: BM2 and BM3. Petroleum in either soil was fully weathered in the field, and the soils were air-dried before any experiments; thus, minimal volatilization of the residual petroleum hydrocarbons caused by gas flow was expected. Table 4.1 compares the physical and chemical properties of BM2 and BM3. Detailed descriptions of BM2 and soil preparation and characterization methods for BM3 can be found in Chen et al. [297] Briefly, BM2 (a sandy loam) had a TPH concentration of ~18,000 mg/kg with an oil API gravity ~20. BM3 (sand), a 50:50 mixture of two petroleum-contaminated soils from two different weathered sites, had a TPH concentration of ~33,000 mg/kg with an oil API gravity of ~40. A higher API value indicates the oil is lighter, having organics that are more volatile and likely more biodegradable. The results of full GC/MS tentative identification of the TPH compositions of BM2 and BM3 are available in Table A1.

Table 4.1. Physical and chemical properties of BM2 and BM3 soils

Parameter	BM2	BM3
Sand	79.5% (wt)	96% (wt)
Silt	5.1% (wt)	1% (wt)
Clay	12.5% (wt)	1.6% (wt)
Al	11800 mg/kg	3000 mg/kg
Ca	37400 mg/kg	3900 mg/kg
Fe	16800 mg/kg	3800 mg/kg
K	2560 mg/kg	580 mg/kg
Mg	6930 mg/kg	1000 mg/kg
Mn	208 mg/kg	50 mg/kg
Na	1480 mg/kg	130 mg/kg
Zn	38 mg/kg	50 mg/kg
P	330 mg/kg	180 mg/kg
S	36000 mg/kg	560 mg/kg
Total Kjeldahl Nitrogen	700 mg/kg	1100 mg/kg
pH	7.9±0.3	7.8±0.2
Total Petroleum Hydrocarbons	18000±600 mg/kg	**33000±500 mg/kg**
Total Organic Carbon	46000±800 mg/kg	58000±1000 mg/kg

All concentrations are normalized to air-dried soil mass.

4.2.2 Ozonation of BM2 and BM3 soils

Our experimental setup was the same as in Chen et al. [136]. O_3 gas (produced from pure O_2 using an Ozonia Triogen laboratory ozone generator) was delivered at a constant flow rate -- 5 L/min at an O_3 concentration of 10,000 ppmv -- to a soil column (20cm x 8cm) with a glass diffuser for even distribution of the inlet gas in an up-flow mode. All the experiments were carried out in a chemical fume hood.

For BM2, we mixed 300 g of air-dried soil with 15 mΩ-cm DI water to reach moisture contents (wt%) of 5%, 7.5%, 10%, 15%, and 20%. Wethen ozonated each soil (also including air-dried soil) until the TPH concentration plateaued or was below 0.1% (1000 mg/kg). During this process, we stopped the ozonation every two hours, remixed the soil, and added water to bring the moisture

content back to its original level, since exothermal reactions and gas flow evaporated some water. We also measured the TPH concentration every two hours.

For BM3, 200 g of soil was used because it has a higher TPH concentration than BM2.Weozonated the soils at 1% (air-dried), 2.5%, 5%, 7.5%, and 10% moisture contents using the same apparatus for one hour (O_3 dose: 0.9 gO_3/g initial TPH). TPH, SCOD, DOC, and TOC were measured after ozonation to determine how water content affected ozonation efficacy. We also selected 5% and 10% for extended ozonation -- 4 h (O_3 dose: 3.5 gO_3/g initial TPH) -- and established a carbon balance (described below) to understand how moisture changed the carbon distribution during ozonation.

4.2.3 BM3 smoldering and its cause analysis

Smoldering occurred at ~20 min with air-dried BM3 and 45 minutes for BM3 soil having 2.5% moisture. We stopped ozonation soon after we documented smoldering. This phenomenon was not observed for BM2 soil with any moisture content. As these experiments were carried out behind shielding in a fully functional fume hood and smoldering ended shortly after ozonation was stopped, the researchers were not exposed to any safety risk.

To gain information into the cause of the smoldering, we repeated the experiments for air-dried and 5% BM3 and monitored the temperature with a thermometer (VWR, PA, USA) embedded in the soil column at ~10 cm from the inlet. During ozonation of BM3 at 5% moisture, we collected the off-gas and had it assayed for combustible volatile organic compounds (VOCs) using EPA standard TO-15 methodology[306] at Eurofins - AirToxics Ltd. (Folsom, CA, USA).

4.2.4 TPH extraction and quantification, Soluble Chemical Oxygen Demand (SCOD), Dissolved Organic Carbon (DOC), Total Organic carbon (TOC), and Ozonation Products identification using GC/MS

We used the same methods for assaying these parameters as in Chen et al. [136].

4.2.5 Carbon distributions of ozonated BM3 soil at 5% and 10% moisture levels before and after ozonation

We assigned organic carbon into four groups: Total organic carbon (TOC), DCM-extractable organic carbon (DeOC), DOC, and residual organic carbon (ROC). TPH carbon was part of the DeOC, and TPH carbon was estimated based on the assumption of 85% of TPH being carbon [297]. DeOC was extracted with DCM and then determined using the TOC solid module SSM-5000A after all the DCM was removed by heating at 70°C for 2 h. ROC represents the organic carbon remained in the soil after DCM extraction. Remaining DOC also was extracted from the soil after DCM extraction. DOC in DeOC was calculated by total DOC subtracting remaining DOC. All carbon fractions were normalized to g C/kg dry soil.

4.3 Results and Discussion

4.3.1 Removal of TPH by ozonation with different moisture contents for BM2:

We investigated how water content affected TPH reduction with ozonation for BM2; the results are illustrated in Figure 4.1. It took 12 hours (O_3 dose: 13.3 gO_3/g initial TPH) for ozonation to reduce TPH to 0.1% for air-dried (≤1% moisture) soil, but the dose was only 11 gO_3/g initial TPH (10 hours) for soil with 5% moisture. That 5% moisture enhanced TPH removal is consistent with the interpretations of Masten and Davies [289], who attributed a similar trend to water displacing PAH in pore space and exposing more PAH to O_3. However, we see two other phenomena as having been relevant. First, 5% moisture was just sufficient to maintain the soil's physical integrity, which mitigated negative impacts of gas channeling [297]. Second, given that BM2 has a higher metal content (Table 4.1), catalytic metal ions, such as Fe(II) and Mn(II), could have dissolved into the soil solution [307], mobilized to O_3-available locations, and led to more hydroxyl radical formation [308, 309], increasing overall oxidation rate.

Water content greater than 5% yielded less TPH reduction for the same amount of O_3 supplied. In addition, at lower moisture level, it was possible to eliminate TPH with ozonation; however, at higher moisture content, even extensive ozonation with re-mixing to improve mass transfer did not eliminate the plateau of TPH at higher ozone dosages. The most likely cause was restricted O_3 mass transfer to TPH or metal oxides when too much water was present. Physical evidence supporting this interpretation is that we observed the BM2 soil self-aggregated with higher water contents, forming large soil aggregates (moisture ≤10%) and even large sticky clods (moisture >10%) that impeded the penetration of O_3 to all the TPH. This implies that an effective means to make ozonation more effective is to lower the moisture content before applying ozone. Moreover, too much water minimized a temperature rise, which should benefit oxidation rate. We examine the effect of water on temperature below.

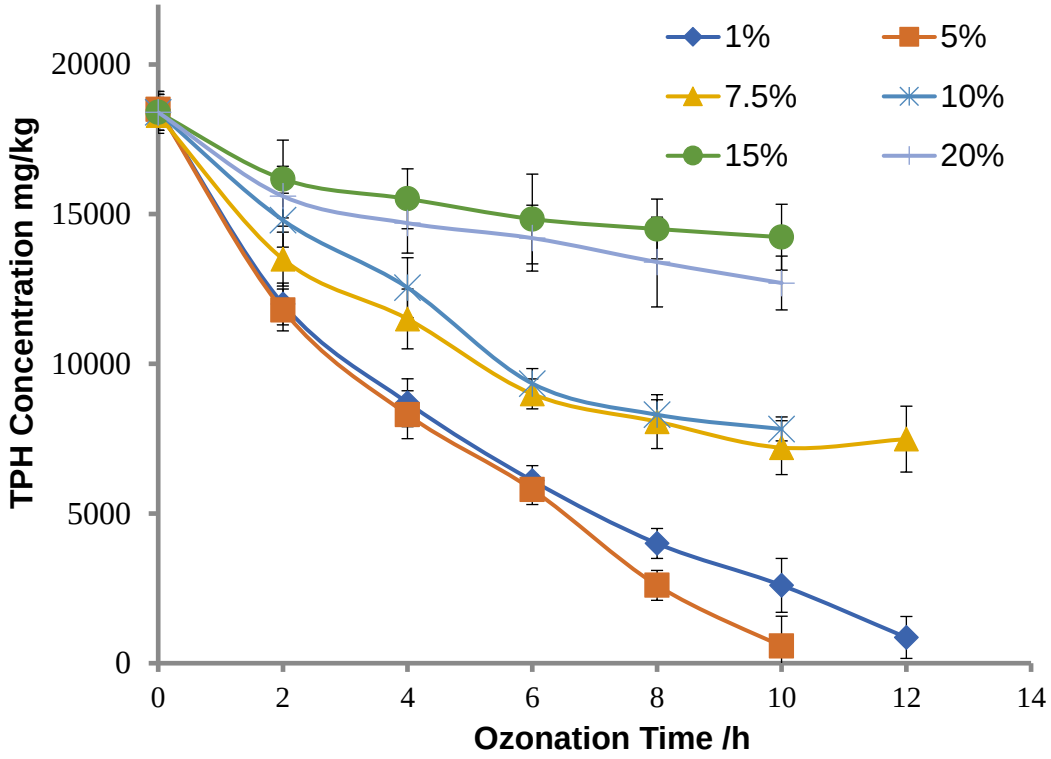

Figure. 4.1. TPH profiles over time of ozonation in BM2 soil having moisture content from 1% to 20%. At the time of sampling for each datum, we mixed the soil with added water to replace moisture loss during ozonation. Error bars represent the standard deviation around the mean (symbol) of 3 assays.

4.3.2 Different moisture contents affect the removal of TPH by ozonation for BM3

Figure. 4.2 illustrates the TPH changes and correlated effects (SCOD, TOC, and DOC) for 1-h (O_3 dose: 0.9 gO_3/g initial TPH) ozonation of BM3 at four water contents. The oxidation effect can be represented by the quantity of produced water-soluble compounds (SCOD and DOC). The trends for the four parameters clearly show that an increase in moisture content decreased the oxidation efficiency of O_3: More TPH remained in soil, and lower concentrations of hydrophilic products were generated. This observation can be ascribed primarily to the same effects observed with > 5% moisture with BM2. An elevated temperature also may contribute to the loss of TPH with lower moisture content by promoting volatilization, which we discuss below in the smoldering section.

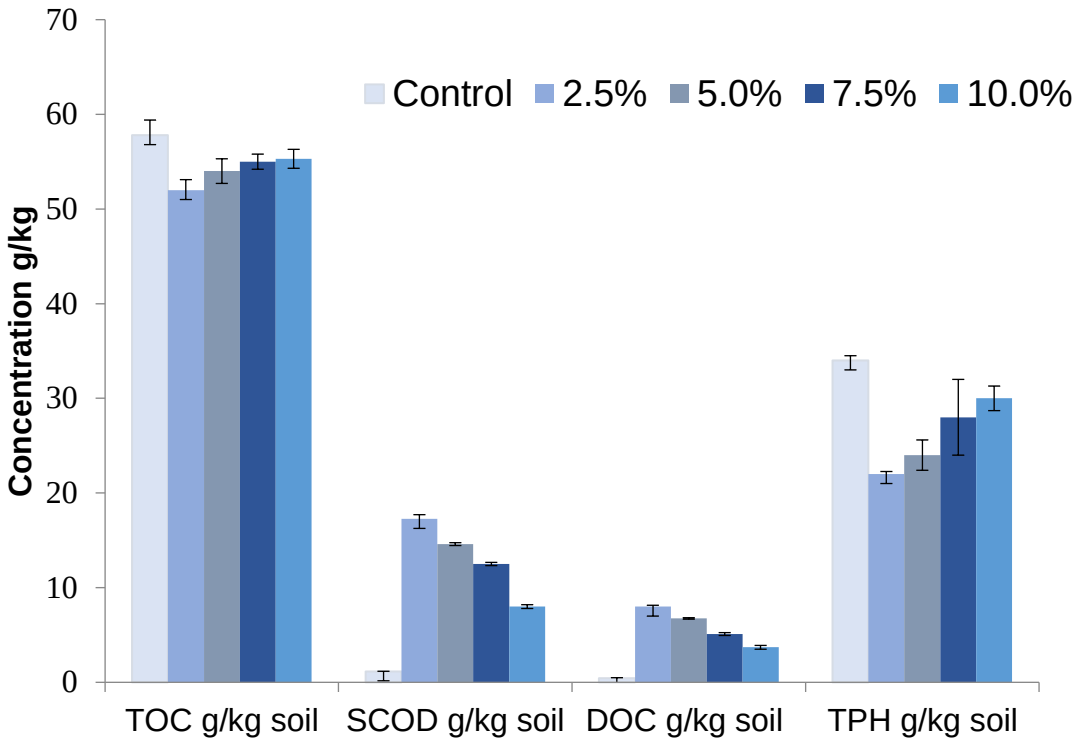

Figure. 4.2. The changes in TOC, SCOD, DOC and TPH after 1-h ozonation (O_3 dose: 0.9 gO_3/g initial TPH) at 3 different moisture contents: 2.5%, 5%, 7.5%, and 10%. The Control is BM3 soil without ozonation. Error bars represent the standard deviation around the mean (symbol) of 3 parallel measurements.

4.3.3 The difference in carbon distribution for 4-h treated samples at 5% and 10% water contents

We extended the ozonation time for BM3 soil having 5% and 10% moisture to 4 hours and then assayed carbon composition in their different pools. As visualized in Figure 4.3, the TOC (the largest box) of the non-ozonated control (top) was partitioned into 63% DeOC (28 g/kg of TPH carbon residing in it) and 32% ROC. The 5% unaccounted carbon could due to detection variability and losses through evaporation and transferring. DOC inside and outside of DeOC were negligible compared to DeOC or ROC.

Ozonation caused minimal TOC loss for the 5% and 10% moisture conditions, although the same O_3 dose of 3.5 gO_3/g initial TPH removed less TOC for 10% than for 5%. The trend was the same for DeOC and TPH, which illustrates the negative impact of soil moisture > 5%. Among these components, TPH was the most reactive with O_3, as it decreased more than DeOC and TOC.

DOC for both soils increased remarkably after ozonation, which demonstrates that substantial hydrophobic organic materials were converted into water-soluble carbon, and this observation is comparable to the DOC change with air-dried BM2 [297], indicating that ozonation created hydrophilic compounds in a manner independent of moisture content, and water merely affected the degree of oxidation, i.e., 5% moisture group gained more DOC (10.3 gC/kg) than did the 10% moisture one (8.2 gC/kg). These observations again point out that more water reduced the oxidation efficiency. The GC-MS-detectable part of the DOC in DeOC, shown by the superimposition of TPH and DOC, was comprised mostly of carboxylic acids, as listed in Table 4.2. Again, 5% moisture generated more GC-MS-detectable carboxylic acids: 1.2 gC/kg for 5%, versus 0.8 gC/kg for 10%, although the compositions were similar.

Table 4.2. Tentative identified carboxylic acids produced during ozonation for BM3

RT /min	Analyte
4.40	Pentanoic acid
5.13	Hexanoic acid
5.84	Heptanoic acid
6.47	Octanoic acid
7.06	Nonanoic acid
7.61	n-Decanoic acid
8.13	Undecanoic acid
8.62	Dodecanoic acid
9.09	Sulfurous acid, cyclohexylme
9.14	Tridecanoic acid
9.29	2-Methyl-E-7-hexadecene
9.33	Pentadecane, 2,6,10,14-tetra
9.59	Tetradecanoic acid
9.64	Cyclohexane, undecyl-
10.39	n-Hexadecanoic acid
13.17	1,3-Benzenedicarboxylic acid

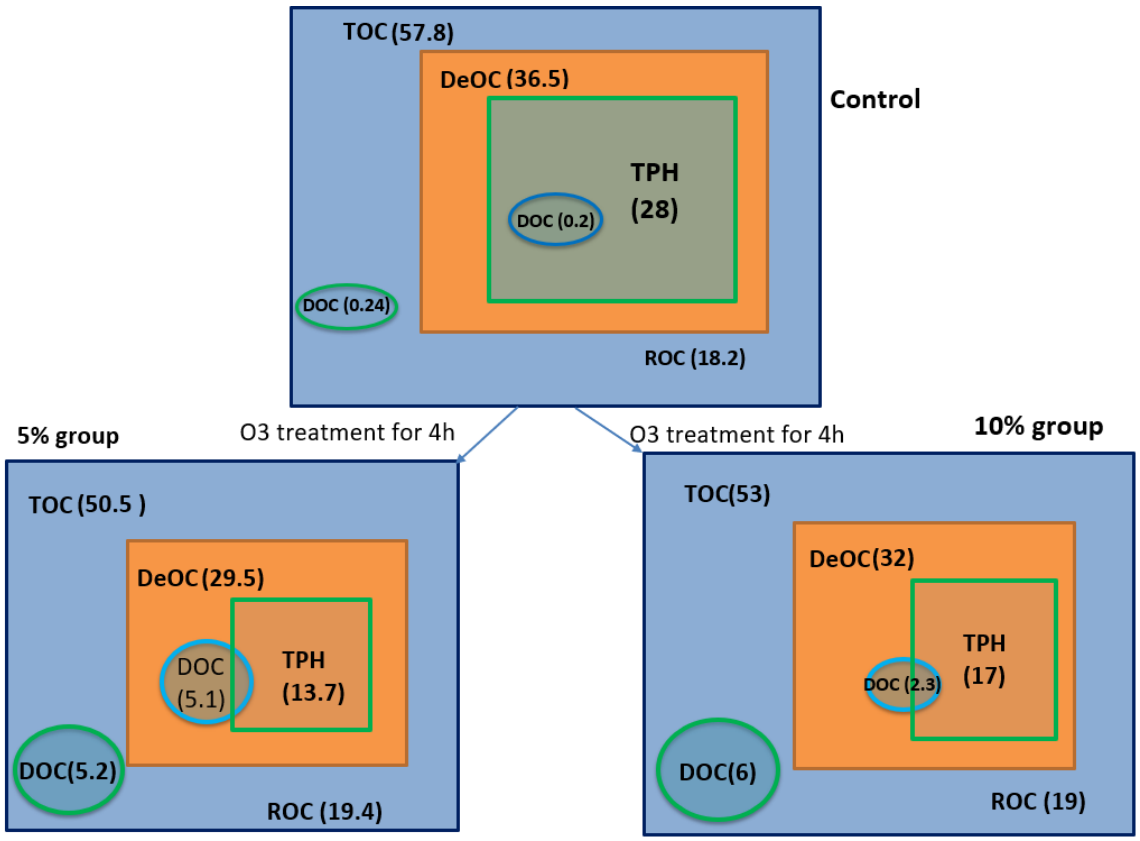

Figure 4.3. Schematic representative of the comparison of organic-carbon distributions between BM3 soil ozonated at 5% or 10% moisture content for 4 h. The top box is for the un-ozonated control, the bottom left is for the soil treated at 5% moisture content, and the right one is for the soil at 10%. Distributions of organic carbon are for the control (non-ozonated), the soil treated for 4 h at 5% moisture content, and the soil treated for 4 h at 10% moisture content. Each the large blue box represents total organic carbon (TOC) of the soil. Inside each of them are DCM-extractable organic carbon (DeOC), dissolvable organic carbon (DOC), and remaining carbon after DCM extraction (ROC). Each component is illustrated by a box or a circle with distinct color, and the size of the box indicates the relative quantity. All carbon fractions are normalized to g C/kg dry soil.

4.3.4 Smoldering and root-cause analysis

Figure. 4.2 does not show results for the air-dried (1%) soil, because the soil began smoldering at ~20 min into the 1-h O_3 treatment; the left panel of Figure. 4.4 shows a picture of the glow of the smoldering soil. After taking the picture, we stopped the treatment immediately to avoid any potential danger. The smoldering phenomenon stopped within 60 seconds of the cessation of ozonation. The soil after smoldering took on a white color (Figure 4.5).

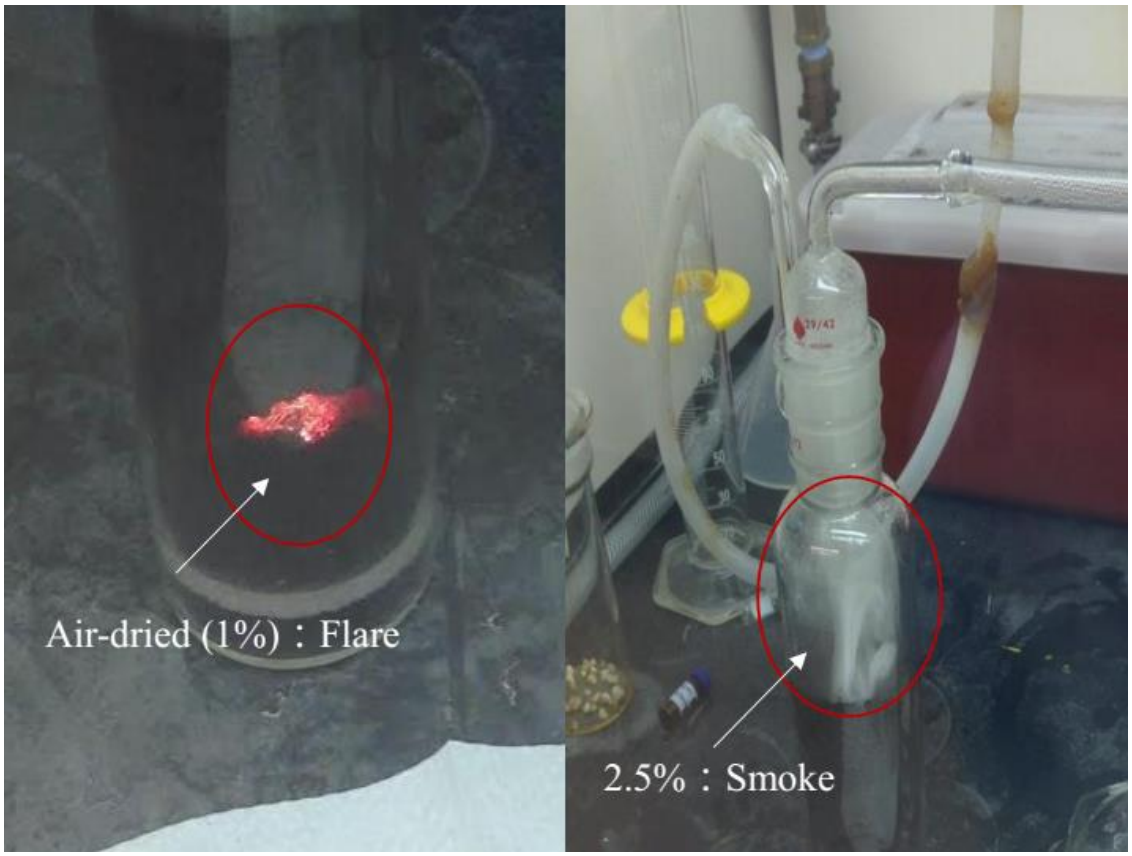

Figure. 4.4. Smoldering at 1% moisture content (left) and smoke emission at 2.5% moisture level (right) during ozonation. The experimental setups were in a closed chemical hood.

Figure 4.5. BM3 soil after smoldering. The soil took on a white color.

Although less dramatic, the BM3 soils with 2.5% moisture generated smoke near the end of the 1-h ozonation; the right panel of Figure. 4.4 shows the smoke. We let this batch run continue for the full 1 h, and its results are in Figure 4.2. BM3 soils with higher moisture contents did not show any sign of smoking or glowing during the 1-h ozonation.

Two factors contributed to smoldering in the experiments with the air-dried BM3 soil, but not in the BM2 soil.

(1) Higher TPH Concentration. The BM3 soil had a higher starting TPH (~33000 mg/kg) compared to BM2 (~18000 mg/kg). Since oxidation of organic materials during ozonation is exothermic, a higher concentration of TPH should lead to a faster reaction rate. Hence, BM3 underwent a more rapid temperature increase (shown below for a follow up experiment) that was continuous, as BM3 had TPH and other petroleum hydrocarbons throughout the experiment. The heat generated during the oxidation reaction was dictated by the enthalpy of reactants and products. We used equation (1) to calculate the two oils' enthalpies[310].

$$H_p = (0.03181T + 0.00001791K_w^{4.693})^{2.2916} \qquad (4.1)$$

where H_p is the enthalpy of petroleum, kJ/kg petroleum; T is the temperature, 23 °C; and K_w, the Watson characterization factor (dimensionless) is linked to specific gravity and mean average boiling point of the oil.

We used an empirical K_w value based on API gravity [311] to calculate H_p in Equation (1) for BM2 and BM3 oils: API gravity of 40 has a K_w of 12, and API gravity of 20 corresponds to a K_w of 10. Then, Equation (1) gives H_{pBM2} and H_{pBM3} values of 210 kJ/kg and 280 kJ/kg of petroleum.

To establish an ΔH analysis, we assumed that the petroleum had a formula of $(CH_2)_n$ (~85% carbon), where n is the number of $-CH_2-$ groups. To estimate the maximum amount of enthalpy release, we assumed that all lost TPH was mineralized.

High Value: $(CH_2)_n + nO_3 == nCO_2 + nH_2O$, $\Delta H = n(H_f(H_2O) + H_f(CO_2) - n(H_f(O_3)) - H_p) = n(-286-393-143-H_p)$ KJ/mol = $-(822n - H_p)$ kJ/mol.

To estimate the minimum enthalpy released, we assume that the lost TPH was converted to CH_2O.

Low Value: $(CH_2)_n + nO_3 == nO_2 + nCH_2O$, $\Delta H = n(H_f(O_2) + H_f(CH_2O) - n(H_f(O_3) - nH_p) = n(-110 - 143-H_p)$ KJ/mol = $-(253n - H_p)$ kJ/mol.

For BM2, the range of ΔH_{BM2} is -256.4n kJ/mol to -825.4n KJ/mol, and for BM3, ΔH_{BM3} is between -257.5n kJ/mol and -826.5n KJ/mol.

The change in TPH concentration of BM3 over any length of time of ozonation was more than twice that of BM2. For example, at 5% moisture content, ozonation for 2 h removed 15 g/kg of TPH for BM3, compared to 6 g/kg of TPH for BM2. Given 300 g of BM2 soil and 200 g of BM3 soil, the heat released for BM2 ranged from 31 kJ to 98 kJ, while it was 49 kJ to 155 KJ for BM3. These calculations indicate that, on average, oxidation of TPH in BM3 generated 35% more energy than for BM2. When normalized to the mass of air-dried soil, the energy release from BM3 (500 kJ/kg soil) was about twice that of BM2 (215 kJ/kg soil), which can be ascribed to the higher concentration and API gravity of BM3 oil. A higher API gravity corresponds to a higher enthalpy (kJ/kg TPH) based on equation (1), and a higher concentration leads to a higher soil mass-based energy. The math here is kJ/kg TPH × kg TPH/kg dry soil (TPH concentration unit) = kJ/kg dry soil.

(2) More Volatile Organics. Fuel vaporization is required for combustion [312, 313]. BM3's petroleum had a higher API gravity than BM2 oil, meaning that BM3 oil had more volatile components than BM2 oil. In particular, higher API gravity corresponds to components with lower boiling points, and it often is associated with a higher K_w [311]. Several potentially ignitable volatiles were present in the off gas from ozonation of BM3; they are highlighted in yellow in Table 3.

Increasing soil temperature leads to more volatilization of the volatile components When the soil temperature exceeds a VOC's auto-ignition point and with an O_2-rich atmosphere, combustion can commence. Furthermore, the pure-oxygen environment present in our ozonation experiments could have lowered the auto-ignition temperatures below those stated in Table 4.3, because higher oxygen partial pressure lowers the minimum ignition energy [314, 315], which reduces the auto-ignition temperature of combustibles. Kuchta and Cato [316] reported a reduction of nearly 100°C in auto-

ignition temperature of engine oil when O_2 reached 1 atm. Hence, a likely scenario is that, with the pure-O_2 conditions in our experiment, the exothermic oxidation of TPH by O_3 generated enough heat to volatilize and ignite one or more of the volatiles (Table 4.3), and the ignition released more heat, triggering a train of ensuing auto-ignitions of other VOCs with low auto-ignition points.

Table 4.3. GC/MS Tentatively identified VOCs in the off-gas during ozonation of BM3 at 5% moisture content. The yellow highlighting indicates the compounds whose auto-ignition temperatures are low enough that they may have been involved in smoldering. The auto-ignition points are at 21% oxygen level.

Tentatively identified VOCs in off-gas	Auto-ignition point/°C
Chloromethane	625
Bromomethane	535
Chloroethane	472
Ethanol	363
Acetone	465
2-Propanol	399
Carbon disulfide	90
Methylene chloride	556
Hexane	234
2-Butanone	404
Tetrahydrofuran	321
Cyclohexane	245
Benzene	560
Heptane	204
4-Methyl-2-Pentanone	460
2-Hexanone	423
Styrene	490
1,3,5-Trimethybenzene	550
Acetic acid	427
Acetaldehyde	175
Acetophenone	571
Butanol	230
2-Pentanone	452
Propanol	371
Propanoic acid	485
Formic acid	480
Benzaldehyde	192
Benzenecarbothoic acid	570
Benzoic acid	574

4.3.5 Temperature control via 5% moisture content

The first time we observed the smoldering phenomena, we did not measure the temperature, because smoldering had never occurred before for our experiments with BM2 or another soil (BM1) [136, 297]. The BM3 samples that showed smoldering were at ≤ 2.5% moisture content.

We repeated the experiments for air-dried and 5% BM3 while monitoring soil temperature. We immediately stopped ozonation for air-dried soil at the smoking point for safety reasons. We recorded temperature profiles for air-dried and 5%-moisture BM3 soil during ozonation up to 4 h, and the results are shown in Fig. 4.6. The sharp increase for the air-dried (<1% moisture) soil, up to 160°C, verifies that heat was continuously produced and accumulated, even though the inlet gas was cooled to 23°C. Within 15 minutes, the air-dried soil reached its smoking point, and we stopped the experiment. In contrast, the temperature of BM3 with 5% moisture group reached a maximum, ~46°C, in less than 3 minutes, and then it gradually declined to around ≤35°C, where it stabilized (Fig. 4.6). At the end of the 4-h dosing, the T was 33°C, and the final moisture of the soil was ~1%. (We did not add water to the soil as the gas flow evaporated the moisture.) The decline and stabilization of the soil's temperature drop were related to the slowdown in oxidation, which lowered the heat generation. The stabilization is illustrated by the TPH trend, also presented in Fig. 5, which has only small losses after 2 h.

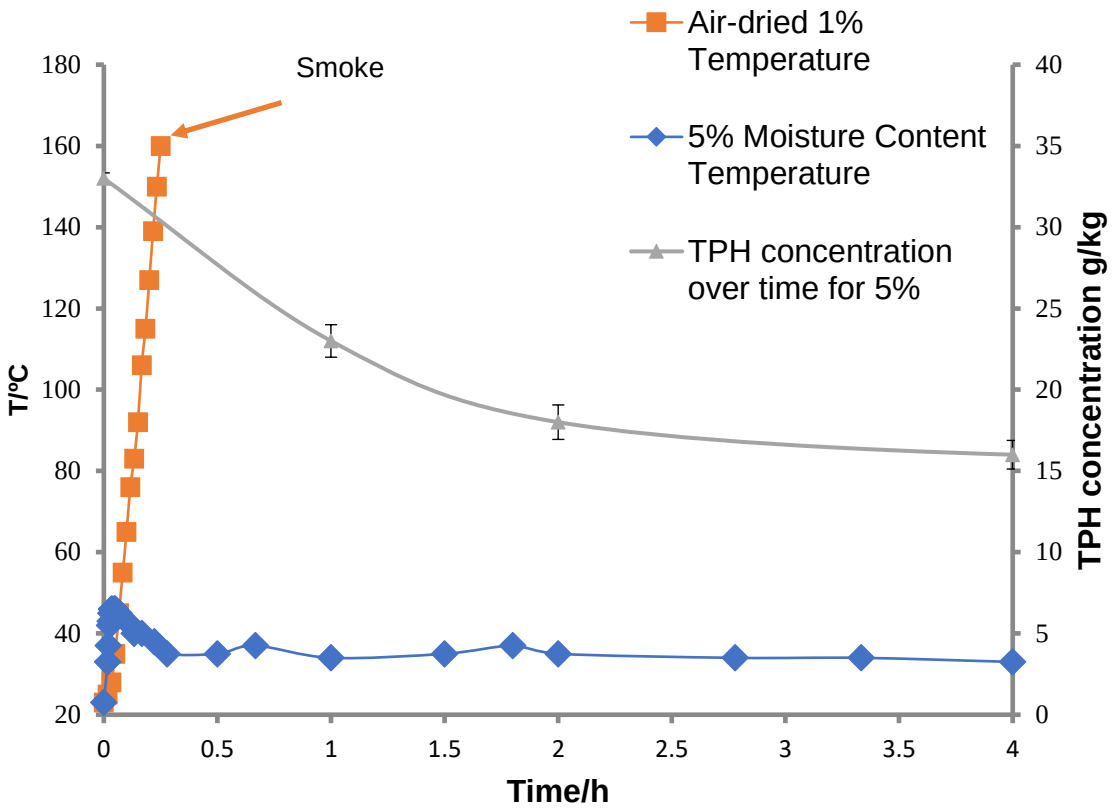

Figure. 4.6. Temperature profiles during the ozonation process for BM-3 soils at ≤1% (air-dried, red) and 5% (blue) moisture levels. The initial T (room T) was 23°C, and the final moisture content of the blue group was ~1%.

We hypothesize that the main function of moisture was to suppress the temperature rise resulting from the exothermic oxidation of organics by ozonation. Water has high specific heat and latent heat of vaporization. Low moisture content minimizes the temperature buffering effects from both mechanisms. The real field moisture varies from 1-2% (considered dry) to ~20% (*de facto* saturated), depending on the climate and the distance of the soil to groundwater. Many soils in the field will have moisture content much higher than 2.5%. Thus, we explored the effect of moisture content on temperature and quantify the energy absorbed by water.

The initial 5% moisture was able to absorb a substantial amount of the heat generated by the ozonation of TPH through its specific heat and latent heat of evaporation.

$$\Delta E = \Delta T^{*}(C_{water+soil}{*}M_{water+soil}) + M_{water}{*}L_{water} \quad (4.2)$$

where ΔE is the heat adsorbed through soil+water specific heat and latent heat of evaporation, $C_{water+soil}$ is the specific heat of water + soil, calculated by equation (3) listed below; L_{water} is latent heat of water vaporization, 2265 kJ/kg; and M_{water} is the mass of water evaporated during the process, ~10 g for the example here with 5% water in our experiments with 200 g of BM3.

$$C_{water+soil} = (C_{soil} + w\, C_{water}) / (1 + w) \quad (4.3)$$

where w is the moisture content, 5% for this example; C_{soil} and C_{water} are the specific heats of soil and water, 800J/kg°C and 4200 J/kg°C, respectively.

ΔE was ~27 kJ for BM3 with 5% moisture, and it could account for 20 to 50% of the heat released through enthalpy change (calculated above). For air-dried BM3, ΔE was only ~5 kJ. Without the addition of water, this low value of ΔE could allow the soil's temperature to increase by ≥34°C, leading to a rapid increase in temperatures that exceeded the self-ignition point for one or more of the VOCs under pure oxygen environment.

It is obvious that a higher water content leads to larger ΔE, or more energy-absorption potential by the soil. Combined with Fig. 2, our evaluation in Fig. 5 and energy computations support that 5% water content was sufficient to prevent smoldering for BM3, but it was also not too much to hinder ozonation efficiency. This implies that moisture control and temperature monitoring will be important for good efficiency and safety with large-scale application of ozone. If the oil has combustible volatiles and a high-enough oil concentration, smoldering might occur when the temperature is not constrained (e.g., by adding water or by pausing ozonation). Also, high-capacity field-scale ozone generators can be fed with air instead of pure O_2, which will lower the possibility of creating a combustion-friendly environment.

4.4 Conclusions

Our results show that, for BM2 soil, a moisture content of 5% benefited oxidation, giving the highest efficiency of ozonation for TPH removal. In contrast, higher moisture content hindered O_3 from oxidizing reactive materials in BM3 soil, which had a higher TPH concentration. This trend was documented by less TPH removal, less generation of soluble and biodegradable organic product, and a carbon balance that showed retarded carbon oxidation. An unexpected phenomenon was smoldering during ozonation of air-dried (< 1% moisture) BM3, which did not occur with the same moisture conditions for BM2. BM3 smoldered was due to its higher TPH content that led to more heat generation during the exothermic ozonation, the pure O_2 environment, and especially volatile organics with low self-ignition points. Smoldering did not occur for ≥ 5% water content, as it suppressed the temperature increase needed to volatilize the organics that initiated smoldering. The findings on smoldering underscore the importance of controlling water content during ozonation of soils containing residual petroleum and propagate the implication of safety awareness on a larger scale implementation.

CHAPTER 5. OPTIMIZATION-BASED MULTI-CYCLE OZONATION-BIOREMEDIATION TREATMENT FOR SOILS CONTAINING RESIDUAL PETROLEUM

This Chapter is in preparation as a manuscript for journal submission, and the author list will include:

Tengfei Chen, Burcu M. Yavuz, Anca G. Delgado, Brielle Januszewski, Yi Zuo, Paul Westerhoff, Rosa Krajmalnik-Brown, and Bruce E. Rittmann.

5.1 Introduction

General information on integrated ozonation and bioremediation already is in Chapter 1. Some will be added here for the manuscript.

Current field-applicable technologies for treating petroleum-contaminated soil include chemical, physical, and biological processes, which can be applied *in situ* or *ex situ*. Most commonly used are bioremediation (e.g., land farming, bioventing, biopile) [38-42], stabilization/solidification [43-45], chemical oxidation [46-48], soil washing [49, 50], and thermal (desorption, incineration) [51-54]. Even direct reuse of the soil as a road material has been reported [55, 56]. Among the technologies, bioremediation is attractive due to its relative cost-effectiveness, simplicity, and good performance in many situations [34, 57-59]. Bioremediation can remove alkanes, branched alkanes, cycloalkanes, and aromatics, and it often can achieve a regulatory treatment goal of ≤ 1% total petroleum hydrocarbon (TPH) after biostimulation or bioaugmentation [31].

Although bioremediation can be effective, it can be slow, and its efficiency depends on a suite of variables, including oxygen availability, moisture level (>10%), TPH concentration, pH (circumneutral), macro and micronutrients, salinity, and temperature [40, 67, 85]. Moreover, one challenge facing bioremediation is a 'residual TPH concentration,' or a TPH plateau at which biodegradation stops, even though biotic conditions are optimal [35, 68, 72, 73]. High residual concentrations often are associated with oils having low API gravity, which is linked to a high concentration of resins and asphaltenes and, thus, lower concentration of the more readily biodegradable hydrocarbons [71]. Poor biodegradability may be due to limited bioavailability, i.e., the microbes cannot access TPH that is very water-insoluble or resides within the soil's pores [74-76], the

inherent recalcitrance of the molecules having complex structures [77, 78], or both [68]. No matter the cause, residual TPH greater than the regulatory standard needs to be treated with more aggressive strategies to reach the cleanup goal.

Chemical oxidation relying on ozone (O_3) to remediate the soil has gained attention over the past few decades. Ozone's strong oxidizing power can help overcome the residual plateau by making the recalcitrant residuals more soluble, simpler in structure, and, thus, more biodegradable. Ozone and the hydroxyl radical (OH•), which can be produced form ozone, react with many types of hydrocarbons, but through different mechanisms. The dominant oxidation pathways for OH• are hydrogen abstraction and OH• addition [182-187]. In contrast, ozone directly attacks hydrocarbons via O_3 molecule 1,3 dipolar cycloaddition, which leads to bond breaking [161, 175, 188].

When applied prior to biodegradation, ozonation can produce soluble and biodegradable compounds to support microbial growth and activity. This pre-ozonation setting is the format used so far for integrated biodegradation and ozonation of soils containing petroleum residuals [227, 239, 317, 318]. However, post-ozonation, i.e., O_3 applied after biodegradation to reduce the residual concentration for a relatively recalcitrant oil, has not been broached. In addition, none of the studies employed sequential ozonation and bioremediation with the ozonation and bio-stimulation processes individually optimized. Furthermore, the fate of dissolved organic carbon (DOC) produced during ozonation has not been tracked. DOC with high polarity cannot be measured by GC-FID tailored for non-polar hydrocarbons [297]; therefore, only monitoring the regulated TPH does not account for the essential remediation of all the introduced carbon, as DOC could still be hazardous contaminant and always contains oxygen demand.

Here, we evaluate multiple-step treatment that alternates ozonation and biodegradation. We do the evaluation with two weathered soils containing distinctly different residual crude oils: Benchmarks 3 (BM3) has relatively biodegradable residual oil, while Benchmark 4 (BM4) has more recalcitrant residual oil. We use moisture and pH conditions to optimize each step: ≤5% water content to achieve fast O_3 reactivity. and ≥10% moisture with near-neutral pH to achieve rapid

biodegradation rate of TPH and ozonation products. The soil acidifies from production of carboxylic acids after ozonation and, therefore, pH adjustment is necessary for biodegradation.

The objectives of this study are to: (1) compare the overall TPH removal efficiencies of pre-ozonation versus post-ozonation method for both soils; (2) track the fate of all carbon pools to understand how they behave relative to TPH; and (3) understand how ozonation improves biodegradation.

5.2 Materials and Methods

5.2.1 Benchmark Soils

We carried out multi-stage ozonation + bioremediation experiments with two soils containing weathered petroleum: BM3 and BM4. Table 5.1 summarizes physical and chemical characteristics of the two soils, which were distinctly different. BM3 had a TPH concentration of 31000 mg/kg with a relatively biodegradable oil (API gravity ~40). BM4's TPH concentration (30000 mg/kg) was close to BM3, but its oil was more recalcitrant. The DCM extract of BM4 was darker than of BM3, indicating a higher asphaltene content and thus a heavier oil in BM4.

Table 5.1. Physical and chemical properties of BM3 and BM4 soils

Parameter	BM3	BM4
Soil Classification	Sand	Loamy Sand
Sand	96% (wt)	73.7% (wt)
Silt	1% (wt)	4.4% (wt)
Clay	1.6% (wt)	11.7% (wt)
Al	3000 mg/kg	7500 mg/kg
Ca	3900 mg/kg	6100 mg/kg
Fe	3800 mg/kg	9000 mg/kg
K	580 mg/kg	1800 mg/kg
Mg	1000 mg/kg	2400 mg/kg
Mn	50 mg/kg	150 mg/kg
Na	130 mg/kg	130 mg/kg
Zn	50 mg/kg	40 mg/kg
P	180 mg/kg	310 mg/kg
S	560 mg/kg	560 mg/kg
TKN	1100 mg/kg	580 mg/kg
pH	7.8±0.2	8.9±0.1
TPH	31000±500 mg/kg	30000±600 mg/kg
TOC	58000±1000 mg/kg	39000±600mg/kg

All concentrations are normalized to air-dried soil mass.

5.2.2 Ozonation setup

The experimental setup, shown in Figure 5.1, was an up-flow column containing BM3 or BM4 soil. The setup was modified from past work [136] by the addition of an anhydrate Na_2SO_4 column (for moisture removal) and the ozone monitor (to track O_3 consumption). The inlet O_3 concentration was set at a constant value (10,000 ppmv, i.e., 20mg/L), and the effluent was connected to an ozone monitor (465M, T-API, CA, USA) for real-time measurement of the O_3 concentration. The gas-flow rate was kept at 5 L/min for all ozonation experiments.

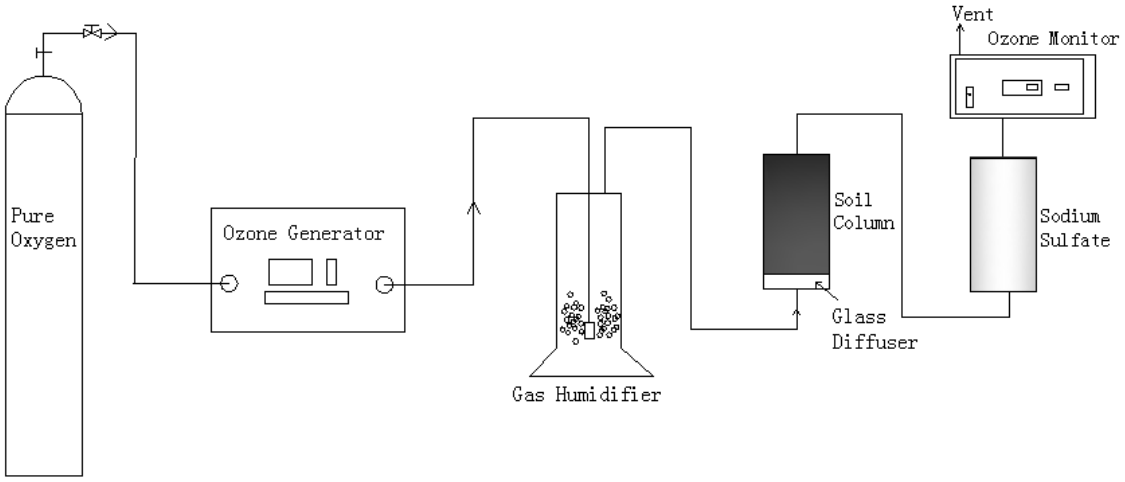

Figure 5.1. Diagram of the updated ozonation system

5.2.3 TPH, DOC, DeOC, and TOC

TPH was assayed by GC-FID for both soils. Carbon was separated into Dissolved organic carbon (DOC), dichloromethane-extractable organic carbon (DeOC), TPH carbon (TPHC), and total organic carbon (TOC). They were measured to establish carbon balances using the methods reported in Chen et al. [136, 297]. TPH is part of DeOC, and TOC contains all pools of carbon. Details of the extraction and analytical methods can be found in Chapters 2 and 3.

5.2.4 Evaluating TPH removal efficiency for BM3

We carried out three groups of multi-cycle biodegradation+ozonation experiments to assess the TPH removal efficiencies for BM3 soil: (1) biostimulation for 12 weeks (the control); (2) ozonation as pre-treatment followed by 4-week biostimulation, followed by two more cycles of the same treatment; and (3) ozonation as post-treatment at the end of week 4 of the biostimulation, followed by two more identical cycles. 1 kg of BM3 soil was used for each group. All ozone treatments were at a soil-moisture level of 5%. We applied the same O_3 mass for each ozonation experiment, which corresponded to a dose of 0.8 g O_3/ g $TPH_{initial}$, or 24 g O_3/ kg dry soil.

The biodegradation experiments mimicked land farming [319]. We placed the 1 kg of soil with pH maintained at ~7.5 (before or after ozonation) in each pan, and we tilled the soil every two days to provide oxygen and stimulate aerobic biodegradation. The soil was moistened with DI water to maintain a 10% of moisture content. The pans were covered with aluminum foil to slow moisture loss and were incubated at 30°C in the dark. To one kg of soil, we added 10 mL salt and macronutrient solution, 1 mL trace mineral A solution, 1 mL trace mineral B solution, and 10 mL of vitamin mix solution. The chemical compositions of these solutions and concentration of each reagent are provided in the Appendix.

5.2.5 Evaluating pre-ozonation versus post-ozonation for BM4:

We also performed three groups of multi-cycle biodegradation + ozonation studies to assess the TPH removal efficiencies and carbon fates for BM4 soil. All experimental conditions were the same as for the BM3 soil. Since BM3 and BM4 have approximately the same TPH initial concentration, the ozone dose, when normalized, also came to 0.8 g O_3/ g $TPH_{initial}$, or 24 g O_3/ kg dry soil.

5.3 Results and Discussion

5.3.1 Integration of Ozonation and Bioremediation for BM3

Figure 5.2 tracks the fates of TPH during the three different treatment scenarios for BM3: biotreatment only (blue diamonds), pre-ozonation (orange squares), and post-ozonation (grey triangles). The green lines are the dividers between phases.

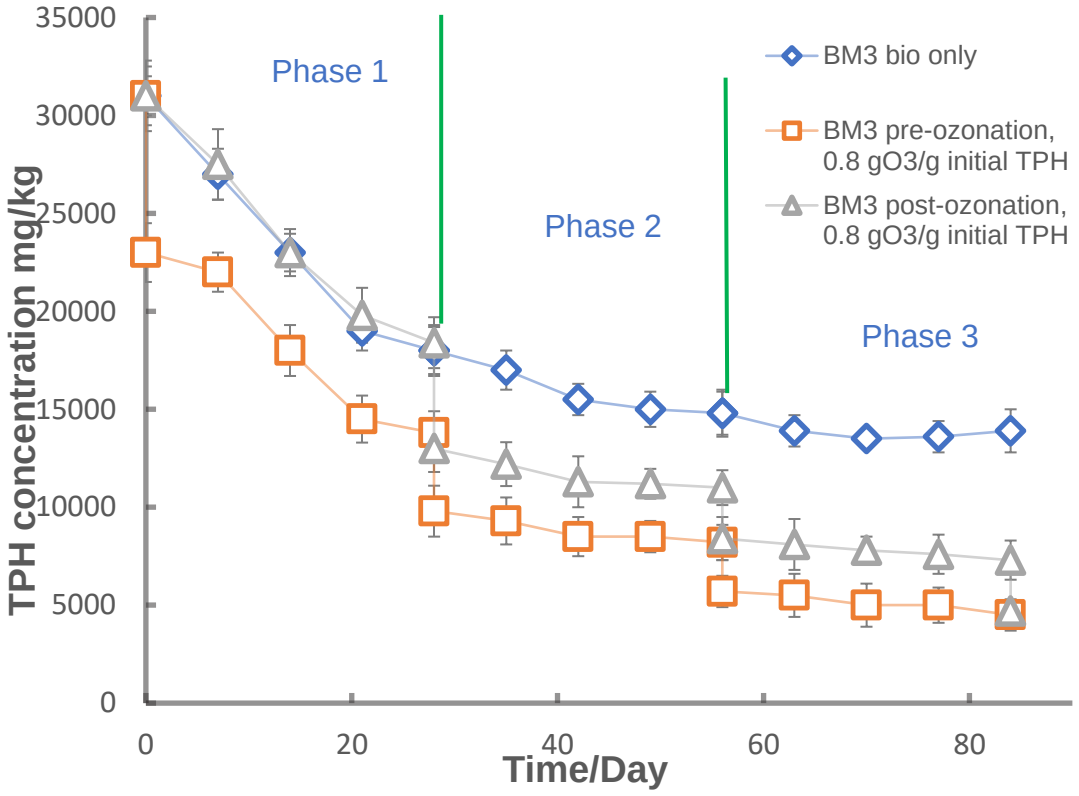

Figure 5.2. The fates of BM3's TPH for the biotreatment control (blue diamonds), pre-ozonation (orange squares), and post-ozonation (grey triangles). The 12-week experiment was divided into three 4-week phases. Each ozone dose was 0.8 gO_3/g initial TPH, corresponding to 24 g O_3/ kg dry soil. Symbols are the means of 3 replicates, and error bars are the standard deviations.

5.3.1.1 Bio-treatment of BM3

Initially, TPH-biodegradation kinetics for biostimulation alone were rapid and followed pseudo-zero-order kinetics. Fast biodegradation in Phase I likely was due to consumption of the lightest portion of BM3's TPH. However, the biodegradation rate slowed in Phase 2, and, by the beginning of Phase 3, TPH plateaued at a concentration of ~ 13500 mg/kg, which can be viewed as the non-biodegradable residual concentration [35]. Biodegradation alone did not meet the TPH regulation (10,000 mg/kg). Figure 5.3 presents that BM3's TOC and DeOC concentrations followed the path of TPH and leveled off in Phase 3 at 48.5 g/kg (declined from 58) and 27 g/kg (declined from 36.5), respectively.

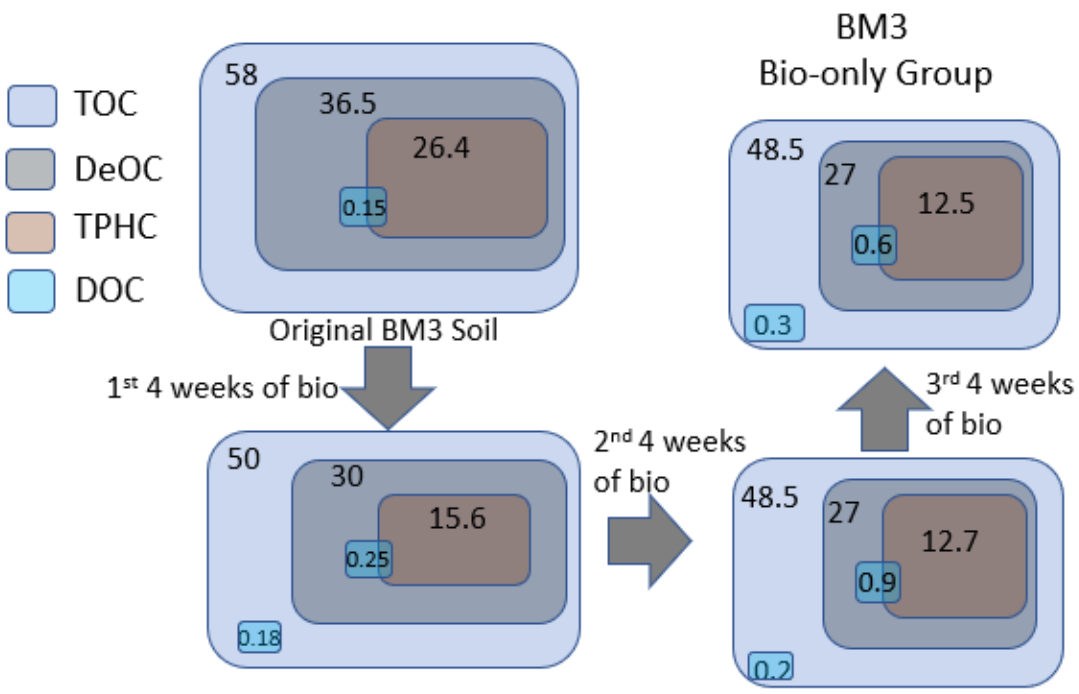

Figure 5.3. Carbon fate of BM3 for bioremediation-only group. Carbon was divided into four categories: Total organic carbon (TOC), DCM-extractable organic carbon (DeOC), TPH carbon (TPHC), and Dissolved organic carbon (DOC). TPH carbon was calculated by TPH concentration x 0.85 (assuming 85% of TPH is carbon). The carbon flow chart presents how each category of carbon evolved throughout the treatment process that followed the same timeline as Figure 5.2, and the 1st, 2nd, and 3rd correspond to phase 1, 2, and 3, respectively. Numbers show the mass of C in grams, and the areas are proportional to the mass.

5.3.1.2 Pre-ozonation of BM3

Pre-ozonation led to a different TPH-removal pattern. The first ozonation dropped the TPH concentration by ~ 8000 mg/kg, and the ensuing bioremediation yielded a TPH-biodegradation rate almost parallel to that of biotreatment. Figure 5.4, which tracks the different carbon components for BM3, shows that ozonation produced 6 g/kg of DOC, with 5 g/kg being non-TPH DOC. Only 0.2 g/kg of non-TPH DOC was utilized in Phase I. This lack of non-TPH DOC biodegradation suggests that light TPH remained abundant after ozonation and outcompeted DOC as a biodegradable substrate.

The second ozone dose removed only about one-half of the TPH removed by the first ozonation. This correlates with having about one-half of TPH already removed, but it also is possible that the remaining TPH was less reactive or had to compete with DOC. The most significant trend is that the preferred substrate for microbial metabolism in Phase 2 shifted from TPH to DOC: biodegradation consumed 6 g/kg of DOC in total, with 1.5 g/kg in DeOC and 4.5 g/kg outside of DeOC, and this was due to that, in Phase I, easily biodegradable TPH were consumed. In contrast, TPH has only a modest decrease, 1.5 g/kg. TOC loss (6 g/kg) was slightly less than the combined losses of DOC and DeOC loss, mostly likely due to net growth of biomass, variability of measurement, or both.

Phase 3 showed similar patterns as Phase 2: The 3rd dose decreased less TPH than the previous one (Figure 5.2), and biodegradation mainly targeted DOC rather than TPH (Figure 2). Overall, the three cycles of ozonation coupled with biodegradation achieved a significant degree of TPH removal: from ~31000 mg/kg to ~5000 mg/kg in 84 days. TOC reduction – from 58 to 34 g/kg – was based on DOC mineralization, with most of the DOC generated by ozonation.

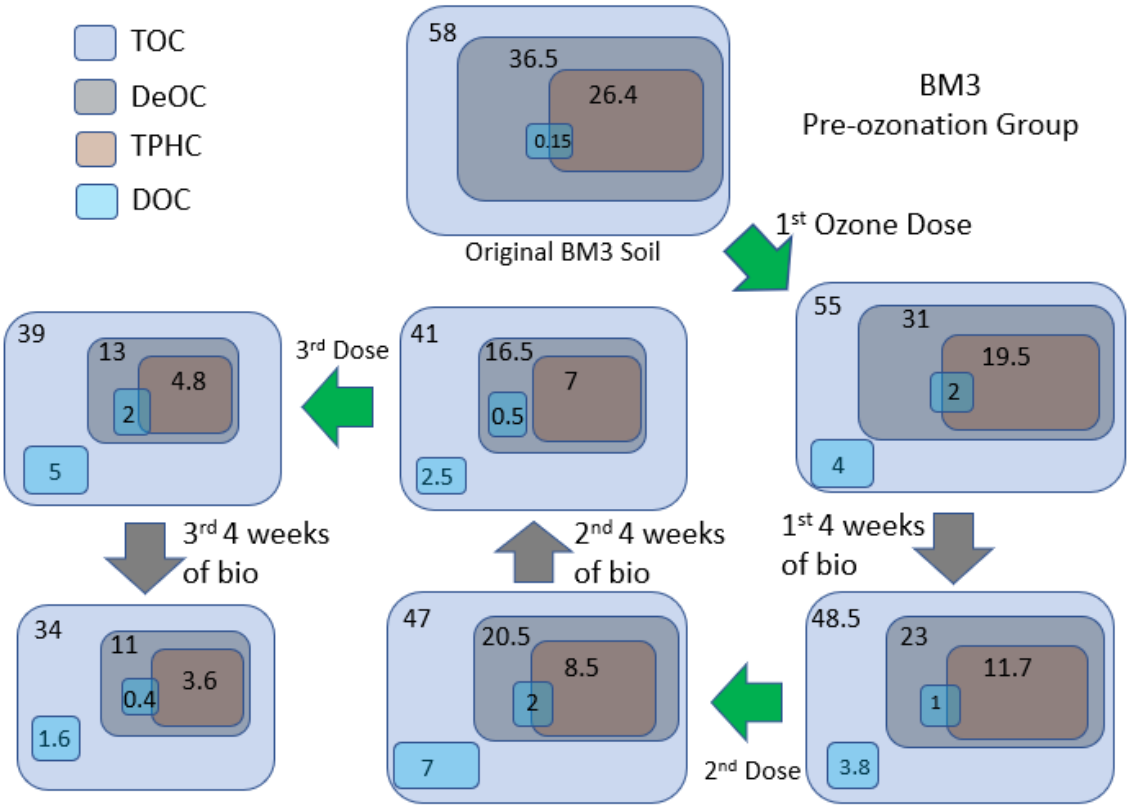

Figure 5.4. Carbon fate for the multi-stage treatment of BM3 using pre-ozonation. Carbon was divided into four categories: Total organic carbon (TOC), DCM-extractable organic carbon (DeOC), TPH carbon (TPHC), and dissolved organic carbon (DOC). TPH carbon was calculated from TPH concentration x 0.85 (i.e., 85% of TPH is carbon). The carbon flow chart presents how each category of carbon evolved throughout the treatment process that follows the same timeline as Figure 1, and the 1st, 2nd, and 3rd correspond to phase 1,2, and 3, respectively. Numbers show the mass of C in grams, and the areas are proportional to the mass. The green arrows indicate an ozone dose.

5.3.1.3 Post-ozonation of BM3

Post-ozonation reached about the same TPH end-point as pre-ozonation, but the route was different (grey triangles in Figure 5.2). The first ozone dose, applied at the end of week 4, led to a sharp drop of TPH, ~5400 mg/kg TPH, but did not cause substantial mineralization; instead, Figure 5.4 shows that the primary effect of ozonation was converting DeOC and TPHC to DOC. The effect of the second ozone dose was similar, but muted.

Figure 5.5 shows that biodegradation in Phases 2 and 3 mirrored the trends of pre-ozonation: rapid DOC mineralization, but limited TPH consumption. This underscores that, when readily biodegradable TPH was depleted, the dominant impact of ozone was to transform TPH, along with some other components in DeOC, into DOC, which then could be biodegraded and mineralized.

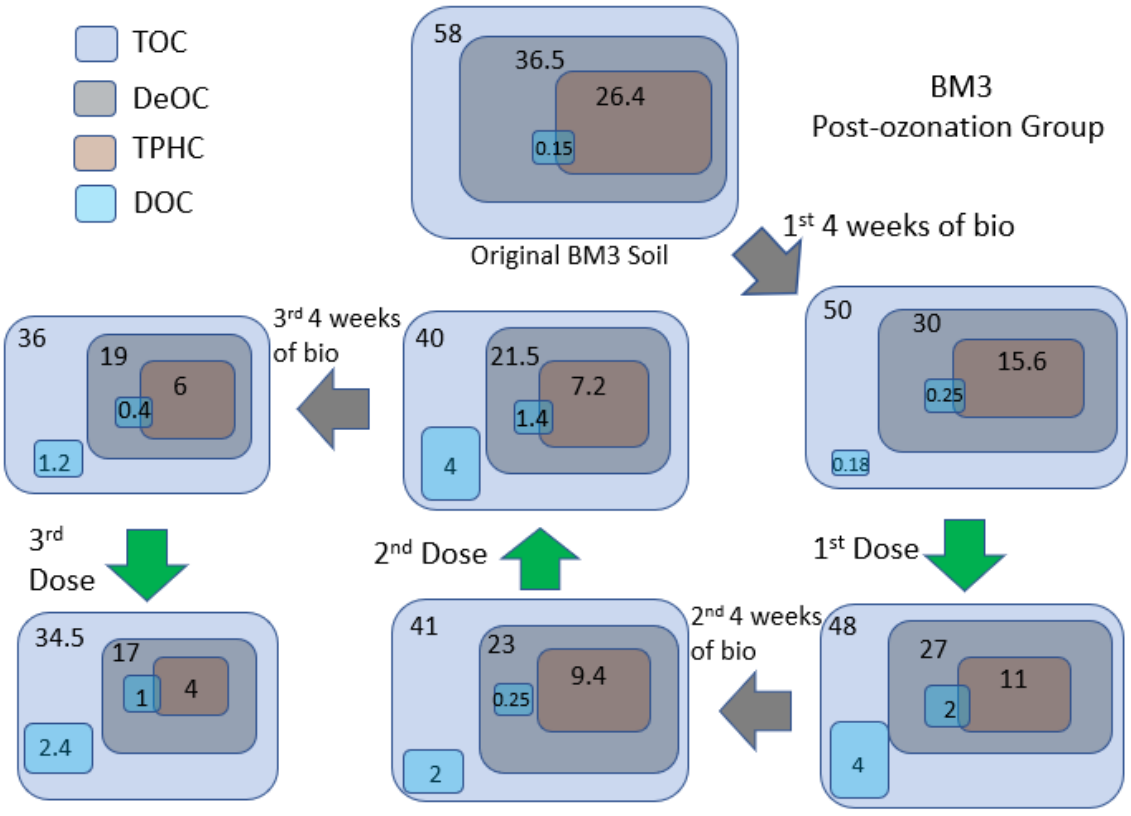

Figure 5.5. Carbon fate for multi-cycle treatment of BM3 using post-ozonation. Carbon was divided into four categories: Total organic carbon (TOC), DCM-extractable organic carbon (DeOC), TPH carbon (TPHC), and dissolved organic carbon (DOC). TPH carbon was calculated by TPH concentration x 0.85 (i.e., 85% of TPH is carbon). The carbon flow chart presents how each category of carbon evolved throughout the treatment process that followed the same timeline as Figure 1, and the 1st, 2nd, and 3rd correspond to phase 1,2, and 3, respectively. Numbers show the mass of C in grams, and the areas are proportional to the mass. The green arrows indicate an ozone dose.

In summary for BM3, when readily biodegradable TPH was available, the microbial community selectively utilized this portion of TPH in preference to non-TPH DOC. Later, DOC became the dominant substrate, since only less-biodegradable TPH remained. Integrating ozonation with biodegradation made it possible to bring TPH level far below the regulated value of 10000 mg/kg while also removing about 40% of the TOC. For BM3, pre-ozonation and post-ozonation were equally efficient, since BM3 contained a significant fraction of readily biodegradable TPH.

5.3.2 Integration of Ozonation and Bioremediation for BM4 soil:

Figure 5.6 compares TPH changes with time among the three treatment processes for BM4: biotreatment only (blue diamonds), pre-ozonation (orange squares), and post-ozonation (grey triangles).

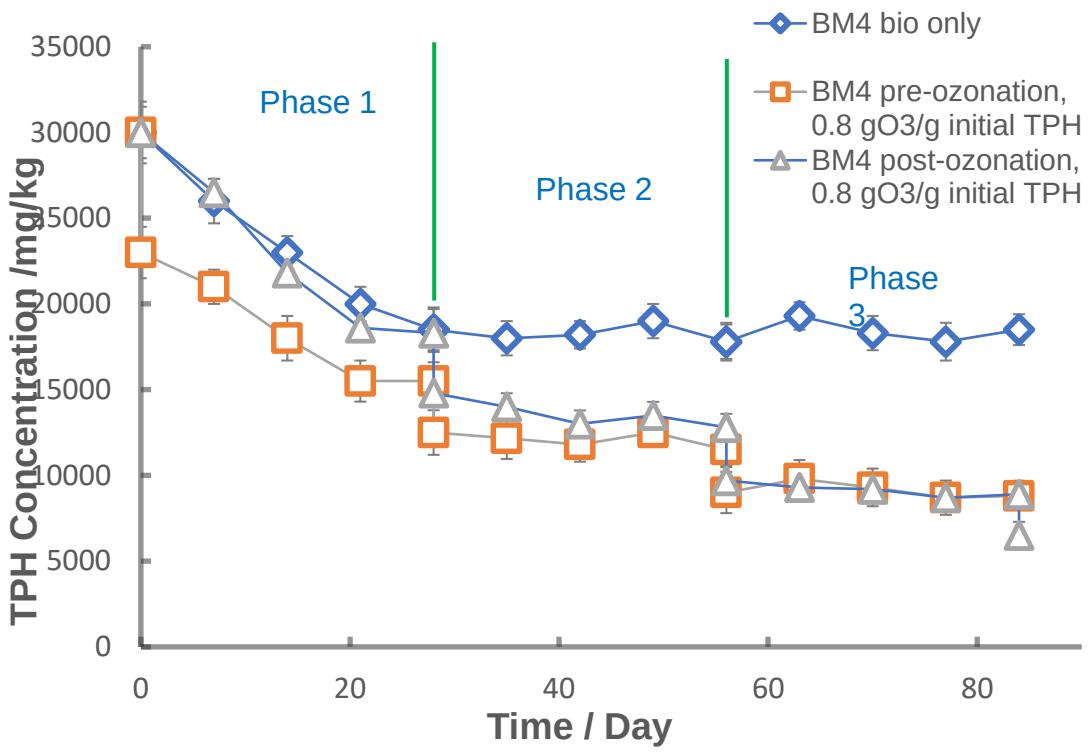

Figure 5.6. The patterns of BM4 TPH concentrations with time for: Biotreatment control (blue diamonds), pre-ozonation (orange squares), and post-ozonation (grey triangles). The 12-week period was divided into three 4-week phases. Each ozone dose was 0.8 gO_3/g initial TPH, which corresponds to 24 gO_3 /kg dry soil. Symbols are the means of 3 replicates, and error bars are the standard deviations.

5.3.2.1 Bio-treatment of BM4

In Phase 1 of biotreatment (control), TPH decreased in a pseudo-zero order pattern from ~ 30,000 mg/kg to ~18,500 mg/kg, presumably due to the biodegradation of the lighter fractions of TPH. Starting in Phase 2, biodegradation stopped, leading to a residual concentration of ~ 5000 mg/kg higher than the residual for BM3. This observation is consistent with a heavier oil corresponding to a higher residual concentration. Again, the final TPH concentration achieved by bioremediation alone did not meet the 10,000 mg/kg standard. Figure 5.7 shows that the TOC reduction (~8 g/kg) was primarily driven by TPHC loss, which led to mineralization.

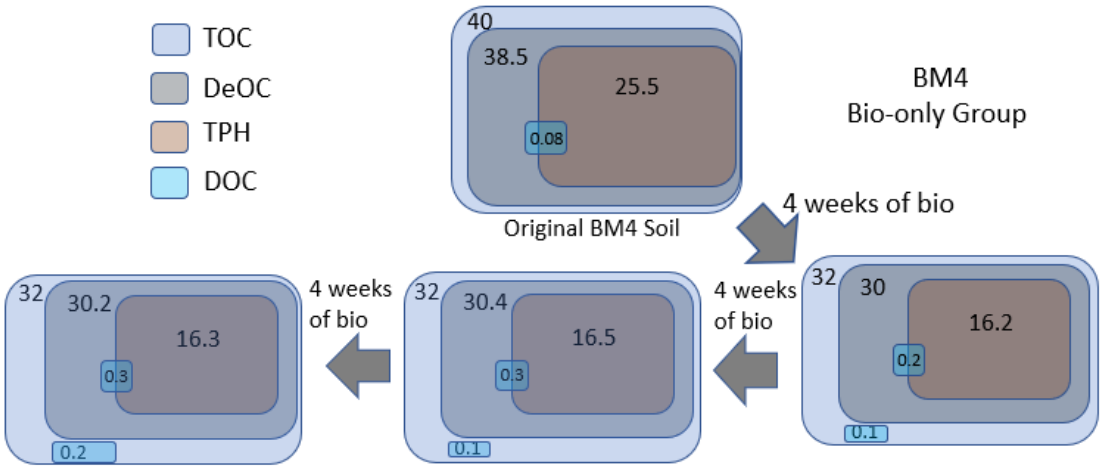

Figure 5.7. Carbon fate of BM4 during biotreatment alone. Carbon was divided into four categories: Total organic carbon (TOC), DCM-extractable organic carbon (DeOC), TPH carbon (TPHC), and Dissolved organic carbon (DOC). TPH carbon was calculated by TPH concentration x 0.85 (assuming 85% of TPH is carbon). The carbon flow chart presents how each category of carbon evolved throughout the treatment process that followed the same timeline as Figure 4, and the 1st, 2nd, and 3rd correspond to phase 1, 2, and 3, respectively. Numbers show the mass of C in grams, and the areas are proportional to the mass.

5.3.2.2 Pre-ozonation of BM4

The overall patterns for TPH and carbon components with BM4 were similar to those for BM3, but important details differed. The first ozone dose resulted in a ~7000 mg/kg TPH reduction, which was followed by another 7000 mg/kg TPH decrease during biodegradation in Phase 1, which brought the TPH concentration ~2000 mg/kg below the residual concentration of biostimulation alone. The 2nd and 3rd ozone doses combined led to less TPH decline than did the 1st dose, which resembled the pattern of BM3. The final TPH was diminished to ~9000 mg/kg, which met the regulatory standard, but was higher than the end-point TPH of BM3.

Figure 5.8, which displays the carbon distribution, shows that, in Phase 1, about 40% of ozone-generated total DOC (3 g/kg) also was biodegraded. Although TOC loss in Phase 1 was dominated by TPHC loss, DOC loss dominated the change in TOC of the second and third phases, and the control was strongest for the DOC outside of DeOC, since this fraction of DOC is more polar and biodegradable.

TOC loss over all phases was ~45%, and it was dominated by mineralization of DOC that was generated from TPH by ozonation (in all phases), although some direct mineralization of TPH also occurred in Phase 1.

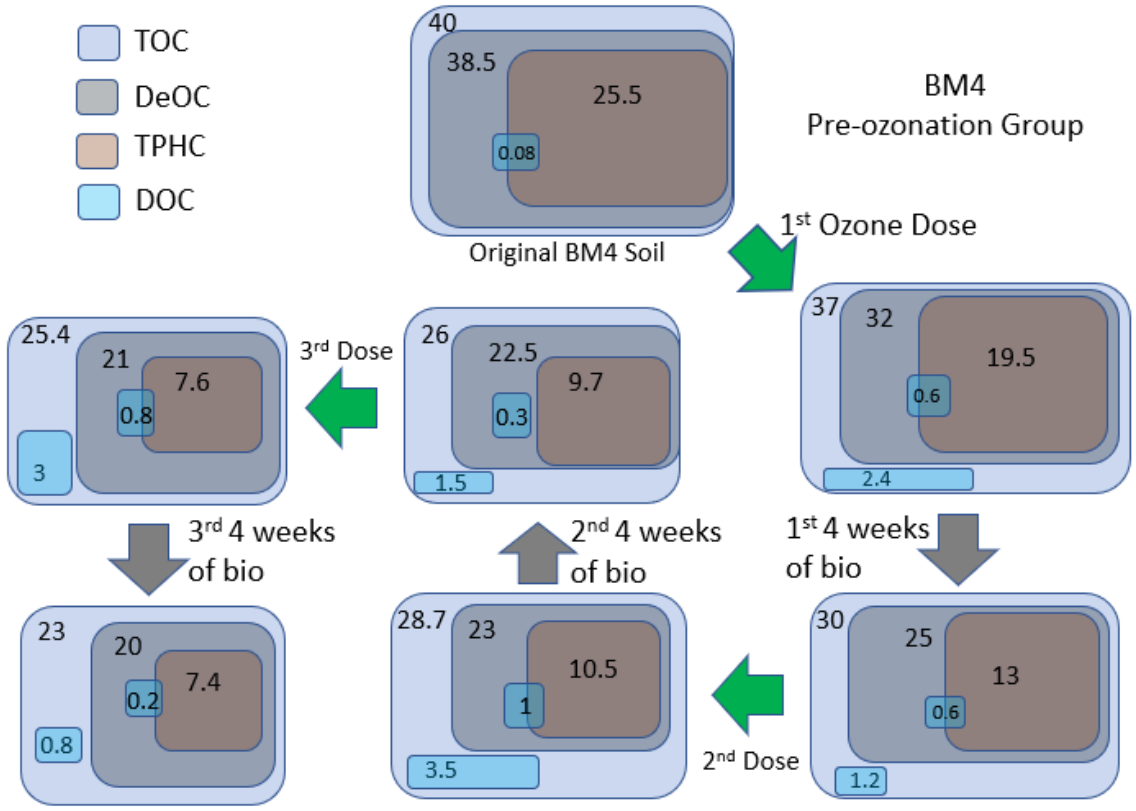

Figure 5.8. Carbon fate of BM4 during pre-ozonation multi-stage treatment. Carbon was divided into four categories: Total organic carbon (TOC), DCM-extractable organic carbon (DeOC), TPH carbon (TPHC), and Dissolved organic carbon (DOC). TPH carbon was calculated by TPH concentration x 0.85 (assuming 85% of TPH is carbon). The carbon flow chart presents how each category of carbon evolved throughout the treatment process that followed the same timeline as Figure 4, and the 1st, 2nd, and 3rd correspond to phase 1, 2, and 3, respectively. Numbers show the mass of C in grams, and the areas are proportional to the mass. The green arrows indicate an ozone dose.

5.3.2.3 Post-ozonation of BM4

Post-ozonation reached the TPH end-point of pre-ozonation before the 3rd ozone dose (Figure 5.6). This faster trajectory occurred because TPH was biodegraded during Phases 2 and 3. Figure 5.9 illustrates that these two phases of biodegradation removed 2.6 g TPHC, a value much larger than the 1 g TPHC for pre-ozonation (Figure 5.8). Thus, the TPH following the 1st ozonation still contained a biodegradable fraction.

Within the DeOC, TPH always was the more reactive component during ozonation or biodegradation. For example, Figure 6 shows that the 1st ozonation removed 3.4 g of TPHC and produced 0.8 g DOC inside DeOC, which created a net loss of 2.6 g, approximately the loss of DeOC. This supports that the change in TOC was mainly controlled by the change of TPHC.

In summary for BM4, the results emphasize that, when only recalcitrant TPH was present, ozonation did not directly enhance the biodegradation rate of the persistent TPH. Instead, it converted the residual TPH into more hydrophilic and biodegradable DOC that could be mineralized by microbial metabolism. Ozonation coupled with biodegradation achieved ~67% removal of TPH and 45% removal of TOC. Delivering the first O_3 dose when biodegradation alone reached a plateau (i.e., post-ozonation) was more efficient for removing and mineralizing recalcitrant TPH. The same overall O3 dose achieved more TPH reduction for post-ozonation than for pre-ozonation. Therefore, the more recalcitrant residual petroleum of BM4 was better treated with post-ozonation, although post- and pre-ozonation were equivalent for BM3.

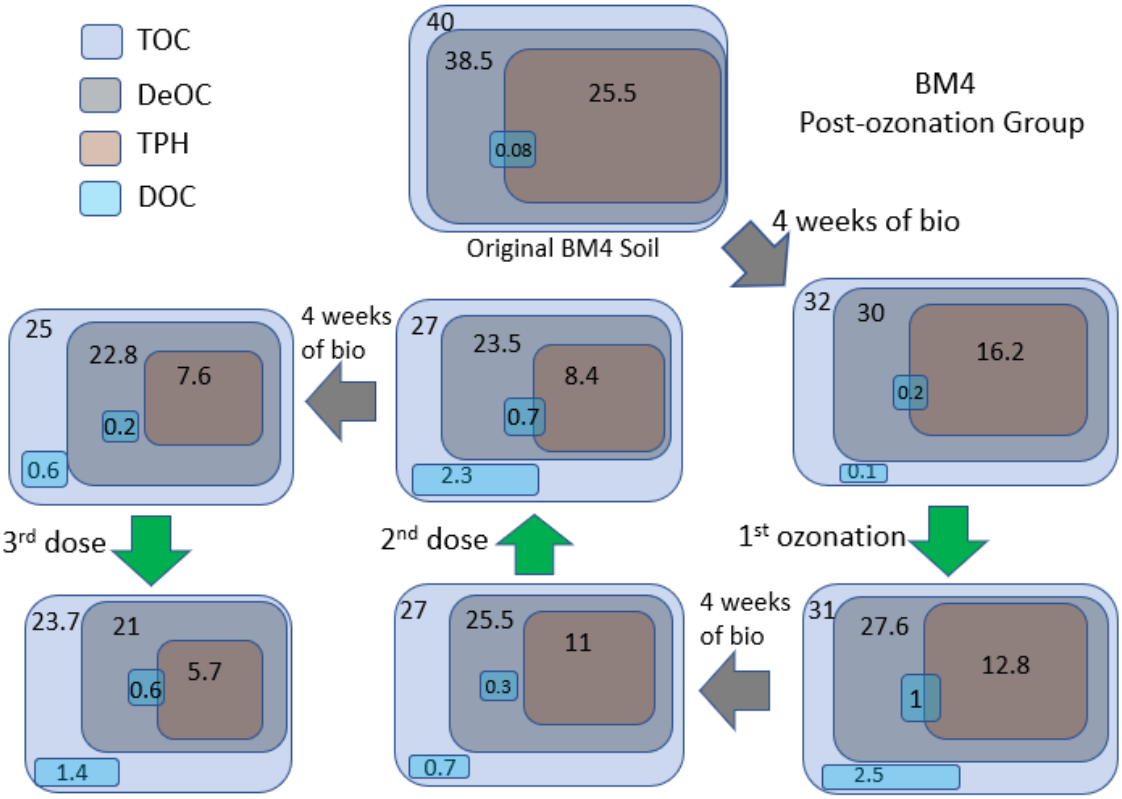

Figure 5.9. Carbon fate of BM4 during post-ozonation multi-cycle treatment. Carbon was divided into four categories: Total organic carbon (TOC), DCM-extractable organic carbon (DeOC), TPH carbon (TPHC), and Dissolved organic carbon (DOC). TPH carbon was calculated by TPH concentration x 0.85 (assuming 85% of TPH is carbon). The carbon flow chart presents how each category of carbon evolved throughout the treatment process that followed the same timeline as Figure 4, and the 1st, 2nd, and 3rd correspond to phase 1, 2, and 3, respectively. Numbers show the mass of C in grams, and the areas are proportional to the mass. The green arrows indicate an ozone dose.

5.4 Conclusion

Optimizing sequential steps of ozonation and biodegradation made it possible to meet the TPH regulatory standard and mineralize 40-45% of the TOC. Pre- and post-ozonation strategies were able to overcome the recalcitrant nature of the residual TPH and TOC. For the relatively biodegradable TPH in BM3, pre-ozonation and post-ozonation strategies were equally effective. in contrast, post-ozonation was more efficient for the less biodegradable TPH in BM4. Tracking the fate of carbon along the treatment timeline revealed that dissolved organic carbon (DOC) was the dominant substrate for microbial consumption only when readily biodegradable TPH was no longer available. TPH carbon was more reactive (by ozonation and biodegradation) than was DeOC, and it dictated the changes of DeOC. However, decreases in TOC relied more on the microbial mineralization of DOC. Ozonation did not directly enhance the biodegradation kinetics of TPH; instead, ozonation converted TPH into DOC that was subsequently mineralized microbially. The results document that multi-stage ozonation + biodegradation is a useful remediation tool for petroleum contamination, and the decision to use pre- versus post-ozonation depends on the biodegradability of the residual petroleum.

CHAPTER 6. SUMMARY

6.1 Summary of results

My research demonstrates the promise and the challenges of using O_3 gas to remove petroleum hydrocarbons in soil, either stand-alone or combined with biodegradation. My work defines ozone's fate and transport in soil, the interactions between O_3 and the organic components in soil matrix (carbon balance), and the interplay between ozone and soil moisture. By using a lab-scale soil column, I was able to identify the barriers facing delivering ozone gas to soil and to fill in the knowledge gaps that might cause inefficiency in implementing the technology. The main research questions remain in the barriers in gas transfer and knowledge gaps in the integration of bioremediation and ozonation, such as how to optimize each process, a need to ensure reliable and cost-effective remediation of soils contaminated with residual petroleum hydrocarbons.

In Chapter 2, I observed a plateau in the increases of BOD_5, SCOD, and DOC and the decline in TPH; from that I, proposed a benchmark dose for BM1 soil. In Chapter 3, the same pattern emerged, and I investigated a physical aspect of the gas-delivery mechanism — gas channeling. This concept was then validated for BM2 via manual mixing of the soil. From this point on, the limitation of gas transfer in the soil became an important research object. Gas preferential pathways only partially contributed to the mass-transfer resistance; moisture also played a key role in compromising TPH removal. Thus, in Chapter 4, I analyzed the effects of a range of moisture levels. High moisture content (10%) inevitably hindered gas-soil contact. The balance between mineralization and producing DOC in Chapter 2, carbon distribution in Chapter 3, and the effect of moisture content in Chapter 4 structured how to efficiently apply O_3 to couple with biodegradation to achieve substantial TPH removal, and this led to Chapter 5.

In Chapter 5, I pursued the theme of optimizing integration through a multi-stage strategy with alternating ozonation and biodegradation. With pH and moisture optimized in each step, the overall TPH removal performance via pre- or post-ozonation was evaluated on two distinct soils (BM3 and BM4). The multi-cycle treatment I implemented successfully reduced TPH below the regulatory

limit for both soils. While pre- and post-ozonation were equally effective for BM3, post-ozonation was more efficient for BM4, which had petroleum that was heavier and less biodegradable.

6.2 Conclusions

My results lead to these major conclusions that answer the questions intended for Chapters 2-5.

- Chapter 2: Does application of gaseous ozone to soil reduce TPH and produce water soluble DOC?
  - Conclusion: Yes, ozonation removed nearly half of the TPH and converted TPH to hydrophilic and biodegradable products and did not severely harm the indigenous microbial community.

- Chapter 3: (1) How can the mass transfer of ozone in petroleum-contaminated soil be improved? (2) What are the interactions between ozone and different organic carbon fractions (TPH, SOM, and DeOC) for a more recalcitrant oil?
  - Conclusions: (1) TPH was the major reactant with ozone, though other organic carbon also consumed ozone. (2) Mixing, which enhanced the mass transfer, improved TPH reduction.

- Chapter 4: What is the effect of water content on TPH transformation and reduction during ozonation?
  - Conclusion: Controlling moisture content was important for ozonation performance. High moisture content slowed ozonation, but some moisture was necessary.

- Chapter 5: (1) Does the sequence of ozonation and biodegradation (pre- versus post-ozonation) affect the overall TPH removal? (2) What synergies exist between ozonation and biodgradation of TPH contaminated soils, for both TPH and DOC removal?
  - Conclusions: (1) Ozonation did not directly enhance the biodegradation rate of the residual TPH after ozonation, but ozone converted TPH into DOC that was then

biodegraded and mineralized. (2) Pre-ozonation and post-ozonation were equally efficient for a biodegradation oil, while post-ozonation was a better option for a more recalcitrant oil. (3) Although residual TPH still persisted, the multi-stage approach was proven to be a useful remediation tool for driving the TPH concentration below regulatory requirements (10,000 mg/kg) and mineralizing a substantial portion of the TOC. (4) Ozone doses ranging from ~2 to ~12 gO_3 g/ $TPH_{removed}$ (Table 6.1) were controlled by the synergy of (i) initial TPH concentration that controlled the kinetics, (ii) soil moisture content that affected gas-mass transfer, (iii) API gravity of the oil that dictated heat production that affects the temperature and kinetics, (iv) sequence of ozonation and biodegradation that changed the quantity of TPH removal, and (v) ozonation time that corresponded to O_3 mass input. Careful sequencing of ozonation + biodegradation could keep ozone dose near the lower end of the range, an important factor for cost-effectiveness.

Table 6.1. O_3 doses for BM1-BM4 soils

Soil	Initial TPH concentration mg/kg	Soil Moisture wt %	O_3 g/g *initial TOC	O_3 g/g initial TPH	O_3 g/g removed TPH	Remark
BM1	10600	1%	1.0	3.6	8.0	
BM1	10600	1%	1.4	4.8	9.0	
BM1	10600	1%	1.8	6.0	10.0	
BM1	10600	1%	2.1	7.2	11.5	
BM2	18000	1%	0.5	1.1	4.0	
BM2	18000	1%	1.0	2.2	6.7	
BM2	18000	1%	1.5	3.4	9.2	
BM2	18000	1%	2.0	4.5	11.4	
BM3	31000	5%	0.4	0.8	1.8	*pre-1st
BM3	31000	5%	0.4	0.8	6.0	pre-2nd
BM3	31000	5%	0.4	0.8	8.8	pre-3rd
BM3	31000	5%	0.4	0.8	4.4	post-1st
BM3	31000	5%	0.4	0.8	9.2	post-2nd
BM3	31000	5%	0.4	0.8	9.5	post-3rd
BM4	30000	5%	0.6	0.8	3.4	pre-1st
BM4	30000	5%	0.6	0.8	8.0	pre-2nd
BM4	30000	5%	0.6	0.8	8.3	pre-3rd
BM4	30000	5%	0.6	0.8	6.9	post-1st
BM4	30000	5%	0.6	0.8	7.7	post-2nd
BM4	30000	5%	0.6	0.8	7.8	post-3rd

* (1) Pre- and post- in the remark column indicate the three ozone doses in a numerical order conferred on BM3 and BM4 soils in Chapter 5.

(2) Initial means the untreated condition.

6.3 Potential Future Work

As outlined in Chapter 3, gas channeling was an obstacle to be overcome to achieve more thorough gas-soil contact; however, gas channeling is unavoidable in a static injecting mode (e.g., *in situ*). Thus, when applying O_3 *in situ*, the configuration of multiple injection points adjacent to each other should be practiced to reduce any 'uncontacted' area. Two approaches can be used to devise a good arrangement of injection points. One is exploiting mathematical modeling to calculate the radius of influence for each injection node. COMSOL can be used to solve the multi-variable, multi-reaction, and multi-phases model focusing on ozone's fate and transport in the soil matrix. Two is testing the overlapping area of two injection points experimentally. DOC, TPH, and pH need to be measured as the indicator to compare the ozonation efficiency of different injection regions, and this can confine the overlapping area. The two methods can be combined to reach a more reliable conclusion, and both are promising research topics to explore as ozonation + biodegradation move towards practical application.

Ex situ application also can be explored using a rotary contactor that will completely eliminate gas channels. Constant mixing will enhance gas transfer, even when the soil moisture level is high. The performance of a rotary reactor depends on the rotary speed, the ratio of the soil-depth to the contactor's diameter, gas-flow rate, and initial soil water content. DOC and TPH should be monitored at different rotary conditions to determine the optimal scenario.

To advance the application of ozone + bioremediation to field scale, I suggest that both scenarios be evaluated systematically by a combination of lab-based and field-based pilot studies. In addition, the toxicity of the TOC that remains after treatment is unknown. DOC, being more mobile and leachable than the residual TPH, is the most critical, and it is produced by ozonation. Therefore, bioassays on the toxicity of the ozonated soil and its leachate are warranted. The acute and chronic toxicities tests can include on seed germination and on soil invertebrate. Seedling tests usually last 14-28 days or until 65% of the seeds germinate, and then germination rate, biomass, and root length will be recorded to provide a statistically robust EC_{50} [320], The growth rate, mortality, and reproduction condition of earthworms in the ozonated soils also can be used to evaluate the acute

and chronic toxicities. These standardized tests have a duration of 28 days, and the results can be converted into LC_{50} or EC_{50} [321].

REFERENCES

（1）Kharaka, Y. K.; Dorsey, N. S., Environmental issues of petroleum exploration and production: Introduction. *Environmental Geosciences* **2005,** *12*, (2), 61-63.

（2）Chand, J., Environmental pollution monitoring in oil exploration and exploitation. In *Condition Monitoring and Diagnostic Engineering Management*, Springer: 1990; pp 218-224.

（3）Nadim, F.; Hoag, G. E.; Liu, S.; Carley, R. J.; Zack, P., Detection and remediation of soil and aquifer systems contaminated with petroleum products: an overview. *Journal of Petroleum Science and Engineering* **2000,** *26*, (1), 169-178.

（4）Adejoh, O. F., Petroleum Pipelines, Spillages and the Environment of the Niger Delta Region of Nigeria. *World Environment* **2014,** *4*, (3), 93-100.

（5）Khaitan, S.; Kalainesan, S.; Erickson, L. E.; Kulakow, P.; Martin, S.; Karthikeyan, R.; Hutchinson, S. L. L.; Davis, L. C.; Illangasekare, T. H.; Ng'oma, C., Remediation of sites contaminated by oil refinery operations. *Environmental Progress* **2006,** *25*, (1), 20-31.

（6）Trench, C. J., How Pipelines Make the Oil Market Work–Their Networks, Operation and Regulation. *A Memorandum Prepared for the Association of Oil Pipe Lines and the American Petroleum Institute's Pipeline Committee, Allegro Energy Group, New York* **2001**.

（7）Brown, D. M.; Bonte, M.; Gill, R.; Dawick, J.; Boogaard, P. J., Heavy hydrocarbon fate and transport in the environment. *Quarterly Journal of Engineering Geology and Hydrogeology* **2017,** *50*, (3), 333.

（8）KURNAZ, S. Ü.; BÜYÜKGÜNGÖR, H., Bioremediation of total petroleum hydrocarbons in crude oil contaminated soils obtained from southeast Anatolia. *Acta Biologica Turcica* **2016,** *29*, (2), 57-60.

（9）Todd, G. D.; Chessin, R. L.; Colman, J., Toxicological profile for total petroleum hydrocarbons (TPH). **1999**.

（10）Cowell, E., The effects of oil pollution on salt-marsh communities in Pembrokeshire and Cornwall. *Journal of Applied Ecology* **1969,** *6*, (2), 133-142.

（11）Baker, J. M., The effects of oils on plants. *Environmental Pollution (1970)* **1970,** *1*, (1), 27-44.

（12）Banks, M. K.; Schultz, K. E., Comparison of Plants for Germination Toxicity Tests in Petroleum-Contaminated Soils. *Water, Air, and Soil Pollution* **2005,** *167*, (1), 211-219.

（13）Besalatpour, A.; Khoshgoftarmanesh, A. H.; Hajabbasi, M. A.; Afyuni, M., Germination and Growth of Selected Plants in a Petroleum Contaminated Calcareous Soil. *Soil and Sediment Contamination: An International Journal* **2008,** *17*, (6), 665-676.

（14）Tang, J.; Wang, M.; Wang, F.; Sun, Q.; Zhou, Q., Eco-toxicity of petroleum hydrocarbon contaminated soil. *Journal of Environmental Sciences* **2011,** *23*, (5), 845-851.

（15）Zhu, Y.; Song, Z.; Chen, J.; Li, C.; Xiao, B.; Wang, Q. In *Effects of oil-contaminated soil on the seed germination and seedling growth of selected crops*, World Automation Congress 2012, 24-28 June 2012, 2012; 2012; pp 1-4.

（16）Shakir Hanna, S. H.; Weaver, R. W., Earthworm survival in oil contaminated soil. *Plant and Soil* **2002,** *240*, (1), 127-132.

（17）Saterbak, A.; Toy, R. J.; Wong, D. C. L.; McMain, B. J.; Williams, M. P.; Dorn, P. B.; Brzuzy, L. P.; Chai, E. Y.; Salanitro, J. P., Ecotoxicological and analytical assessment of hydrocarbon-contaminated soils and application to ecological risk assessment. *Environmental Toxicology and Chemistry* **1999,** *18*, (7), 1591-1607.

（18）SOIL, P. H. P. I., CANADA-WIDE STANDARDS for PETROLEUM HYDROCARBONS (PHC) IN SOIL. **2008**.

（19）Jones, O. A.; Spurgeon, D. J.; Svendsen, C.; Griffin, J. L., A metabolomics based approach to assessing the toxicity of the polyaromatic hydrocarbon pyrene to the earthworm Lumbricus rubellus. *Chemosphere* **2008,** *71*, (3), 601-609.

（20）De Jong, E., The effect of a crude oil spill on cereals. *Environmental Pollution Series A, Ecological and Biological* **1980,** *22*, (3), 187-196.

（21）Ibemesim, R., Effect of salinity and wytch farm crude oil on Paspalum conjugatum Bergius (Sour Grass). *J Biol Sci* **2010,** *10*, 122-130.

（22）Nsobilaatibila, E. Using nitrogen and phosphorus to stimulate microbial degradation of diesel oil in four Ghanaian soils. University of Ghana, 2013.

（23）Canada-Wide Standard for Petroleum Hydrocarbons (PHC)in Soil: Scientific Rationale In Environment, C. C. o. M. o. t., Ed. 2008; Vol. ISBN 978-1-896997-77-3.

（24）McMillen, S. J.; Magaw, R. I.; Carovillano, R. L., *Risk-based decision-making for assessing petroleum impacts at exploration and production sites*. US Department of Energy: 2001.

（25）Edwards, D.; Andriot, M.; Amoruso, M.; Tummey, A.; Bevan, C.; Tveit, A.; Hayes, L.; Youngren, S.; Nakles, D., Development of fraction specific reference doses (RfDs) and refernce concentrations (RfCs) for total petroleum hydrocarbons (TPH). *Total petroleum hydrocarbon criteria working group series* **1997,** *4*.

（26）Edwards, D. A.; Tveit, A.; Emerson, M., Development of Reference Doses for Heavy Total Petroleum Hydrocarbon (TPH) Fractions. *Risk-Based Decision-Making for Assessing Petroleum Impacts at Exploration and Production Sites* **2001**, 111.

（27）Roberts, S. M.; James, R. C.; Williams, P. L., *Principles of toxicology: environmental and industrial applications*. John Wiley & Sons: 2014.

（28）Karleskint, G.; Turner, R.; Small, J., *Introduction to marine biology*. Cengage Learning: 2012.

（29）McMillen, S.; Rhodes, I.; Nakles, D. V.; Sweeney, R. E., Application of the Total Petroleum Hydrocarbon Criteria Working Group (TPHCWG) methodology to crude oils and gas condensates. *Risk-based decision-making for assessing petroleum impacts at exploration and production sites: USA Petroleum Environmental Research Foundation and The United States Department of Energy* **2001**, 58-76.

（30）USEPA, Non-Halogenated Organics using GC/FID, Method 8015C. In **2007**.

（31）Hamilton, W. A.; Sewell, H. J.; Deeley, G. In *Technical basis for current soil management levels of total petroleum hydrocarbons*, Risk-Based Decision-Making for Assessing Petroleum Impacts at Exploration and Production Sites. SJ McMillen, RI Magaw and RL Carovillano. Tulsa, Oklahoma, US Dept. of Energy and the Petroleum Environmental Research Forum, 2001; 2001; pp 36-45.

（32）Tomlinson, P.; Ruby, M. V., State and federal cleanup levels for petroleum hydrocarbons in soil: state of the states and implications for the future. *Human and Ecological Risk Assessment: An International Journal* **2016,** *22*, (4), 911-926.

（33）Mercer, J. W.; Cohen, R. M., A review of immiscible fluids in the subsurface: properties, models, characterization and remediation. *Journal of Contaminant Hydrology* **1990,** *6*, (2), 107-163.

（34）Das, N.; Chandran, P., Microbial degradation of petroleum hydrocarbon contaminants: an overview. *Biotechnology research international* **2010,** *2011*.

（35）Nocentini, M.; Pinelli, D.; Fava, F., Bioremediation of a soil contaminated by hydrocarbon mixtures: the residual concentration problem. *Chemosphere* **2000,** *41*, (8), 1115-1123.

（36）Aeppli, C.; Nelson, R. K.; Radović, J. R.; Carmichael, C. A.; Valentine, D. L.; Reddy, C. M., Recalcitrance and degradation of petroleum biomarkers upon abiotic and biotic natural weathering of Deepwater Horizon oil. *Environmental science & technology* **2014,** *48*, (12), 6726-6734.

（37）Khan, F. I.; Husain, T.; Hejazi, R., An overview and analysis of site remediation technologies. *Journal of environmental management* **2004,** *71*, (2), 95-122.

（38）Balba, M. T.; Al-Awadhi, N.; Al-Daher, R., Bioremediation of oil-contaminated soil: microbiological methods for feasibility assessment and field evaluation. *Journal of Microbiological Methods* **1998,** *32*, (2), 155-164.

（39）Maila, M. P.; Cloete, T. E., Bioremediation of petroleum hydrocarbons through landfarming: Are simplicity and cost-effectiveness the only advantages? *Reviews in Environmental Science and Biotechnology* **2004,** *3*, (4), 349-360.

（40）Riser-Roberts, E., *Remediation of petroleum contaminated soils: biological, physical, and chemical processes*. CRC Press: 1998.

（41）Dupont, R. R., Fundamentals of bioventing applied to fuel contaminated sites. *Environmental Progress* **1993,** *12*, (1), 45-53.

（42）Li, P.; Sun, T.; Stagnitti, F.; Zhang, C.; Zhang, H.; Xiong, X.; Allinson, G.; Ma, X.; Allinson, M., Field-scale bioremediation of soil contaminated with crude oil. *Environmental engineering science* **2002,** *19*, (5), 277-289.

（43）Mater, L.; Sperb, R. M.; Madureira, L. A. S.; Rosin, A. P.; Correa, A. X. R.; Radetski, C. M., Proposal of a sequential treatment methodology for the safe reuse of oil sludge-contaminated soil. *Journal of Hazardous Materials* **2006,** *136*, (3), 967-971.

（44）Shah, S. J.; Shroff, A. V.; Patel, J. V.; Tiwari, K. C.; Ramakrishnan, D., Stabilization of fuel oil contaminated soil—A case study. *Geotechnical & Geological Engineering* **2003,** *21*, (4), 415-427.

（45）Meegoda, J. N., Stabilization/solidification of petroleum-contaminated soils with asphalt emulsions. *Practice Periodical of Hazardous, Toxic, and Radioactive Waste Management* **1999,** *3*, (1), 46-55.

（46）USEPA, Field Applications of In Situ Remediation Technologies: chemical oxidation. In Publication # EPA 542-R-98-008: Washington, DC, 1998.

（47）Ferguson, S. H.; Woinarski, A. Z.; Snape, I.; Morris, C. E.; Revill, A. T., A field trial of in situ chemical oxidation to remediate long-term diesel contaminated Antarctic soil. *Cold Regions Science and Technology* **2004,** *40*, (1), 47-60.

（48）Petroleum Hydrocarbon Remediation by In-situ Chemical Oxidation at Colorado Sites In Safety, T. C. D. o. L. a. E. D. o. O. a. P., Ed. 2007.

（49）Kang, W.-H.; Cheong, J.-G.; Kim, K.; Chae, H.; Chang, C.-H. In *Restoration of petroleum-contaminated soils by field-scale soil washing system*, International Conference on Environmental Science and Technology IPCBEE, 2012; 2012.

（50）Barnes, D. L.; Laderach, S. R.; Showers, C., Treatment of petroleum-contaminated soil in cold, wet, remote regions. In US Forest Service, T. a. D. P., Missoula, MT., Ed. 2002.

（51）Vidonish, J. E.; Zygourakis, K.; Masiello, C. A.; Sabadell, G.; Alvarez, P. J. J., Thermal Treatment of Hydrocarbon-Impacted Soils: A Review of Technology Innovation for Sustainable Remediation. *Engineering* **2016,** *2*, (4), 426-437.

（52）Troxler, W.; Yezzi, J.; Cudahy, J.; Rosenthal, S. *Thermal desorption of petroleum contaminated soils*; Foster Wheeler Enviresponse, Inc., Livingston, NJ (United States): 1992.

（53）Ezeji, U.; Anyadoh, S.; Ibekwe, V., Clean up of Crude Oil-Contaminated Soil. *Terrestrial and Aquatic Environmental Toxicology* **2007,** *1*, (2), 54-59.

（54）Reeves, T. C. On-site incineration of contaminated soil: a study into US Navy applications. Monterey, California. Naval Postgraduate School, 1991.

（55）Hassan, H. F.; Taha, R.; Al Rawas, A.; Al Shandoudi, B.; Al Gheithi, K.; Al Barami, A. M., Potential uses of petroleum-contaminated soil in highway construction. *Construction and Building Materials* **2005,** *19*, (8), 646-652.

（56）Pamukcu, S.; Hijazi, M.; Fang, H., Study of possible reuse of stabilized petroleum contaminated soils as construction material. *Petroleum Contaminated Soils* **1990**, 203-14.

（57）Singh, S.; Kumari, B.; Mishra, S., Microbial degradation of alkanes. In *Microbial degradation of xenobiotics*, Springer: 2012; pp 439-469.

（58）Wilson, S. C.; Jones, K. C., Bioremediation of soil contaminated with polynuclear aromatic hydrocarbons (PAHs): a review. *Environmental pollution* **1993,** *81*, (3), 229-249.

（59）Okoh, A.; Trejo-Hernandez, M., Remediation of petroleum hydrocarbon polluted systems: exploiting the bioremediation strategies. *African Journal of Biotechnology* **2006,** *5*, (25).

（60）Morgan, P.; Atlas, R. M., Hydrocarbon degradation in soils and methods for soil biotreatment. *Critical reviews in biotechnology* **1989,** *8*, (4), 305-333.

（61）Margesin, R.; Schinner, F., Biodegradation and bioremediation of hydrocarbons in extreme environments. *Applied microbiology and biotechnology* **2001,** *56*, (5-6), 650-663.

（62）Tyagi, M.; da Fonseca, M. M. R.; de Carvalho, C. C., Bioaugmentation and biostimulation strategies to improve the effectiveness of bioremediation processes. *Biodegradation* **2011,** *22*, (2), 231-241.

（63）Huesemann, M. H.; Hausmann, T. S.; Fortman, T. J., Does bioavailability limit biodegradation? A comparison of hydrocarbon biodegradation and desorption rates in aged soils. *Biodegradation* **2004,** *15*, (4), 261-274.

（64）Woo, S. H.; Rittmann, B. E., Microbial energetics and stoichiometry for biodegradation of aromatic compounds involving oxygenation reactions. *Biodegradation* **2000,** *11*, (4), 213-227.

（65）Bamforth, S. M.; Singleton, I., Bioremediation of polycyclic aromatic hydrocarbons: current knowledge and future directions. *Journal of Chemical Technology and Biotechnology* **2005,** *80*, (7), 723-736.

（66）Haritash, A. K.; Kaushik, C. P., Biodegradation aspects of Polycyclic Aromatic Hydrocarbons (PAHs): A review. *Journal of Hazardous Materials* **2009,** *169*, (1–3), 1-15.

（67）Leahy, J. G.; Colwell, R. R., Microbial degradation of hydrocarbons in the environment. *Microbiological reviews* **1990,** *54*, (3), 305-315.

（68）Huesemann, M. H., Incomplete hydrocarbon biodegradation in contaminated soils: Limitations in bioavailability or inherent recalcitrance? *Bioremediation Journal* **1997,** *1*, (1), 27-39.

（69）Bost, F.; Frontera-Suau, R.; McDonald, T.; Peters, K.; Morris, P., Aerobic biodegradation of hopanes and norhopanes in Venezuelan crude oils. *Organic Geochemistry* **2001,** *32*, (1), 105-114.

（70）Labud, V.; Garcia, C.; Hernandez, T., Effect of hydrocarbon pollution on the microbial properties of a sandy and a clay soil. *Chemosphere* **2007,** *66*, (10), 1863-1871.

（71）McMillen, S. J.; Kerr, J. M.; Nakles, D. V., Composition of crude oils and gas condensates. *Risk-Based Decision-Making for Assessing Petroleum Impacts at Exploration and Production Sites* **2001**, 46.

（72）Huesemann, M. H., Predictive Model for Estimating the Extent of Petroleum Hydrocarbon Biodegradation in Contaminated Soils. *Environmental Science & Technology* **1995,** *29*, (1), 7-18.

（73）McMillen, S. J.; Young, G.; Davis, P.; Cook, P.; Kerr, J.; Gray, N.; Requejo, A. *Bioremediation potential of crude oil spilled on soil*; Battelle Press, Columbus, OH (United States): 1995.

（74）Alexander, M., Aging, Bioavailability, and Overestimation of Risk from Environmental Pollutants. *Environmental Science & Technology* **2000,** *34*, (20), 4259-4265.

（75）Cuypers, C.; Clemens, R.; Grotenhuis, T.; Rulkens, W., Prediction of Petroleum Hydrocarbon Bioavailability in Contaminated Soils and Sediments. *Soil and Sediment Contamination: An International Journal* **2001,** *10*, (5), 459-482.

（76）Weissenfels, W. D.; Klewer, H.-J.; Langhoff, J., Adsorption of polycyclic aromatic hydrocarbons (PAHs) by soil particles: influence on biodegradability and biotoxicity. *Applied Microbiology and Biotechnology* **1992,** *36*, (5), 689-696.

（77）Singh, A.; Ward, O. P., *Applied bioremediation and phytoremediation*. Springer Science & Business Media: 2004; Vol. 1.

（78）Gough, M.; Rowland, S., Characterization of unresolved complex mixtures of hydrocarbons in petroleum. *Nature* **1990,** *344*, 648-650.

（79）Lyons, W. C.; Plisga, G. J., *Standard handbook of petroleum and natural gas engineering*. Gulf Professional Publishing: 2011.

（80）McCain, W. D., *The properties of petroleum fluids*. PennWell Books: 1990.

（81）Hunt, M., *Petroleum geochemistry and geology*. WH Freeman and company: 1979.

（82）Selley, R. C.; Sonnenberg, S. A., *Elements of petroleum geology*. Academic Press: 2014.

（83）Mansoori, G. A., A unified perspective on the phase behaviour of petroleum fluids. *International Journal of Oil, Gas and Coal Technology* **2009,** *2*, (2), 141-167.

（84）Akbarzadeh, K.; Hammami, A.; Kharrat, A.; Zhang, D.; Allenson, S.; Creek, J.; Kabir, S.; Jamaluddin, A.; Marshall, A. G.; Rodgers, R. P., Asphaltenes—problematic but rich in potential. *Oilfield Review* **2007,** *19*, (2), 22-43.

（85）Atlas, R. M., Microbial degradation of petroleum hydrocarbons: an environmental perspective. *Microbiological reviews* **1981,** *45*, (1), 180.

（86）McKenna, A. M.; Donald, L. J.; Fitzsimmons, J. E.; Juyal, P.; Spicer, V.; Standing, K. G.; Marshall, A. G.; Rodgers, R. P., Heavy petroleum composition. 3. Asphaltene aggregation. *Energy & Fuels* **2013,** *27*, (3), 1246-1256.

（87）McKenna, A. M.; Marshall, A. G.; Rodgers, R. P., Heavy Petroleum Composition. 4. Asphaltene Compositional Space. *Energy & Fuels* **2013,** *27*, (3), 1257-1267.

（88）Podgorski, D. C.; Corilo, Y. E.; Nyadong, L.; Lobodin, V. V.; Bythell, B. J.; Robbins, W. K.; McKenna, A. M.; Marshall, A. G.; Rodgers, R. P., Heavy Petroleum Composition. 5. Compositional and Structural Continuum of Petroleum Revealed. *Energy & Fuels* **2013,** *27*, (3), 1268-1276.

（89）McKenna, A. M.; Nelson, R. K.; Reddy, C. M.; Savory, J. J.; Kaiser, N. K.; Fitzsimmons, J. E.; Marshall, A. G.; Rodgers, R. P., Expansion of the Analytical Window for Oil Spill Characterization by Ultrahigh Resolution Mass Spectrometry: Beyond Gas Chromatography. *Environmental Science & Technology* **2013,** *47*, (13), 7530-7539.

（90）Tissot, B.; Welte, D., " Petroleum Formation and Occurrence.". In Springer, Berlin: 1984.

（91）Boduszynski, M. M.; Altgelt, K. H., *Composition and analysis of heavy petroleum fractions*. CRC Press: 1994.

（92）McKenna, A. M.; Purcell, J. M.; Rodgers, R. P.; Marshall, A. G., Heavy Petroleum Composition. 1. Exhaustive Compositional Analysis of Athabasca Bitumen HVGO Distillates by Fourier Transform Ion Cyclotron Resonance Mass Spectrometry: A Definitive Test of the Boduszynski Model. *Energy & Fuels* **2010,** *24*, (5), 2929-2938.

（93）McKenna, A. M.; Blakney, G. T.; Xian, F.; Glaser, P. B.; Rodgers, R. P.; Marshall, A. G., Heavy Petroleum Composition. 2. Progression of the Boduszynski Model to the Limit of Distillation by Ultrahigh-Resolution FT-ICR Mass Spectrometry. *Energy & Fuels* **2010,** *24*, (5), 2939-2946.

（94）Gustafson, S.; Tell, S.; Orem, D., Selection of Representative Total Petroleum Hydrocarbon (TPH) Fractions Based on Fate and Transport Considerations. *Total Petroleum Hydrocarbon Criteria Working Group Series* **1997,** *3*.

（95）Fathepure, B. Z., Recent studies in microbial degradation of petroleum hydrocarbons in hypersaline environments. *Frontiers in microbiology* **2014,** *5*.

（96）Tissot, B.; Welte, D., *Petroleum formation and occurrence: a new approach to oil and gas exploration*. Springer Science & Business Media: 2012.

（97）Wentzel, A.; Ellingsen, T. E.; Kotlar, H.-K.; Zotchev, S. B.; Throne-Holst, M., Bacterial metabolism of long-chain n-alkanes. *Applied microbiology and biotechnology* **2007,** *76*, (6), 1209-1221.

（98）Madigan, M. T.; Martinko, J. M.; Parker, J., *Brock biology of microorganisms*. prentice hall Upper Saddle River, NJ: 1997; Vol. 514.

（99）Whyte, L. G.; Hawari, J.; Zhou, E.; Bourbonnière, L.; Inniss, W. E.; Greer, C. W., Biodegradation of Variable-Chain-Length Alkanes at Low Temperatures by a Psychrotrophic Rhodococcussp. *Applied and environmental microbiology* **1998,** *64*, (7), 2578-2584.

（100）Jansen, G. A.; Wanders, R. J. A., Alpha-Oxidation. *Biochimica et Biophysica Acta (BBA) - Molecular Cell Research* **2006,** *1763*, (12), 1403-1412.

（101）Mikolasch, A.; Klenk, H.-P.; Schauer, F., Degradation of the multiple branched alkane 2, 6, 10, 14-tetramethyl-pentadecane (pristane) in Rhodococcus ruber and Mycobacterium neoaurum. *International Biodeterioration & Biodegradation* **2009,** *63*, (2), 201-207.

（102）Peters, K. E.; Moldowan, J. M.; McCaffrey, M. A.; Fago, F. J., Selective biodegradation of extended hopanes to 25-norhopanes in petroleum reservoirs. Insights from molecular mechanics. *Organic Geochemistry* **1996,** *24*, (8), 765-783.

（103）Koma, D.; Sakashita, Y.; Kubota, K.; Fujii, Y.; Hasumi, F.; Chung, S.; Kubo, M., Degradation pathways of cyclic alkanes in Rhodococcus sp. NDKK48. *Applied microbiology and biotechnology* **2004,** *66*, (1), 92-99.

（104）van Beilen, J. B.; Funhoff, E. G., Alkane hydroxylases involved in microbial alkane degradation. *Applied Microbiology and Biotechnology* **2007,** *74*, (1), 13-21.

（105）Perry, J. J., Microbial cooxidations involving hydrocarbons. *Microbiological Reviews* **1979,** *43*, (1), 59.

（106）Ember, G., Initiated peroxidation of secondary carbon in alkanes and cycloalkanes. In Google Patents: 1993.

（107）Horvath, R. S., Microbial co-metabolism and the degradation of organic compounds in nature. *Bacteriological Reviews* **1972,** *36*, (2), 146.

（108）Cheng, Q.; Thomas, S.; Rouviere, P., Biological conversion of cyclic alkanes and cyclic alcohols into dicarboxylic acids: biochemical and molecular basis. *Applied microbiology and biotechnology* **2002,** *58*, (6), 704-711.

（109）Sinninghe Damsté, J. S.; Kock-van Dalen, A. C.; Albrecht, P. A.; De Leeuw, J. W., Identification of long-chain 1,2-di-n-alkylbenzenes in Amposta crude oil from the Tarragona Basin, Spanish Mediterranean: Implications for the origin and fate of alkylbenzenes. *Geochimica et Cosmochimica Acta* **1991,** *55*, (12), 3677-3683.

（110）Yang, C.; Zhang, G.; Wang, Z.; Yang, Z.; Hollebone, B.; Landriault, M.; Shah, K.; Brown, C. E., Development of a methodology for accurate quantitation of alkylated polycyclic aromatic hydrocarbons in petroleum and oil contaminated environmental samples. *Analytical Methods* **2014,** *6*, (19), 7760-7771.

（111）Zeigler, C. D.; Robbat Jr, A., Comprehensive profiling of coal tar and crude oil to obtain mass spectra and retention indices for alkylated PAH shows why current methods err. *Environmental science & technology* **2012,** *46*, (7), 3935-3942.

（112）Juhasz, A. L.; Naidu, R., Bioremediation of high molecular weight polycyclic aromatic hydrocarbons: a review of the microbial degradation of benzo [a] pyrene. *International biodeterioration & biodegradation* **2000,** *45*, (1), 57-88.

（113）Beam, H.; Perry, J., Co-metabolism as a factor in microbial degradation of cycloparaffinic hydrocarbons. *Archiv für Mikrobiologie* **1973,** *91*, (1), 87-90.

（114）Fan, X.-L.; Wang, X.-Q.; Wang, J.-T.; Li, H.-D., Structural and electronic properties of linear and angular polycyclic aromatic hydrocarbons. *Physics Letters A* **2014,** *378*, (20), 1379-1382.

（115）Abdel-Shafy, H. I.; Mansour, M. S. M., A review on polycyclic aromatic hydrocarbons: Source, environmental impact, effect on human health and remediation. *Egyptian Journal of Petroleum* **2016,** *25*, (1), 107-123.

（116）Estévez-Fregoso, M.; Hernández-Trujillo, J., Electron delocalization and electron density of small polycyclic aromatic hydrocarbons in singlet excited states. *Physical Chemistry Chemical Physics* **2016,** *18*, (17), 11792-11799.

（117）Gardiner, W. W.; Word, J. Q.; Word, J. D.; Perkins, R. A.; McFarlin, K. M.; Hester, B. W.; Word, L. S.; Ray, C. M., The acute toxicity of chemically and physically dispersed crude oil to key arctic species under arctic conditions during the open water season. *Environmental Toxicology and Chemistry / Setac* **2013,** *32*, (10), 2284-2300.

（118）Wammer, K. H.; Peters, C. A., Polycyclic Aromatic Hydrocarbon Biodegradation Rates: A Structure-Based Study. *Environmental Science & Technology* **2005,** *39*, (8), 2571-2578.

（119）Knightes, C. D.; Peters, C. A., Aqueous Phase Biodegradation Kinetics of 10 PAH Compounds. *Environmental Engineering Science* **2003,** *20*, (3), 207-218.

（120）Leblond, J. D.; Wayne Schultz, T.; Sayler, G. S., Observations on the preferential biodegradation of selected components of polyaromatic hydrocarbon mixtures. *Chemosphere* **2001,** *42*, (4), 333-343.

（121）Seo, J.-S.; Keum, Y.-S.; Li, Q. X., Bacterial Degradation of Aromatic Compounds. *International Journal of Environmental Research and Public Health* **2009,** *6*, (1), 278-309.

（122）Malmquist, L. M. V.; Selck, H.; Jørgensen, K. B.; Christensen, J. H., Polycyclic Aromatic Acids Are Primary Metabolites of Alkyl-PAHs—A Case Study with Nereis diversicolor. *Environmental Science & Technology* **2015,** *49*, (9), 5713-5721.

（123）Mahajan, M. C.; Phale, P. S.; Vaidyanathan, C. S., Evidence for the involvement of multiple pathways in the biodegradation of 1- and 2-methylnaphthalene by Pseudomonas putida CSV86. *Archives of Microbiology* **1994,** *161*, (5), 425-433.

（124）Davis, J.; Raymond, R., Oxidation of alkyl-substituted cyclic hydrocarbons by a Nocardia during growth on n-alkanes. *Applied microbiology* **1961,** *9*, (5), 383-388.

（125）Si-Zhong, Y.; Hui-Jun, J.; Zhi, W.; Rui-Xia, H.; Yan-Jun, J.; Xiu-Mei, L.; Shao-Peng, Y., Bioremediation of oil spills in cold environments: a review. *Pedosphere* **2009,** *19*, (3), 371-381.

（126）Ferguson, S. H.; Franzmann, P. D.; Snape, I.; Revill, A. T.; Trefry, M. G.; Zappia, L. R., Effects of temperature on mineralisation of petroleum in contaminated Antarctic terrestrial sediments. *Chemosphere* **2003,** *52*, (6), 975-987.

（127）Delille, D.; Coulon, F.; Pelletier, E., Effects of temperature warming during a bioremediation study of natural and nutrient-amended hydrocarbon-contaminated sub-Antarctic soils. *Cold Regions Science and Technology* **2004,** *40*, (1), 61-70.

（128）Siron, R.; Pelletier, E.; Brochu, C., Environmental factors influencing the biodegradation of petroleum hydrocarbons in cold seawater. *Archives of Environmental Contamination and Toxicology* **1995,** *28*, (4), 406-416.

（129）Balks, M. R.; Paetzold, R. F.; Kimble, J. M.; AISLABIE, J.; Campbell, I. B., Effects of hydrocarbon spills on the temperature and moisture regimes of Cryosols in the Ross Sea region. *Antarctic Science* **2002,** *14*, (04), 319-326.

（130）Dibble, J.; Bartha, R., Effect of environmental parameters on the biodegradation of oil sludge. *Applied and environmental microbiology* **1979,** *37*, (4), 729-739.

（131）Thavasi, R.; Jayalakshmi, S.; Balasubramanian, T.; Banat, I. M., Effects of Salinity, Temperature, Ph and Crude Oil Concentration on Biodegradation of Crude Oil by Pseudomonas Aeruginosa. *Journal of Biological and Environmental Sciences* **2007,** *1*, (2).

（132）Rahman, K.; Thahira-Rahman, J.; Lakshmanaperumalsamy, P.; Banat, I., Towards efficient crude oil degradation by a mixed bacterial consortium. *Bioresource technology* **2002,** *85*, (3), 257-261.

（133）Hambrick, G. A.; DeLaune, R. D.; Patrick, W., Effect of estuarine sediment pH and oxidation-reduction potential on microbial hydrocarbon degradation. *Applied and Environmental Microbiology* **1980,** *40*, (2), 365-369.

（134）Bossert, I.; Bartha, R., The fate of petroleum in soil ecosystems. **1984**.

（135）Verstraete, W.; Vanloocke, R.; DeBorger, R.; Verlinde, A. In *Modelling of the breakdown and the mobilization of hydrocarbons in unsaturated soil layers*, proceedings of the Third international Biodegradation symposium. Applied Science Publishers,(JM Sharpley, AM Kaplan, eds.), 1976; 1976; pp 99-112.

（136）Chen, T.; Delgado, A. G.; Yavuz, B. M.; Proctor, A. J.; Maldonado, J.; Zuo, Y.; Westerhoff, P.; Krajmalnik-Brown, R.; Rittmann, B. E., Ozone enhances biodegradability of heavy hydrocarbons in soil. *Journal of Environmental Engineering and Science* **2016,** *11*, (1), 7-17.

（137）Liang, Y.; Van Nostrand, J. D.; Wang, J.; Zhang, X.; Zhou, J.; Li, G., Microarray-based functional gene analysis of soil microbial communities during ozonation and biodegradation of crude oil. *Chemosphere* **2009,** *75*, (2), 193-199.

（138）Chaineau, C.; Rougeux, G.; Yepremian, C.; Oudot, J., Effects of nutrient concentration on the biodegradation of crude oil and associated microbial populations in the soil. *Soil biology and biochemistry* **2005,** *37*, (8), 1490-1497.

（139）Smith, V. H.; Graham, D. W.; Cleland, D. D., Application of resource-ratio theory to hydrocarbon biodegradation. *Environmental science & technology* **1998,** *32*, (21), 3386-3395.

（140）Ogboghodo, I.; Iruaga, E.; Osemwota, I.; Chokor, J., An assessment of the effects of crude oil pollution on soil properties, germination and growth of maize (Zea mays) using two crude types–Forcados light and Escravos light. *Environmental Monitoring and Assessment* **2004,** *96*, (1-3), 143-152.

（141）Bona, C.; Rezende, I. M. d.; Santos, G. d. O.; Souza, L. A. d., Effect of soil contaminated by diesel oil on the germination of seeds and the growth of Schinus terebinthifolius Raddi (Anacardiaceae) seedlings. *Brazilian Archives of Biology and Technology* **2011,** *54*, (6), 1379-1387.

（142）Wang, Y.; Feng, J.; Lin, Q.; Lyu, X.; Wang, X.; Wang, G., Effects of crude oil contamination on soil physical and chemical properties in Momoge wetland of China. *Chinese geographical science* **2013,** *23*, (6), 708-715.

（143）Adesina, G. O.; Adelasoye, K. A., Effect of crude oil pollution on heavy metal contents, microbial population in soil, and maize and cowpea growth. *Agricultural Sciences* **2014,** *2014*.

（144）Okolo, J. In *Effects of soil treatments containing poultry manure on crude oil degradation in a sandy loam soil*, Applied Ecology and Environmental Research, 2005; Citeseer: 2005; pp 47-53.

（145）Xu, Y.; Lu, M., Bioremediation of crude oil-contaminated soil: comparison of different biostimulation and bioaugmentation treatments. *Journal of hazardous materials* **2010,** *183*, (1), 395-401.

（146）Chorom, M.; Sharifi, H.; Motamedi, H., Bioremediation; Fertilizer; Heterotrophic bacteria; Crude oil; Normal paraffin. **2011**.

（147）Yan, N.; Marschner, P.; Cao, W.; Zuo, C.; Qin, W., Influence of salinity and water content on soil microorganisms. *International Soil and Water Conservation Research* **2015,** *3*, (4), 316-323.

（148）Singh, K., Microbial and enzyme activities of saline and sodic soils. *Land Degradation & Development* **2016,** *27*, (3), 706-718.

（149）Minai-Tehrani, D.; Herfatmanesh, A.; Azari-Dehkordi, F.; Minuoi, S., Effect of salinity on biodegradation of aliphatic fractions of crude oil in soil. *Pak. J. Biol. Sci* **2006,** *9*, (8), 1531-1535.

（150）Hong, R.; Kang, T. Y.; Michels, C. A.; Gadura, N., Membrane lipid peroxidation in copper alloy-mediated contact killing of Escherichia coli. *Applied and environmental microbiology* **2012,** *78*, (6), 1776-1784.

（151）Lemire, J. A.; Harrison, J. J.; Turner, R. J., Antimicrobial activity of metals: mechanisms, molecular targets and applications. *Nature Reviews Microbiology* **2013,** *11*, (6), 371-384.

（152）Ward, D. M.; Brock, T., Hydrocarbon biodegradation in hypersaline environments. *Applied and Environmental Microbiology* **1978,** *35*, (2), 353-359.

（153）Qin, X.; Tang, J.; Li, D.; Zhang, Q., Effect of salinity on the bioremediation of petroleum hydrocarbons in a saline‐alkaline soil. *Letters in applied microbiology* **2012,** *55*, (3), 210-217.

（154）Rhykerd, R. L.; Weaver, R. W.; McInnes, K. J., Influence of salinity on bioremediation of oil in soil. *Environmental Pollution* **1995,** *90*, (1), 127-130.

（155）Eriksson, M. Ozone chemistry in aqueous solution: ozone decomposition and stabilisation. KTH, 2005.

（156）Batakliev, T.; Georgiev, V.; Anachkov, M.; Rakovsky, S., Ozone decomposition. *Interdisciplinary toxicology* **2014,** *7*, (2), 47-59.

（157）Miller, G. W., *An assessment of ozone and chlorine dioxide technologies for treatment of municipal water supplies*. Environmental Protection Agency, Office of Research and Development, Municipal Environmental Research Laboratory: 1978; Vol. 1.

（158）Guzel-Seydim, Z. B.; Greene, A. K.; Seydim, A. C., Use of ozone in the food industry. *LWT - Food Science and Technology* **2004,** *37*, (4), 453-460.

（159）Koike, K.; Nifuku, M.; Izumi, K.; Nakamura, S.; Fujiwara, S.; Horiguchi, S., Explosion properties of highly concentrated ozone gas. *Journal of Loss Prevention in the Process Industries* **2005,** *18*, (4), 465-468.

（160）Gonçalves, A. A., Ozone: an emerging technology for the seafood industry. *Brazilian archives of Biology and Technology* **2009,** *52*, (6), 1527-1539.

（161）Beltran, F. J., *Ozone reaction kinetics for water and wastewater systems*. crc Press: 2003.

（162）Rice, R. G.; Bollyky, L. J.; Lacy, W. J. *Analytical aspects of ozone treatment for water and wastewater*; International Ozone Assoc.: 1986.

（163）Smith, W., Principles of ozone generation. *Watertec Engineering Pty Ltd., Australia* **2011**.

（164）Mustafa, M. G., Biochemical basis of ozone toxicity. *Free Radical Biology and Medicine* **1990,** *9*, (3), 245-265.

（165）Wolfenden, J.; Wellburn, A. R., Effects of Summer Ozone on Membrane Lipid Composition During Subsequent Frost Hardening in Norway Spruce [Picea abies (L.) Karst]. *The New Phytologist* **1991,** *118*, (2), 323-329.

（166）Uppu, R. M.; Cueto, R.; Squadrito, G. L.; Pryor, W. A., What Does Ozone React with at the Air Lung Interface? Model Studies Using Human Red Blood Cell Membranes. *Archives of Biochemistry and Biophysics* **1995,** *319*, (1), 257-266.

（167）Mehlman, M. A.; Borek, C., Toxicity and biochemical mechanisms of ozone. *Environmental Research* **1987,** *42*, (1), 36-53.

（168）Menzel, D. B., Ozone: An overview of its toxicity in man and animals. *Journal of Toxicology and Environmental Health* **1984,** *13*, (2-3), 181-204.

（169）Lippmann, M., HEALTH EFFECTS OF OZONE A Critical Review. *JAPCA* **1989,** *39*, (5), 672-695.

（170）Lippmann, M., Effects of ozone on respiratory function and structure. *Annual review of public health* **1989,** *10*, (1), 49-67.

（171）Koren, H. S.; Devlin, R. B.; Graham, D. E.; Mann, R.; McGee, M. P.; Horstman, D. H.; Kozumbo, W. J.; Becker, S.; House, D. E.; McDonnell, W. F., Ozone-induced inflammation in the lower airways of human subjects. *American review of respiratory disease* **1989,** *139*, (2), 407-415.

（172）Buckley, R. D.; Hackney, J. D.; Clark, K.; Posin, C., Ozone and human blood. *Archives of Environmental Health: An International Journal* **1975,** *30*, (1), 40-43.

（173）Raub, J. A.; Miller, F. J.; Graham, J. A., Effects of low level ozone exposure on pulmonary function in adult and neonatal rats. *Advances in Modern Environmental Toxicology* **1983,** *5*, 363-7.

（174）Wegner, C.; Jackson, A.; Berry, J.; Gillespie, J. In *THE EFFECTS OF LONG-TERM, LOW-LEVEL OZONE EXPOSURE ON STATIC, DYNAMIC AND OSCILLATORY PULMONARY MECHANICS IN MONKEYS*, AMERICAN REVIEW OF RESPIRATORY DISEASE, 1982; AMER LUNG ASSOC 1740 BROADWAY, NEW YORK, NY 10019: 1982; pp 147-147.

（175）Gottschalk, C.; Saupe, A.; Libra, J. A., *Ozonation of Water and Waste Water: A Practical Guide to Understanding Ozone and Its Application*. Wiley: 2000.

（176）von Gunten, U., Ozonation of drinking water: Part I. Oxidation kinetics and product formation. *Water Research* **2003,** *37*, (7), 1443-1467.

（177）Kim, J.; Choi, H., Modeling in situ ozonation for the remediation of nonvolatile PAH-contaminated unsaturated soils. *Journal of Contaminant Hydrology* **2002,** *55*, (3–4), 261-285.

（178）Choi, H.; Lim, H.-N.; Kim, J.; Hwang, T.-M.; Kang, J.-W., Transport characteristics of gas phase ozone in unsaturated porous media for in-situ chemical oxidation. *Journal of Contaminant Hydrology* **2002,** *57*, (1–2), 81-98.

（179）Yu, D.-Y.; Bae, W.; Kang, N.; Banks, M. K.; Choi, C.-H., Characterization of Gaseous Ozone Decomposition in Soil. *Soil and Sediment Contamination: An International Journal* **2005,** *14*, (3), 231-247.

（180）Jung, H.; Choi, H., Effects of in situ ozonation on structural change of soil organic matter. *Environmental engineering science* **2003,** *20*, (4), 289-299.

（181）Staehelin, J.; Hoigne, J., Decomposition of ozone in water: rate of initiation by hydroxide ions and hydrogen peroxide. *Environmental Science & Technology* **1982,** *16*, (10), 676-681.

（182）Zavitsas, A. A.; Melikian, A. A., Hydrogen abstractions by free radicals. Factors controlling reactivity. *Journal of the American Chemical Society* **1975,** *97*, (10), 2757-2763.

（183）Chen, Y.; Tschuikow-Roux, E., Mechanism of hydrogen abstraction reactions by free radicals: simple metathesis or involving intermediate complex? *The Journal of Physical Chemistry* **1993,** *97*, (15), 3742-3749.

（184）Allodi, M. A.; Kirschner, K. N.; Shields, G. C., Thermodynamics of the Hydroxyl Radical Addition to Isoprene. *The Journal of Physical Chemistry A* **2008,** *112*, (30), 7064-7071.

（185）Hoigné, J.; Bader, H., The role of hydroxyl radical reactions in ozonation processes in aqueous solutions. *Water Research* **1976,** *10*, (5), 377-386.

（186）Francés-Monerris, A.; Merchán, M.; Roca-Sanjuán, D., Mechanism of the OH Radical Addition to Adenine from Quantum-Chemistry Determinations of Reaction Paths and Spectroscopic Tracking of the Intermediates. *The Journal of Organic Chemistry* **2017,** *82*, (1), 276-288.

（187）Atkinson, R., Kinetics and mechanisms of the gas-phase reactions of the hydroxyl radical with organic compounds under atmospheric conditions. *Chemical Reviews* **1986,** *86*, (1), 69-201.

（188）Yu, D.-Y.; Kang, N.; Bae, W.; Banks, M. K., Characteristics in oxidative degradation by ozone for saturated hydrocarbons in soil contaminated with diesel fuel. *Chemosphere* **2007,** *66*, (5), 799-807.

（189）Munter, R., Advanced oxidation processes–current status and prospects. *Proc. Estonian Acad. Sci. Chem* **2001,** *50*, (2), 59-80.

（190）Kim, J.; Choi, H., Modeling in situ ozonation for the remediation of nonvolatile PAH-contaminated unsaturated soils. *Journal of contaminant hydrology* **2002,** *55*, (3), 261-285.

（191）Kulik, N.; Goi, A.; Trapido, M.; Tuhkanen, T., Degradation of polycyclic aromatic hydrocarbons by combined chemical pre-oxidation and bioremediation in creosote contaminated soil. *Journal of Environmental Management* **2006,** *78*, (4), 382-391.

（192）Park, J.-S.; Choi, H.; Cho, J., Kinetic decomposition of ozone and para-chlorobenzoic acid (pCBA) during catalytic ozonation. *Water research* **2004,** *38*, (9), 2285-2292.

（193）Choi, H.; Lim, H.-N.; Kim, J.; Hwang, T.-M.; Kang, J.-W., Transport characteristics of gas phase ozone in unsaturated porous media for in-situ chemical oxidation. *Journal of contaminant hydrology* **2002,** *57*, (1), 81-98.

（194）Markham, O., *The UV/Oxidation Handbook*. Canada, 1994.

（195）Hellman, T. M.; Hamilton, G. A., Mechanism of alkane oxidation by ozone in the presence and absence of iron(III) chloride. *Journal of the American Chemical Society* **1974,** *96*, (5), 1530-1535.

（196）Popov, A. A.; Rakovskii, S. K.; Shopov, D. M.; Ruban, L. V., Mechanism of the reaction of saturated hydrocarbons with ozone. *Bulletin of the Academy of Sciences of the USSR, Division of chemical science* **1976,** *25*, (5), 958-966.

（197）Cerkovnik, J.; Eržen, E.; Koller, J.; Plesničar, B., Evidence for HOOO Radicals in the Formation of Alkyl Hydrotrioxides (ROOOH) and Hydrogen Trioxide (HOOOH) in the Ozonation of C−H Bonds in Hydrocarbons1. *Journal of the American Chemical Society* **2002,** *124*, (3), 404-409.

（198）Plesničar, B.; Cerkovnik, J.; Tuttle, T.; Kraka, E.; Cremer, D., Evidence for the HOOO- Anion in the Ozonation of 1,3-Dioxolanes: Hemiortho Esters as the Primary Products. *Journal of the American Chemical Society* **2002,** *124*, (38), 11260-11261.

（199）Lee, R.; Coote, M. L., Mechanistic insights into ozone-initiated oxidative degradation of saturated hydrocarbons and polymers. *Physical Chemistry Chemical Physics* **2016,** *18*, (35), 24663-24671.

（200）Von Sonntag, C.; Von Gunten, U., *Chemistry of ozone in water and wastewater treatment*. IWA publishing: 2012.

（201）Bailey, P. S., *Ozonation in Organic Chemistry V2: Nonolefinic Compounds*. Elsevier: 1982; Vol. 2.

（202）Greiner, N. R., Hydroxyl Radical Kinetics by Kinetic Spectroscopy. VI. Reactions with Alkanes in the Range 300–500°K. *The Journal of Chemical Physics* **1970,** *53*, (3), 1070-1076.

（203）Hashimoto, T.; Iwata, S., Theoretical Study on the Weakly-Bound Complexes in the Reactions of Hydroxyl Radical with Saturated Hydrocarbons (Methane, Ethane, and Propane). *The Journal of Physical Chemistry A* **2002,** *106*, (11), 2652-2658.

（204）Gottschalk, C.; Libra, J. A.; Saupe, A., *Ozonation of water and waste water: A practical guide to understanding ozone and its applications*. John Wiley & Sons: 2009.

（205）Criegee, R., Mechanism of ozonolysis. *Angewandte Chemie International Edition in English* **1975,** *14*, (11), 745-752.

（206）Wilmarth, W. K.; Haim, A., Peroxide reaction mechanisms. *Interscience, New York* **1962**, 175.

（207）Zeng, Y.; Hong, P. K. A.; Wavrek, D. A., Integrated Chemical-Biological Treatment of Benzo[a]pyrene. *Environmental Science & Technology* **2000,** *34*, (5), 854-862.

（208）Ananthula, R.; Yamada, T.; Taylor, P. H., Kinetics of OH Radical Reaction with Anthracene and Anthracene-d10. *The Journal of Physical Chemistry A* **2006,** *110*, (10), 3559-3566.

（209）Benzinger, S. B. Reaction of hydroxyl radical with aromatic hydrocarbons. Ball State University, 2010.

（210）Bunce, N. J.; Liu, L.; Zhu, J.; Lane, D. A., Reaction of Naphthalene and Its Derivatives with Hydroxyl Radicals in the Gas Phase. *Environmental Science & Technology* **1997,** *31*, (8), 2252-2259.

（211）Kenley, R. A.; Davenport, J. E.; Hendry, D. G., Gas-phase hydroxyl radical reactions. Products and pathways for the reaction of hydroxyl with aromatic hydrocarbons. *The Journal of Physical Chemistry* **1981,** *85*, (19), 2740-2746.

（212）Dang, J.; Shi, X.; Hu, J.; Chen, J.; Zhang, Q.; Wang, W., Mechanistic and kinetic studies on OH-initiated atmospheric oxidation degradation of benzo[α]pyrene in the presence of O2 and NOx. *Chemosphere* **2015,** *119*, 387-393.

（213）Jung, H.; Ahn, Y.; Choi, H.; Kim, I. S., Effects of in-situ ozonation on indigenous microorganisms in diesel contaminated soil: Survival and regrowth. *Chemosphere* **2005,** *61*, (7), 923-932.

（214）Javorská, H.; Tlustoš, P.; Komárek, M.; Leštan, D.; Kaliszová, R.; Száková, J., Effect of ozonation on polychlorinated biphenyl degradation and on soil physico-chemical properties. *Journal of hazardous materials* **2009,** *161*, (2), 1202-1207.

（215）Russo, L.; Rizzo, L.; Belgiorno, V., Ozone oxidation and aerobic biodegradation with spent mushroom compost for detoxification and benzo (a) pyrene removal from contaminated soil. *Chemosphere* **2012,** *87*, (6), 595-601.

（216）Rivas, F. J., Polycyclic aromatic hydrocarbons sorbed on soils: a short review of chemical oxidation based treatments. *Journal of Hazardous Materials* **2006,** *138*, (2), 234-251.

（217）O'Mahony, M. M.; Dobson, A. D.; Barnes, J. D.; Singleton, I., The use of ozone in the remediation of polycyclic aromatic hydrocarbon contaminated soil. *Chemosphere* **2006,** *63*, (2), 307-314.

（218）Zeng, Y.; Hong, P. A.; Wavrek, D. A., Integrated chemical-biological treatment of benzo [a] pyrene. *Environmental science & technology* **2000,** *34*, (5), 854-862.

（219）Bijan, L.; Mohseni, M., Integrated ozone and biotreatment of pulp mill effluent and changes in biodegradability and molecular weight distribution of organic compounds. *Water Research* **2005,** *39*, (16), 3763-3772.

（220）Adams, C. D.; Cozzens, R. A.; Kim, B. J., Effects of ozonation on the biodegradability of substituted phenols. *Water research* **1997,** *31*, (10), 2655-2663.

（221）Crittenden, J. C.; Trussell, R. R.; Hand, D. W.; Howe, K. J.; Tchobanoglous, G., *MWH's Water Treatment: Principles and Design*. Wiley: 2012.

（222）Cheng, M.; Zeng, G.; Huang, D.; Lai, C.; Xu, P.; Zhang, C.; Liu, Y., Hydroxyl radicals based advanced oxidation processes (AOPs) for remediation of soils contaminated with organic compounds: A review. *Chemical Engineering Journal* **2016,** *284*, 582-598.

（223）Zhu, M.; Wang, H.; Su, H.; You, X.; Jin, W., Study on oxidation effect of ozone on petroleum-based pollutants in water. *Modern Applied Science* **2009,** *4*, (1), p6.

（224）Hoof, F. v.; Janssens, J.; Dyck, H. v., Formation of oxidation by products in surface water preozonation and their behaviour in water treatment. *Water supply* **1986,** *4*, (3), 93-102.

（225）Scott, J. P.; Ollis, D. F., Integration of chemical and biological oxidation processes for water treatment: review and recommendations. *Environmental Progress* **1995,** *14*, (2), 88-103.

（226）Camel, V.; Bermond, A., The use of ozone and associated oxidation processes in drinking water treatment. *Water Research* **1998,** *32*, (11), 3208-3222.

（227）Goi, A.; Kulik, N.; Trapido, M., Combined chemical and biological treatment of oil contaminated soil. *Chemosphere* **2006,** *63*, (10), 1754-1763.

（228）Wu, J. J.; Wu, C.-C.; Ma, H.-W.; Chang, C.-C., Treatment of landfill leachate by ozone-based advanced oxidation processes. *Chemosphere* **2004,** *54*, (7), 997-1003.

（229）Rittmann, B. E.; Stilwell, D.; Garside, J. C.; Amy, G. L.; Spangenberg, C.; Kalinsky, A.; Akiyoshi, E., Treatment of a colored groundwater by ozone-biofiltration: pilot studies and modeling interpretation. *Water research* **2002,** *36*, (13), 3387-3397.

（230）Brame, J. A.; Hong, S. W.; Lee, J.; Lee, S.-H.; Alvarez, P. J., Photocatalytic pre-treatment with food-grade TiO_2 increases the bioavailability and bioremediation potential of weathered oil from the Deepwater Horizon oil spill in the Gulf of Mexico. *Chemosphere* **2013,** *90*, (8), 2315-2319.

（231）Keen, O. S.; Baik, S.; Linden, K. G.; Aga, D. S.; Love, N. G., Enhanced biodegradation of carbamazepine after UV/H2O2 advanced oxidation. *Environmental science & technology* **2012,** *46*, (11), 6222-6227.

（232）Li, G.; Park, S.; Rittmann, B. E., Degradation of reactive dyes in a photocatalytic circulating-bed biofilm reactor. *Biotechnology and bioengineering* **2012,** *109*, (4), 884-893.

（233）Bavel, B. v., Comparison of Fenton's Reagent and Ozone Oxidation of Polycyclic Aromatic Hydrocarbons in Aged Contaminated Soils (7 pp). *Journal of Soils and Sediments* **2006,** *6*, (4), 208-214.

（234）Mohan, S. V.; Kisa, T.; Ohkuma, T.; Kanaly, R. A.; Shimizu, Y., Bioremediation technologies for treatment of PAH-contaminated soil and strategies to enhance process efficiency. *Reviews in Environmental Science and Bio/Technology* **2006,** *5*, (4), 347-374.

（235）Lee, B.-T.; Kim, K.-W., Ozonation of diesel fuel in unsaturated porous media. *Applied geochemistry* **2002,** *17*, (8), 1165-1170.

（236）Ahn, Y.; Jung, H.; Tatavarty, R.; Choi, H.; Yang, J.-w.; Kim, I., Monitoring of petroleum hydrocarbon degradative potential of indigenous microorganisms in ozonated soil. *Biodegradation* **2005,** *16*, (1), 45-56.

（237）Wang, J.; Zhang, X.; Li, G., Compositional changes of hydrocarbons of residual oil in contaminated soil during ozonation. *Ozone: Science & Engineering* **2013,** *35*, (5), 366-374.

（238）Ranc, B.; Faure, P.; Croze, V.; Simonnot, M., Selection of oxidant doses for in situ chemical oxidation of soils contaminated by polycyclic aromatic hydrocarbons (PAHs): A review. *Journal of Hazardous Materials* **2016,** *312*, 280-297.

（239）Haapea, P.; Tuhkanen, T., Integrated treatment of PAH contaminated soil by soil washing, ozonation and biological treatment. *Journal of hazardous materials* **2006,** *136*, (2), 244-250.

（240）Palmer, G.; Dixit, S.; MacArthur, J.; Smol, J., Elemental analysis of lake sediment from Sudbury, Canada, using particle-induced X-ray emission. *Science of the total environment* **1989,** *87*, 141-156.

（241）Jones, D.; Willett, V., Experimental evaluation of methods to quantify dissolved organic nitrogen (DON) and dissolved organic carbon (DOC) in soil. *Soil Biology and Biochemistry* **2006,** *38*, (5), 991-999.

（242）Kim, H. W.; Vannela, R.; Zhou, C.; Rittmann, B. E., Nutrient acquisition and limitation for the photoautotrophic growth of Synechocystis sp. PCC6803 as a renewable biomass source. *Biotechnology and bioengineering* **2011,** *108*, (2), 277-285.

（243）Pierzynski, G. M., Methods of phosphorus analysis for soils, sediments, residuals, and waters. In 2000.

（244）A.D. Eaton, M. A. H. F., Standard Methods for the Examination of Water and Wastewater, 5210—Biochemical Oxygen Demand (BOD)(21st ed.). In Association, A. P. H., Ed. American Public Health Association 2005.

（245）Delgado, A.; Fajardo-Williams, D.; Popat, S.; Torres, C.; Krajmalnik-Brown, R., Successful operation of continuous reactors at short retention times results in high-density, fast-rate Dehalococcoides dechlorinating cultures. *Applied microbiology and biotechnology* **2014,** *98*, (6), 2729-2737.

（246）Herzfelder, E. R.; Golledge, R. W., Method for the determination of extractable petroleum hydrocarbons (EPH). *Massachusetts Department of Environmental Protection, Boston* **2004,** *39*.

（247）Caporaso, J. G.; Lauber, C. L.; Walters, W. A.; Berg-Lyons, D.; Huntley, J.; Fierer, N.; Owens, S. M.; Betley, J.; Fraser, L.; Bauer, M., Ultra-high-throughput microbial community analysis on the Illumina HiSeq and MiSeq platforms. *The ISME journal* **2012,** *6*, (8), 1621-1624.

（248）Caporaso, J. G.; Kuczynski, J.; Stombaugh, J.; Bittinger, K.; Bushman, F. D.; Costello, E. K.; Fierer, N.; Pena, A. G.; Goodrich, J. K.; Gordon, J. I., QIIME allows analysis of high-throughput community sequencing data. *Nature methods* **2010,** *7*, (5), 335-336.

（249）Edgar, R. C., Search and clustering orders of magnitude faster than BLAST. *Bioinformatics* **2010,** *26*, (19), 2460-2461.

（250）Delgado, A. G.; Kang, D.-W.; Nelson, K. G.; Fajardo-Williams, D.; Miceli III, J. F.; Done, H. Y.; Popat, S. C.; Krajmalnik-Brown, R., Selective Enrichment Yields Robust Ethene-Producing Dechlorinating Cultures from Microcosms Stalled at cis-Dichloroethene. *PloS one* **2014,** *9*, (6), e100654.

（251）Sutton, N. B.; Grotenhuis, T.; Rijnaarts, H. H., Impact of organic carbon and nutrients mobilized during chemical oxidation on subsequent bioremediation of a diesel-contaminated soil. *Chemosphere* **2014,** *97*, 64-70.

（252）Lehtola, M. J.; Miettinen, I. T.; Vartiainen, T.; Myllykangas, T.; Martikainen, P. J., Microbially available organic carbon, phosphorus, and microbial growth in ozonated drinking water. *Water research* **2001,** *35*, (7), 1635-1640.

（253）Jones, D.; Douglas, A.; Parkes, R.; Taylor, J.; Giger, W.; Schaffner, C., The recognition of biodegraded petroleum-derived aromatic hydrocarbons in recent marine sediments. *Marine Pollution Bulletin* **1983,** *14*, (3), 103-108.

（254）Adebusoye, S. A.; Ilori, M. O.; Amund, O. O.; Teniola, O. D.; Olatope, S., Microbial degradation of petroleum hydrocarbons in a polluted tropical stream. *World journal of Microbiology and Biotechnology* **2007,** *23*, (8), 1149-1159.

（255）Daugulis, A. J.; McCracken, C. M., Microbial degradation of high and low molecular weight polyaromatic hydrocarbons in a two-phase partitioning bioreactor by two strains of Sphingomonas sp. *Biotechnology letters* **2003,** *25*, (17), 1441-1444.

（256）van Beilen, J. B.; Neuenschwander, M.; Smits, T. H.; Roth, C.; Balada, S. B.; Witholt, B., Rubredoxins involved in alkane oxidation. *Journal of bacteriology* **2002,** *184*, (6), 1722-1732.

（257）Paslawski, J. C.; Headley, J. V.; Hill, G. A.; Nemati, M., Biodegradation kinetics of trans-4-methyl-1-cyclohexane carboxylic acid. *Biodegradation* **2009,** *20*, (1), 125-133.

（258）Young, R. F.; Cheng, S. M.; Fedorak, P. M., Aerobic biodegradation of 2, 2′-dithiodibenzoic acid produced from dibenzothiophene metabolites. *Applied and environmental microbiology* **2006,** *72*, (1), 491-496.

（259）Jamieson, W. D.; Pehl, M. J.; Gregory, G. A.; Orwin, P. M., Coordinated surface activities in Variovorax paradoxus EPS. *BMC microbiology* **2009,** *9*, (1), 124.

（260）Salam, L.; Obayori, O.; Raji, S., Biodegradation of Used Engine Oil by a Methylotrophic Bacterium, Methylobacterium Mesophilicum Isolated from Tropical Hydrocarbon-contaminated Soil. *Petroleum Science and Technology* **2015,** *33*, (2), 186-195.

（261）Van Aken, B.; Yoon, J. M.; Schnoor, J. L., Biodegradation of nitro-substituted explosives 2, 4, 6-trinitrotoluene, hexahydro-1, 3, 5-trinitro-1, 3, 5-triazine, and octahydro-1, 3, 5, 7-tetranitro-1, 3, 5-tetrazocine by a phytosymbiotic Methylobacterium sp. associated with poplar tissues (Populus deltoides× nigra DN34). *Applied and environmental microbiology* **2004,** *70*, (1), 508-517.

（262）Qiu, L.; Chen, W.; Zhong, L.; Wu, W.; Wu, S.; Chen, J.; Zhang, F.; Zhong, W., Formaldehyde biodegradation by immobilized Methylobacterium sp. XJLW cells in a three-phase fluidized bed reactor. *Bioprocess and biosystems engineering* **2014,** *37*, (7), 1377-1384.

（263）Gan, S.; Lau, E.; Ng, H., Remediation of soils contaminated with polycyclic aromatic hydrocarbons (PAHs). *Journal of Hazardous Materials* **2009,** *172*, (2), 532-549.

（264）Caliman, F. A.; Robu, B. M.; Smaranda, C.; Pavel, V. L.; Gavrilescu, M., Soil and groundwater cleanup: benefits and limits of emerging technologies. *Clean Technologies and Environmental Policy* **2011,** *13*, (2), 241-268.

（265）Masten, S. J.; Davies, S. H., Efficacy of in-situ for the remediation of PAH contaminated soils. *Journal of contaminant hydrology* **1997,** *28*, (4), 327-335.

（266）Huling, S. G.; Pivetz, B. E. *In-situ chemical oxidation*; DTIC Document: 2006.

（267）Park, H.; Choi, W., Photocatalytic conversion of benzene to phenol using modified TiO 2 and polyoxometalates. *Catalysis Today* **2005,** *101*, (3), 291-297.

（268）Mantzavinos, D.; Psillakis, E., Enhancement of biodegradability of industrial wastewaters by chemical oxidation pre-treatment. *Journal of Chemical Technology and Biotechnology* **2004,** *79*, (5), 431-454.

（269）Chamarro, E.; Marco, A.; Esplugas, S., Use of Fenton reagent to improve organic chemical biodegradability. *Water research* **2001,** *35*, (4), 1047-1051.

（270）Apul OG; Dahlen P; Delgado AG; Sharif F; P, W., Treatment of heavy, long-chain petroleum-hydrocarbon contaminated soils using chemical oxidation. *Journal of Environmental Engineering* **2016,** *3*, (5), 997-1002.

（271）Element, C., METHOD 3051A MICROWAVE ASSISTED ACID DIGESTION OF SEDIMENTS, SLUDGES, SOILS, AND OILS. **2007**.

（272）IP143, Determination of asphaltenes (heptane insolubles) in crude petroleum and petroleum products. **2004**.

（273）Brooks, M. C.; Wise, W. R.; Annable, M. D., Fundamental changes in in situ air sparging how patterns. *Groundwater Monitoring & Remediation* **1999,** *19*, (2), 105-113.

（274）Rittmann, B. E.; McCarty, P. L., Environmental biotechnology: principles and applications. . *New York, USA: McGraw-Hill Series in Water Resources & Environmental Engineering* **2001,** *173*, 569-570.

（275）Wang, J.; Zhang, X.; Li, G., Detailed characterization of polar compounds of residual oil in contaminated soil revealed by Fourier transform ion cyclotron resonance mass spectrometry. *Chemosphere* **2011,** *85*, (4), 609-615.

（276）Georges, M. K.; Veregin, R. P.; Kazmaier, P. M.; Hamer, G. K., Narrow molecular weight resins by a free-radical polymerization process. *Macromolecules* **1993,** *26*, (11), 2987-2988.

（277）Keoshkerian, B.; Georges, M. K.; Boils-Boissier, D., Living free-radical aqueous polymerization. *Macromolecules* **1995,** *28*, (18), 6381-6382.

（278）Hodges, J. C.; Harikrishnan, L. S.; Ault-Justus, S., Preparation of designer resins via living free radical polymerization of functional monomers on solid support. *Journal of combinatorial chemistry* **2000,** *2*, (1), 80-88.

（279）Shalabi, M. A.; Baldwin, R. M.; Bain, R. L.; Gary, J. H.; Golden, J. O., Noncatalytic coal liquefaction in a donor solvent. Rate of formation of oil, asphaltenes, and preasphaltenes. *Industrial & Engineering Chemistry Process Design and Development* **1979,** *18*, (3), 474-479.

（280）Carlson, C.; Langer, A.; Stewart, J.; Hill, R., Thermal hydrogenation. Transfer of hydrogen from tetralin to cracked residua. *Industrial & Engineering Chemistry* **1958,** *50*, (7), 1067-1070.

（281）Mare, M.; Waldner, G.; Bauer, R.; Jacobs, H.; Broekaert, J., Degradation of nitrogen containing organic compounds by combined photocatalysis and ozonation. *Chemosphere* **1999,** *38*, (9), 2013-2027.

（282）Swift, R.; Posner, A., Nitrogen, phosphorus and sulphur contents of humic acids fractionated with respect to molecular weight. *Journal of Soil Science* **1972,** *23*, (1), 50-57.

（283）Faria, P.; Órfão, J.; Pereira, M., Catalytic ozonation of sulfonated aromatic compounds in the presence of activated carbon. *Applied Catalysis B: Environmental* **2008,** *83*, (1), 150-159.

（284）Kostecki, P. T., *Hydrocarbon Contaminated Soils and Groundwater: Analysis, Fate, Environmental & Public Health Effects, & Remediation*. CRC Press: 1991; Vol. 1.

（285）Valentín, L.; Nousiainen, A.; Mikkonen, A., Introduction to Organic Contaminants in Soil: Concepts and Risks. In *Emerging Organic Contaminants in Sludges: Analysis, Fate and Biological Treatment*, Vicent, T.; Caminal, G.; Eljarrat, E.; Barceló, D., Eds. Springer Berlin Heidelberg: Berlin, Heidelberg, 2013; pp 1-29.

（286）Fabietti, G.; Biasioli, M.; Barberis, R.; Ajmone-Marsan, F., Soil contamination by organic and inorganic pollutants at the regional scale: the case of Piedmont, Italy. *Journal of Soils and Sediments* **2010,** *10*, (2), 290-300.

（287）Cunningham, S. D.; Anderson, T. A.; Schwab, A. P.; Hsu, F., Phytoremediation of soils contaminated with organic pollutants. *Advances in agronomy* **1996,** *56*, (1), 55-114.

（288）O'Mahony, M. M.; Dobson, A. D.; Barnes, J. D.; Singleton, I., The use of ozone in the remediation of polycyclic aromatic hydrocarbon contaminated soil. *Chemosphere* **2006,** *63*, (2), 307-14.

（289）Masten, S. J.; Davies, S. H. R., Efficacy of in-situ for the remediation of PAH contaminated soils. *Journal of Contaminant Hydrology* **1997,** *28*, (4), 327-335.

（290）USEPA, Field applications of in situ remediation technologies: chemical oxidation. In US Environmental Protection Agency Washington, DC, 1998; Vol. EPA 542-R-98-008.

（291）USEPA, Abstracts of remediation case studies 6. Office of SolidWaste and Emergency Response. In US Environmental Protection Agency Washington, DC, 2002; Vol. EPA-542-C-02-004.

（292）USEPA, Abstracts of remediation case studies 7. Office of SolidWaste and Emergency Response. In US Environmental Protection Agency Washington,DC, 2003; Vol. EPA 542-R-03-011.

（293）Lim, H.-N.; Choi, H.; Hwang, T.-M.; Kang, J.-W., Characterization of ozone decomposition in a soil slurry: kinetics and mechanism. *Water research* **2002,** *36*, (1), 219-229.

（294）Lens, P., *Soil and sediment remediation: mechanisms, technologies and applications*. IWA Publishing: 2005.

（295）Nam, K.; Kukor, J. J., Combined ozonation and biodegradation for remediationof mixtures of polycyclic aromatic hydrocarbons in soil. *Biodegradation* **2000,** *11*, (1), 1-9.

（296）Goi, A.; Trapido, M.; Kulik, N.; Palmroth, M. R. T.; Tuhkanen, T., Ozonation and Fenton Treatment for Remediation of Diesel Fuel Contaminated Soil. *Ozone: Science & Engineering* **2006,** *28*, (1), 37-46.

（297）Chen, T.; Delgado, A. G.; Yavuz, B. M.; Maldonado, J.; Zuo, Y.; Kamath, R.; Westerhoff, P.; Krajmalnik-Brown, R.; Rittmann, B. E., Interpreting Interactions between Ozone and Residual Petroleum Hydrocarbons in Soil. *Environmental Science & Technology* **2017,** *51*, (1), 506-513.

（298）Chorom, M.; Sharifi, H.; Motamedi, H., Bioremediation of a crude oil-polluted soil by application of fertilizers. *Iranian Journal of Environmental Health Science & Engineering* **2010,** *7*, (4), 319.

（299）Goi, A.; Trapido, M., Degradation of polycyclic aromatic hydrocarbons in soil: The fenton reagent versus ozonation. *Environmental Technology* **2004,** *25*, (2), 155-164.

（300）Luster-Teasley, S.; Ubaka-Blackmoore, N.; Masten, S. J., Evaluation of soil pH and moisture content on in-situ ozonation of pyrene in soils. *Journal of Hazardous Materials* **2009,** *167*, (1–3), 701-706.

（301）Gomez-Alvarez, M.; Poznyak, T.; Rios-Leal, E.; Silva-Sanchez, C., Anthracene decomposition in soils by conventional ozonation. *J Environ Manage* **2012,** *113*, 545-51.

（302）Albers, P. H., Petroleum and individual polycyclic aromatic hydrocarbons. *Handbook of ecotoxicology* **1995,** *2*.

（303）Pampanin, D. M.; Sydnes, M. O., Polycyclic aromatic hydrocarbons a constituent of petroleum: presence and influence in the aquatic environment. *Hydrocarbon. Rijeka: InTech Prepress* **2013**, 83-118.

（304）Ramasamy, R. K.; Rahman, N. A.; San, W. C., Effect of temperature on the ozonation of textile waste effluent. *Coloration Technology* **2001,** *117*, (2), 95-97.

（305）Hirata, T.; Shimura, A.; Morita, S.; Suzuki, M.; Motoyama, N.; Hoshikawa, H.; Moniwa, T.; Kaneko, M., The effect of temperature on the efficacy of ozonation for inactivating Cryptosporidium parvum oocysts. *Water Science and Technology* **2001,** *43*, (12), 163-166.

（306）USEPA, Air Method, Toxic Organics-15 (TO-15): Compendium of Methods for the Determination of Toxic Organic Compounds in Ambient Air Second Edition: Determination of Volatile Organic Compounds (VOCs) in Air Collected in Specially-Prepared Canisters and Analyzed by Gas Chromatography/Mass Spectrometry (GC/MS). **1999,** *EPA 625/R-96/010b*.

（307）McLean, J. E.; Bledsoe, B. E., Behavior of Metals in Soils. *EPA Environmental Assessment Sourcebook* **1996,** *19*.

（308）Legube, B.; Karpel Vel Leitner, N., Catalytic ozonation: a promising advanced oxidation technology for water treatment. *Catalysis Today* **1999,** *53*, (1), 61-72.

（309）Kasprzyk-Hordern, B.; Ziółek, M.; Nawrocki, J., Catalytic ozonation and methods of enhancing molecular ozone reactions in water treatment. *Applied Catalysis B: Environmental* **2003,** *46*, (4), 639-669.

（310）Moharam, H. M.; Braek, A. M.; Fahim, M. A., A Simple Method of Estimating the Enthalpy of Petroleum Fractions. *Industrial & Engineering Chemistry Research* **1998,** *37*, (12), 4898-4902.

（311）Riazi, M., *Characterization and properties of petroleum fractions*. ASTM international: 2005; Vol. 50.

（312）Law, C. K., Recent advances in droplet vaporization and combustion. *Progress in Energy and Combustion Science* **1982,** *8*, (3), 171-201.

（313）Glassman, I.; Yetter, R. A.; Glumac, N. G., *Combustion*. Academic press: 2014.

（314）Affens, W. A.; Carhart, H. W. *Ignition Studies. Part 7. The Determination of Autoignition Temperatures of Hydrocarbon Fuels*; DTIC Document: 1974.

（315）McManus, N., *Safety and health in confined spaces*. CRC Press: 1998.

（316）Kuchta, J. M.; Cato, R. J., Ignition and Flammability Properties of Lubricants. In SAE International: 1968.

（317）Liang, Y.; Nostrand, J. D. V.; Wang, J.; Zhang, X.; Zhou, J.; Li, G., Microarray-based functional gene analysis of soil microbial communities during ozonation and biodegradation of crude oil. *Chemosphere* **2009,** *75*, (2), 193-199.

（318）Ahn, Y.; Jung, H.; Tatavarty, R.; Choi, H.; Yang, J.-w.; Kim, I. S., Monitoring of petroleum hydrocarbon degradative potential of indigenous microorganisms in ozonated soil. *Biodegradation* **2005,** *16*, (1), 45-56.

（319）Apul OG, D. A., Arrowsmith S, Alam F, Hall C, Miranda EM, Sra K, Kamath R, Dahlen P, McMillen S, Westerhoff P, Krajmalnik-Brown R, Biodegradation of petroleum hydrocarbons in crude oil-containing soils is inhibited by addition of peroxide oxidants. *Journal of Hazardous Materials* **2018,** *In Review*

（320）USEPA, Ecological Effects Test Guidelines OCSPP 850.4100: Seedling Emergence and Seedling Growth. **2012**.

（321）USEPA, Ecological Effects Test Guideline OPPTS 850.6200 Earthworm Subchronic Toxicity Test. **1996,** *EPA 712-C-96-167*.

APPENDIX A

NUTRIENTS AND TRACE METALS FOR BIOREMEDIATION

Macronutrients and salt solution:

Reagent	Amount for 1 L stock solution
NaCl	10 g
$MgCl_2$ x $6H_20$	5 g
KH_2PO_4	20 g
NH_4Cl	40 g
Na_2SO_4	20 g
KCl	30 g
$CaCl_2$ x $2H_20$	0.5 g

Trace element solution A:

Reagent	Amount for 1 L stock solution
HCl (25% solution, w/w)	10 mL
$FeCl_2$ x $4H_20$	1.5 g
$CoCl_2$ x $6H_20$	0.19 g
$MnCl_2$ x $4H_20$	0.1 g
$ZnCl_2$	70 mg
H_3BO_3	6 mg
Na_2MoO_3 x $2H_20$	36 mg
$NiCl_2$ x $6H_20$	24 mg
$CuCl_2$ x $2H_20$	2 mg

Trace element solution B:

Reagent	Amount for 1 L stock solution
Na_2SeO_3 x $5H_20$	6 mg
Na_2WO_4 x $2H_20$	8 mg
NaOH	0.5 g

Vitamin mix stock solution

Reagent	Amount for 1 L stock solution
Folic acid	2 mg
Pyridoxine hydrochloride	10 mg
Riboflavin	5 mg
Biotin	2 mg
Nicotinic acid	5 mg
Thiamine	5 mg
Calcium Pantothenate	5 mg
Vitamin B_{12}	0.1 mg
p-Aminobenzoic acid	5 mg
Thioctic acid	5 mg
Monopotassium phosphate	900 mg

Table A1. Tentatively identified TPH compositions of BM2 and BM3

BM2 Analytes	BM3 Analytes
Cyclohexene	Cyclohexane, pentyl-
Hexadecane	Undecane, 3-methyl-
Naphthalene, 2,3,6-trimethyl-	Dodecane, 6-methyl-
Octadecane	Naphthalene, 1,2,3,4-tetrahydro-2-methyl
Tridecane	Cyclohexane, octyl-
Pentadecane, 2,6,10,14-tetramethyl-	Dodecane, 4-methyl-
1-Methyl-3-piperidyl cyclopentylphenylgl	Octane, 2,6-dimethyl-
Tridecane	Naphthalene, 1,2,3,4-tetrahydro-5-methyl
Heptadecane	Cyclotridecane
Tetradecane	Cyclopentane, 1-ethyl-3-methyl-, cis-
Heptadecane	Naphthalene, 1,2,3,4-tetrahydro-6-methyl
Dibenzothiophene, 3-methyl-	Naphthalene, 1-methyl-
Nonadecane	Dodecanoic acid, 2-hexen-1-yl ester
Dibenzothiophene, 3-methyl-	Naphthalene, 1,2,3,4-tetrahydro-1,4-dime
Sulfurous acid, 2-propyl tridecyl ester	Heptylcyclohexane
Anthracene, 1-methyl-	Tridecane, 4-methyl-
Tetradecane	Dodecane, 2,6,11-trimethyl-
Dibenzothiophene, 4,6-dimethyl-	3-Tetradecene, (E)-
2-Bromo dodecane	Cyclopentane, 1-ethyl-3-methyl-, trans-
2,7-Dimethyldibenzothiophene	Sulfurous acid, cyclohexylmethyl hexadec
1,7-Dimethyldibenzothiophene	Benzene, 1,3,5-trimethyl-2-(1-methylethe
Nornicotine	Sulfurous acid, cyclohexylmethyl heptade
Hexadecane	Naphthalene, 2,7-dimethyl-
Cyclohexane, tetradecyl-	Cyclohexane, octyl-
Heneicosane	7-Oxabicyclo[4.1.0]heptan-2-one, 4,4,6-t
Cyclic octaatomic sulfur	1-Pentadecene
Hexadecane	Sulfurous acid, cyclohexylmethyl pentade
5(10H)-Pyrido[3,4-b]quinolone, 7-methoxy	Cyclohexanecarboxylic acid, 1-ethyl-, me
Eicosane	Oxalic acid, cyclohexylmethyl decyl este
Phenanthrene, 2,3,5-trimethyl-	Cyclohexane, octyl-
(2,4,6-Trimethyl-phenoxy)-acetic acid be	Naphthalene, 2,3,6-trimethyl-
Pentacosane	Hexane, 2-phenyl-3-propyl-
Oxalic acid, 6-ethyloct-3-yl isobutyl es	7-Tetradecene, (E)-
3,4-Diethyl hexane	Cycloundecane, (1-methylethyl)-
Heptadecane, 3-methyl-	Oxalic acid, cyclohexylmethyl isohexyl e
Heneicosane	Pentadecane, 2,6,10-trimethyl-
Nonadecane	Cyclohexane, decyl-
Eicosane	1-Decanol, 2-hexyl-
Bacchotricuneatin c	Cyclohexane, 1-methyl-2-pentyl-

Eicosane, 10-methyl-	Bacchotricuneatin c
Pentane, 3-ethyl-	Oxalic acid, bis(6-ethyloct-3-yl) ester
Octadecane	Cyclohexane, undecyl-
cis-3-Phenyl-perhydrocyclopenta[d]pyrimi	2-(p-Tolyl)ethylamine
Heptacosane	Heptadecane, 2,6,10,15-tetramethyl-
Sulfurous acid, pentadecyl 2-propyl este	Heptadecane, 8-methyl-
Eicosane	Dodecylcyclohexane
5-Chloro-3-[2-tetrahydropyranylmethyl]-4	Dodecylcyclohexane
Cyclohexanecarboxylic acid, 4-heptyl-, 4	Hexadecane
Nonadecane	Cyclopentane, 1-pentyl-2-propyl-
Tetradecane	Ethanone, 1,2-di-2-furanyl-2-hydroxy-
Eicosane	Phenanthrene, 1-methyl-
Phenylalanine, N-trifluoroacetyl-4-amino	1H-Cyclopropa[l]phenanthrene,1a,9b-dihyd
3-Methylphenanthro[9,10-b]thiophene	n-Tridecylcyclohexane
4-Piperidinecarboxylic acid, 1-methyl-4-	1,4-Dithiepan-2-one, 3-phenyl-
2-methyloctacosane	Benzene, (1-methyldodecyl)-
Thiophene-2-acetic acid, nonyl ester	1,2-Dodecanediol
Octadecane	Tetratriacontyl trifluoroacetate
Pentadecane, 8-heptyl-	Furan, 2,5-dihydro-2,2,4-trimethyl-
2,6,6-Trimethyl-9-undecen-1-ol	5-Amino-3-methylpyrazole
Heptacosane, 1-chloro-	2-Naphthalenamine, 5,6,7,8-tetrahydro-
3,7,11,15-trimethylhexadecanoic acid, 2,	Methyl-3,4-O-furylidene.beta.l-arabinopy
Nonacosane	Phenanthrene, 2,3-dimethyl-
4-Propyl-10H-acridine-9-thione	n-Heptadecylcyclohexane
Hexacosane	Anthracene, 2-ethyl-
Phenol, 2-(4-diethylaminophenyliminometh	4-[2-(4-Oxo-4H-benzo[d][1,3]oxazin-2-yl)
Heptadecane	Phenanthrene, 2,7-dimethyl-
Phenol, 2-amino-4-methyl-	Oxalic acid, cyclohexylmethyl tridecyl e
1-Bromomethylenedecahydronaphthalene	Sulfurous acid, cyclohexylmethyl octadec
7-Methoxy-1-phenyl-4,5-dihydro-1H-benzo[	3,4-Difluorobenzaldehyde
Coprostane	Cyclohexane, decyl-
Heptadecane, 9-octyl-	Pentadecane
Benzoic acid, 3-(3-fluorobenzoylamino)-2	Bicyclo[3.1.1]heptan-3-one, 2,6,6-trimet
Silane, dimethyl-2-propenyl[(6,6,9-trime	Sulfurous acid, cyclohexylmethyl octadec
Pyrene, hexadecahydro-	5-Amino-3-methylpyrazole
Succinamic acid, N-(3-trifluoromethylphe	Tridecane, 1-iodo-
5-(7a-Isopropenyl-4,5-dimethyl-octahydro	Oxalic acid, monoamide, N-cycloheptyl-,
Pentacosane	Cyclohexane, undecyl-
Nickel(II), [bis(4-methylsalicylidene)ac	2-Hexyldodecyl butyrate
Ethion	Pyrene, 4-methyl-
d-Norpregnane (5.alpha.,14.alpha.)	1,2,3,4,5,6-Hexahydrochrysene

Tetracosane	n-Heptadecylcyclohexane
Acetic acid, 2-(5,6,7,8,9,10-hexahydro-3	Benzo[b]naphtho[2,3-d]thiophene, 7,8,9,1
Octacosane	Cyclohexane, 1-ethyl-1-methyl-
28-Nor-17.beta.(H)-hopane	Pyrene, 1,3-dimethyl-
Benzamide, N,N-didecyl-3-methyl-	4,6-O-Furylidene-d-glucopyranose
23,28-Bisnor-17.alpha.(H)-hopane	2-methyltetracosane
1-Penten-3-one, 1-(2,6,6-trimethyl-1-cyc	N-(O-Nitrobenzyl)aniline
4,4'-Furfurylidenebis(2,6-di-tert-butylp	Thenyldiamine
1-Penten-3-one, 1-(2,6,6-trimethyl-1-cyc	1H-Pyrrole-2-acetonitrile, 1-methyl-
1-Penten-3-one, 1-(2,6,6-trimethyl-1-cyc	2-Chloro-4,6-bis(3-furanyl)pyrimidine
.beta.-iso-Methyl ionone	Benzamide, N,N-diheptyl-4-methyl-
	1H-Benz[f]indene, 2-phenyl-
	Cyclohexane, 1-ethyl-1-methyl-
	9H-Cyclopenta[a]pyrene
	Heptadecane
	1,3-Benzenedicarboxylic acid, bis(2-ethy
	Chrysene, 5-ethyl-
	Hexadecane
	Triallylmethylsilane
	4-Fluoro-N-(1H-tetrazol-5-yl)benzamide
	Heptadecane
	Benz[e]acephenanthrylene
	Benzene, 1-(1-buten-3-yl)-4-decyl-
	Eicosane
	Thiophene-2-acetic acid, 4-hexadecyl est
	Benz[j]aceanthrylene, 3-methyl-
	Benz[j]aceanthrylene, 3-methyl-